

Thesis of Doctor of Philosophy

**“DEVELOPMENT OF A VACUUM
ARC THRUSTER FOR
NANOSATELLITES”**

by

Kateryna Aheieva

St. # 13589502

Supervisor: Associate Professor

Kazuhiro Toyoda

Laboratory of Spacecraft Environment Interaction Engineering

(LaSeine)

Department of Electrical and Electronic Engineering

Faculty of Engineering

Kyushu Institute of Technology

7 July, 2016

Publications

Below is a list of journal articles, conference papers produced prior to publication of this work:

1. “Development of a CFRP based Vacuum Arc Thruster for a Nano-Satellite Horyu-IV”

Proceedings of the 65th International Astronautical Congress (2014 年 9 月)

著者: K. Aheieva, S. Fuchikami, K. Toyoda, M. Cho

2. “Deorbit System based on Vacuum Arc Thruster for Microsatellites”

Proceedings of the 66th International Astronautical Congress (2015 年 10 月)

著者: K. Aheieva, K. Toyoda, M. Cho

3. “Development of a Direct Drive Vacuum Arc Thruster Passively Ignited for Nanosatellite”

IEEE Transaction on Plasma Science, Vol. 44, No. 1, pp.100-107 (2016 年 1 月)

著者: K. Aheieva, K. Toyoda, M. Cho

4. “Vacuum Arc Thruster Development and Testing for Micro- and Nano-Satellites”

The 30 ISTS Special Issue of Transaction of JSASS, Aerospace Technology Japan
(2016 年 9 月)

著者: K. Aheieva, K. Toyoda, M. Cho

Acknowledgements

To my supervisor, Associate Professor Kazuhiro Toyoda – thank you for having the faith in me, generous advice, inspiring guidance and encouragement throughout my research for this work. Your guidance and suggestions provided clarity and depth on many technical issues. Your valuable feedback over the many months and years has challenged and grown me.

To Professor Mengu Cho – thank you for significant and constructive suggestions into my research work, for your involvement me in the Horyu-IV project. I got a great experience.

To Kyushu Insitute of Technology staff – Minoru Iwata, Hirokazu Masui, Arifur Khan, George Maeda, Pauline Faure, Tatsuo Shimizu, thank you for putting in so many hours towards building and all the equipment and tools I needed for this project. Your patience and kindness was instrumental to my success.

To all Laboratory of Spacecraft Environment Interaction Engineering (LaSEINE) members- thank you for keeping me sane and reminding me that there was life outside the lab.

To my family– thank you for your endless patience with me and for being a constant source of encouragement and support when things got tough.

This work was partially supported by JSPS KAKENHI Grant Number 25220915

Content

Publications	2
Acknowledgements	3
Abbreviations	6
List of Figures	7
List of Tables.....	11
1. Introduction.	12
1.1. Background and motivation.....	12
1.2. Vacuum Arc Thruster.	15
1.2.1. Vacuum arc.....	19
1.2.2. Cathode material and geometry.	20
1.3. Development effective satellite deorbit system based on Vacuum Arc Thruster.....	21
1.4. Novelty.....	24
1.5. Objectives.	25
2. Experimental apparatus and test setup.	26
2.1. LEO chamber.....	26
2.2. Quadruple Mass Spectrometer.	28
2.3. General purpose chamber.	29
2.3.1. Igniter system.....	30
2.4. Thruster's electric circuit.....	31
3. Vacuum Arc Thruster.....	35
3.1. An Introduction to Vacuum Arc Thruster.	35
3.2. VAT theory and Performance.....	35
3.3. Design of Vacuum Arc Thruster.....	38
3.4. Vacuum Arc Thruster's propellants.	40
3.5. Vacuum Arc Thruster's work parameters.	44
3.6. Impulse bit measurement.....	48

3.7. Methods of efficiency improving.....	51
3.7.1. Water adopt propellant testing.....	52
3.8. Magnet system.....	56
3.9. Applied nozzle to the VAT head	59
3.10. Long life test for VAT	62
3.10.1. Arc rate after long life test.	63
3.11. VAT testing with different capacitors.....	65
4. Satellite deorbit system based on the Vacuum Arc Thruster.....	71
4.1. Requirements for the satellite deorbit system.....	71
4.2. Satellite deorbit time realized by Vacuum Arc Thruster.....	75
4.2.1. VAT testing with DCDC converter.....	82
5. Vacuum Arc Thruster on-board satellite Horyu-4	86
5.1. Horyu-4 satellite project.	86
5.2. Vacuum Arc Thruster sub-system.	87
6. Conclusions	92
References	96

Abbreviations

LEO	Low Earth Orbit
MEO	Medium Earth Orbit
GEO	Geostationary Earth Orbit
VAT	Vacuum Arc Thruster
PPT	Pulsed Plasma Thruster
SPT	Stationary plasma thruster
RIT	Radiofrequency ion thruster
FEEP	Field Emission Electric Propulsion
CFRP	Carbon Fiber Reinforced Plastic
DCDC	Digital converter
HVSA	High Voltage Solar Array
QMS	Quadrupole Mass Spectrometer
ECR	Electron Cyclotron Resonance
OBO	On-board oscilloscope
DLP	Double Langmuir probe
ELF	Electron emitting film

List of Figures

Figure 1. Satellite possible missions.

Figure 2. Vacuum Arc Thruster circuit.

Figure 3. Micro-Cathode Arc Thruster.

Figure 4. Magnetically enhanced Vacuum Arc Thruster

Figure 5. VAT posion on-board 2U CubeSat and VAT geometry.

Figure 6. Model of space debris around the Earth.

Figure 7. Concept for self-consuming satellite (splar cells arc used as the cathode in a vacuum arc propulsion system).

Figure 8. LEO vacuum chamber.

Figure 9. LEO's chamber apparatus.

Figure 10. ECR plasma power source.

Figure 11. Quadrupole Mass Spectrometer.

Figure 12. General Purpose Chamber (GPC).

Figure 13. Igniter system.

Figure 14. Electric circuit for the test performed in the LEO chamber.

Figure 15. Current and voltage probe connections.

Figure 16. Power source.

Figure 17. Oscilloscope "Wavesurfer 3024".

Figure 18. Delay pulse generator

Figure 19. Quick look camera.

Figure 20. Electric circuit for the test performed in the GPC.

Figure 21. Kyutech's vacuum arc thruster

Figure 22. Vacuum arc thruster head

Figure 23. Schematic of thruster head

Figure 24. VAT's assembling

Figure 25. VAT mounting to the satellite wall.

Figure 26. VAT's electric circuit.

Figure 27. Aluminum sample

Figure 28. Tungsten sample

Figure 29. CFRP sample

Figure 30. Scheme of experiments to measure average velocity

Figure 31. QMS output signal

Figure 32. Velocity distribution

Figure 33. Weighted velocity distribution

Figure 34. Average velocity vs. vacuum arc energy

Figure 35. VAT setup condition.

Figure 36. Discharge parameters for VAT with CFRP

Figure 37. Arc rate data of VAT

Figure 38. Discharge current waveforms for 300V-800V voltage level.

Figure 39. CFRP with 45 degree carbon fiber direction and test configuration

Figure 40. Experiment setup for impulse bit measurement.

Figure 41. VAT's discharge.

Figure 42. Target displacement after the discharge.

Figure 43. Impulse bit data for VAT with CFRP

Figure 44. The Mechanism of water adopt CFRP propellant development.

Figure 45. Water adopt CFRP propellant, silica powder and "Araldite" glue.

Figure 46. Water adopt CFRP configurations.

Figure 47. Water adopt propellant's discharges

Figure 48. Arc rate data for each water adopt propellant (#1, #2, #3)

Figure 49. Discharge current of VAT with water adopt CFRP (#1, #2, #3)

Figure 50. Comparison of VAT's propellant material.

Figure 51. Impulse bit measurement for water adopt CFRP with Al and Cu anode.

Figure 52. Permanent magnet

Figure 53. VAT's configuration with permanent magnet

Figure 54. Impulse bit for VAT with water adopt CFRP and permanent magnet ob the different configuration.

Figure 55. Impulse bit for VAT with the CFRP commercial with 0 degree and water adopt CFRP in different configuration with permanent magnet.

Figure 56. VAT configuration with nozzle.

Figure 57. VAT's discharges for configuration with nozzle.

Figure 58. Impulse bit for VAT configuration with 5 mm nozzle and without nozzle.

Figure 59. Cathode profile in term of long life test

Figure 60. 10 uF capacitor impulse bit test.

Figure 61. 14 uF capacitor impulse bit test.

Figure 62. Discharge current waveforms for test with 10 uF and 14 uF capacitors with four VAT's configurations.

Figure 63. Impulse bit for VAT with commercial CFRP (8 mm) and current waveforms.

Figure 64. Arc rate test for commercial CFRP and water adopt CFRP.

Figure 65. Space debris classification. Classification by size in all altitudes and in the LEO orbit.

Figure 66. Effective object numbers on the orbits (collision results for the cataloged and non-cataloged objects with size >10 cm)

Figure 67. VAT position on the RAM side.

Figure 68. Impulse bit data equation predicted by "Curve Expert".

Figure 69. CubeSat deorbit time, realized by VAT.

Figure 70. DCDC converter configuration.

Figure 71. VAT's arc rate with DCDC.

Figure 72. Deorbit time for thruster's circuit configuration without and with DCDC.

Figure 73. VAT efficiency in configuration with commercial CFRP propellant.

Figure 74. VAT efficiency in configuration with water adopt CFRP propellant.

Figure 75. Horyu-IV satellite and sub-system description.

Figure 76. Big Apple mission board.

Figure 77. VAT mounting to the capacitor circuit.

Figure 78. VAT position on-board satellite Horyu-IV.

Figure 79. OBO current waveform and commercial oscilloscope current waveform.

Figure 90. VAT' discharge detected by AVC (end-to-end test).

List of Tables

Table 1. Comparison of propulsion schemes for microsatellites.

Table 2. VAT's arc rate.

Table 3. Permanent magnet parameters.

Table 4. Arc rate data for VAT before and after the long life test.

Table 5. Arc rate depends to the voltage.

Table 6. Arc rate dates for the commercial CFRP and for the water adopt CFRP.

Table 7. Number of pulses needed for 1U CubeSat deorbit (VAT configuration with commercial CFRP).

Table 8. Number of pulses needed for 1U CubeSat deorbit (VAT configuration with water adopt CFRP).

Table 9. Deorbit time for CubeSat for the commercial CFRP and for the water adopt CFRP.

Table 10. Propellant consumption.

Table 11. Deorbit results for VAT with Cu electrode (8 mm depth).

1. Introduction.

This chapter describes background and motivation for the research about Vacuum Arc Thruster. Present a novelty and objectives to be achieved in this work. Describes principle of VAT and the vacuum arc in passive ignition (no igniter). Was done overview about necessity of a deorbiting system for nanosatellites regarding to the high spacecraft population on the LEO orbit.

1.1. Background and motivation.

Traditionally the satellite-building industry differentiated things by size or mass, by power consumption, and by place of development (university, industry, or government). In recent years, micro- and nano- satellites have become popular in part because more and more universities are actively engaged satellite development programs. The “cost-of-entry barrier” has come down significantly.

Formation of a satellite constellation, where each is an individual part of a bigger system, is an important aspect of small satellites potential. Other positive attributes are: low cost, quick response to the mission, flexibility of the operation, and long operational life-time in orbit (> 10 years). Small microsatellites use a cost-effective method for the detailed space study and physical phenomena research. This method could provide new spacecraft design and instruments concepts that will be demonstrated in space, with support to new satellite and instrument projects, international missions also, and to scientific research.

For example, a constellation of nanosatellites may each carry one or two scientific instruments to collectively perform the research of a single large satellite. Payload separation here into smaller segments can reduce a risk for the main mission. In addition, nanosatellites may be launched over an extended period of time, thereby allowing greater flexibility in mission capability, cost and lifetime. A spread network of satellites can collect data and perform experiments on a much larger scale than any single satellite could achieve. Constellations can also converge at a point of interest to study a particular region of the earth's surface.

Some examples of satellite formation flying are shown in Figure 1 [1].

From the Figure 1, satellites used for: weather information, climate research, transportation and logistics (navigation (GPS)), multimedia communication (television, telephones), safety, security and rescue, space research, Earth remote sensing etc. Mostly supplemented micro- and nano- satellites, such as: space research, earth remote sensing, early warning and disaster management.

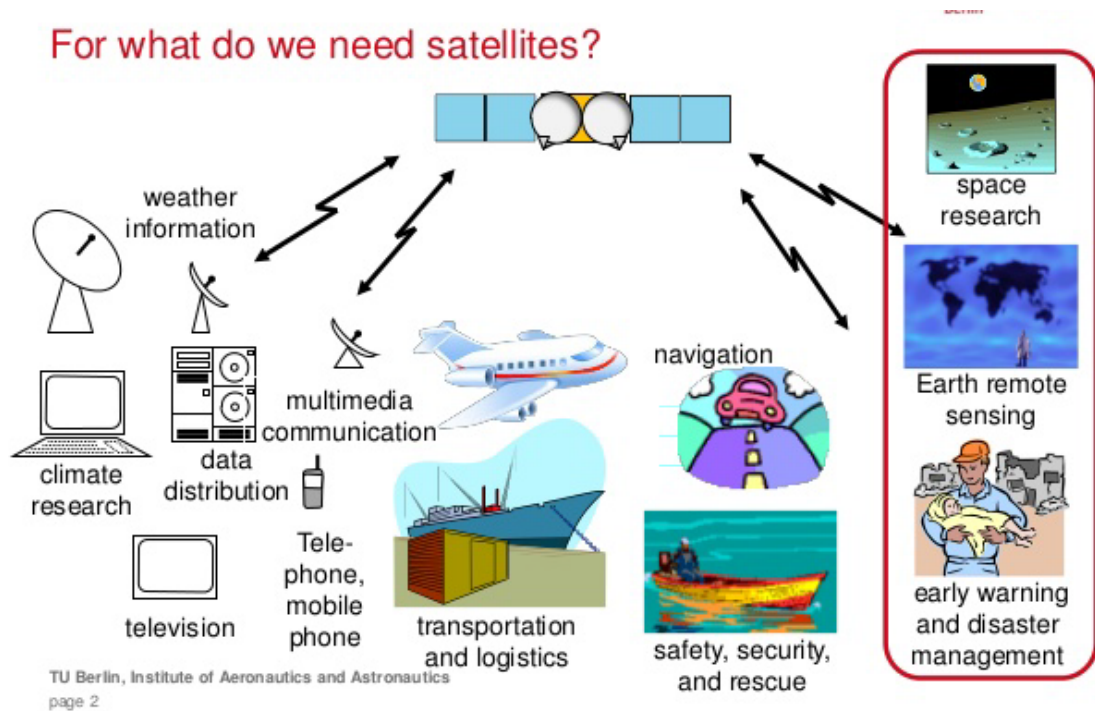


Figure 1. Satellite possible missions.

For now, the total number of operating satellites is around 1,305. Among these are: in Low Earth Orbit (LEO) are 696 satellites, in Elliptical orbit are 41 satellites, in Geostationary Orbit (GEO) are 481 satellites, and in Medium Earth Orbit (MEO) are 87 satellites. The payload breakdown by country is: USA- 549 satellites, Russia- 131 satellites, China- 142 satellites, others- 483 satellites.

For some satellite missions it is necessary to have a payload that can control attitude and satellite orientation. Some on-board propulsion could be used for this control. For now, the most popular method for attitude control is electric propulsion, where the acceleration process is based on the electric field generation

between electrodes. On-board electric propulsions that are commonly used are: Pulsed Plasma Thruster (PPT), Stationary Plasma Thruster (SPT), Radiofrequency Ion Thruster (RIT), and Vacuum Arc Thruster (VAT).

If satellite safety matters are considered, propulsion methods that exclude pipes, valves and tank systems are preferable. The best candidate is a Vacuum Arc Thruster. This propulsion system has a simple design, a great source, absence of valves - and so it is a good candidate for small satellites.

Table 1 shows a comparison between various micro-propulsion schemes developed for satellite missions [2]. Vacuum Arc Thruster, which will be discussed further, is shown in the last column. Thrusters are classified according to the total system mass, specific impulse, efficiency and thrust to total system mass ratio. As we can see, efficiency is lowest for VAT- compared for example with Electrospray thruster method. But specific impulse is higher than Pulsed Plasma Thruster (PPT of Clyde Space), which is the nearest competitor to VAT. Nevertheless, VAT wins by the system mass and mass shot per one pulse/discharge, using passive ignition that avoid pipes, valves and tank in the system as for example for Electrospray (MIT) propulsion. To sum up, Vacuum Arc Thruster method has a simple design, absence of valves with leads to increased system reliability, small weight that is the most important for satellite as CubeSat with a small weight (1 kg) and great source.

Table 1. Comparison of propulsion schemes for microsattellites.

Thruster type	uCAT	PPT (Clyde space)	PPT (Busek Co)	Electrospray (MIT)	VAT (Alameda)	VAT (KIT)
System mass, gr	200	160	550	45	600	35
Propellant	Metal	Teflon	Teflon	Liquid	Metal	CFRP
Isp, s	3000	590	700	3000	1500	1200
Propellant mass, gr	40	10	36	20	40	1.8

efficiency, %	15	4.7	16	71	9.4	2.6
Thrust to mass ratio, uN/gr	0.63	0.03	0.18	0.5	0.22	1.60E-03

Table 1 (continue). Comparison of propulsion schemes for microsattellites.

1.2. Vacuum Arc Thruster.

The vacuum arc thruster was ultimately chosen for study due to its novelty of using Carbon based propellant, low power consumption, variable-thrust capability and low system mass and unless igniter system, when the discharge is occurred by the passive ignition in LEO plasma condition. The vacuum arc thruster consists of anode and cathode electrodes that separated by the insulator between them. The cathode in plasma condition emits electrons and by the potential difference on the cathode surface (consist of a metal and a dielectric) provides discharges. The action of the vacuum arc forms hot microscopic cathode spots on the cathode surface, which emits vaporized cathode material [Schein et al.]. This material becomes ionized within the arc region and expands outward as dense high-speed plasma, achieving velocities as high as 15-20 km/s [3]. The vacuum arc pulses within the VAT are generated by a power circuit comprised of a network of capacitors (Figure 2). Typical thrust values from a VAT are on the order of a few mN per pulse, where pulses are usually 50–500 μ s in length and fired at a rate of 1–50 Hz. Typical impulses (or impulse bits) are in the μ Ns range.

The VAT falls under the category of a microthruster, which is a propulsion system that gives small satellites (typically 1–100 kg mass) the ability to perform orbital maneuvers, drag compensation and station keeping. These capabilities are highly attractive because they allow a satellite to orient itself, perform orbit positioning and extend mission lifetime. A large variety of micro thrusters exist and continue to be developed to address the technical challenges of miniaturizing propulsion systems. Examples include Pulsed Plasma Thrusters (PPT), Stationary plasma thruster, Field Emission Electric Propulsion (FEEP).

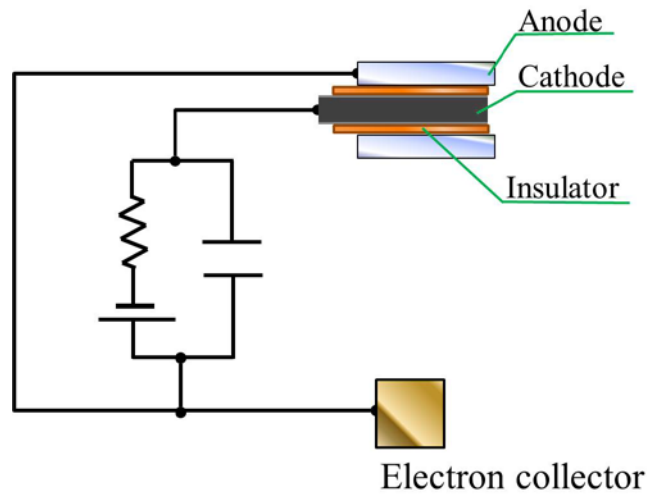


Figure 2. Vacuum Arc Thruster circuit.

One of the Vacuum Arc Thruster was developed in George Washington University and called Micro-Cathode Arc Thruster. This thruster was developed in a frame of PhoneSat program but has not been not launched. The thruster consists of titanium cathode and similar diameter copper anode. The annual ceramic between cathode and anode has the same diameter. Thruster cross section is 5 mm and a mass together with a power processing unit about 200 gramm that is quite big for example for CubeSats. Cathode material eroded and accelerated by the Lorentz force between the cathode and anode electrodes, discharge is occurred and thrust is produced. The advantage of this thruster that thrust could be controlled by the frequency of discharges (for 1-50 Hz it is 1 uN-0.05 mN). During erosion test thruster demonstrated operational lifetime over two months. Micro-Cathode Arc Thruster has impulse bit around 0.11-1.1 uNs (without or with permanent magnet). Duration of one discharge is about 100 usec (Figure 3).

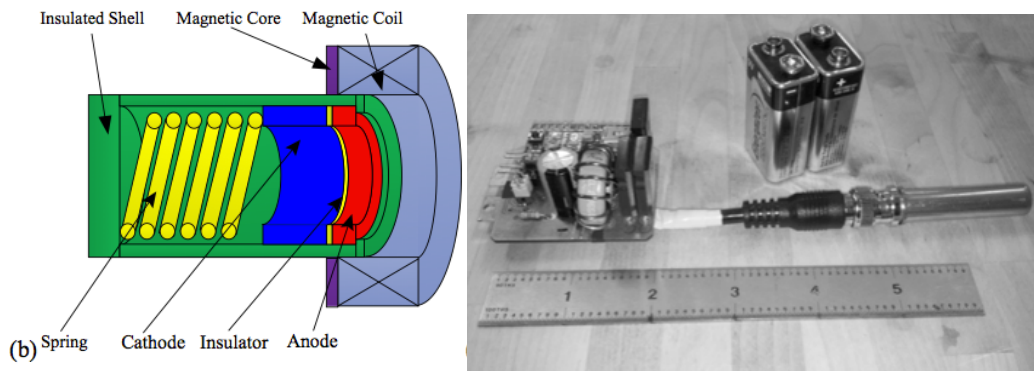


Figure 3. Micro-Cathode Arc Thruster.

Another type of a Vacuum Arc Thruster is Magnetically enhanced Vacuum Arc Thruster (M. Keidar and further development contributed to Alameda Applied Science Corporation). Thruster use metal solid propellant, low voltage operation (~ 100 V) and has 1000 s of specific impulse and 20% of efficiency. Voltage applied from the power processing unit (5-24 V) and converts into an adequate power. Thruster provide ~ 1 uNs of impulse bit and has a total system mass < 300 gram (Figure 4).

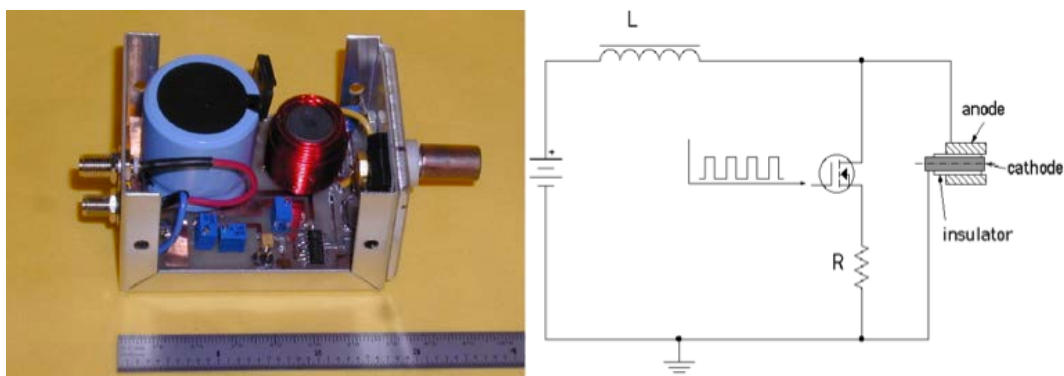


Figure 4. Magnetically enhanced Vacuum Arc Thruster

By Alameda Applied Science Corporation for 2U CubeSat (10 x 10 x 20 cm) propulsion system was developed another Vacuum Arc Thruster [J. Schein] (Figure 5).

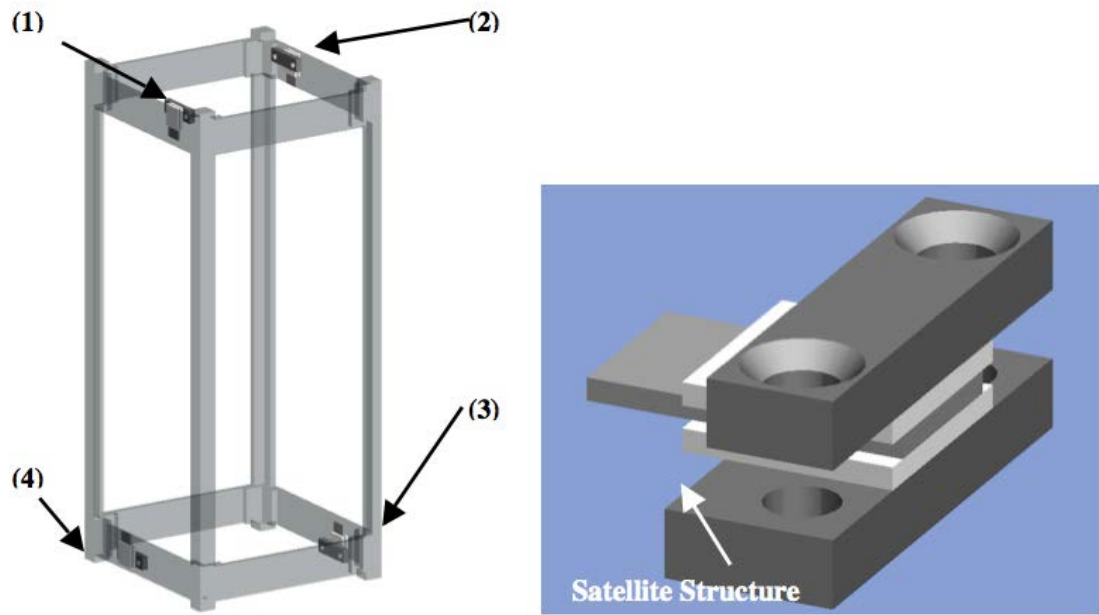


Figure 5. VAT position on-board 2U CubeSat and VAT geometry.

Vacuum arc thruster presented a sandwich structure mounted to the satellite walls. Operation voltage is $\sim 200\text{V}$, discharge period for $<1\text{ }\mu\text{s}$, specific impulse $>1000\text{ sec}$, impulse bit $\sim 0.25\text{ }\mu\text{Ns}$ - $50\text{ }\mu\text{Ns}$ with discharge frequency varying from 1-1000 Hz. Cathode material is Chromium with average velocity of molecules $\sim 17000\text{ m/sec}$. In this project, VAT dry mass of less than 300 gr, together with power processing unit and efficiency about 5%.

The VAT has a huge potential due to the low system mass, low power consumption, great source and simple design. A propulsion system, such as VAT, based on the solid propellant, avoid valves, tank system, piping system and decrease failure modes that associates with that. This potential benefit thruster system has been recognized by several research groups who present developing VAT propulsion system hardware for space flight [4]. Additionally, the VAT is still a relatively new propulsion technology compared to many other commercial systems such as a PPT, which has almost 50 years of development and flight. So, there exists much opportunity to enhance, optimize VAT technology in order to achieve its wider acceptance by the small satellite community as an attractive and viable propulsion solution.

So, this work will present Vacuum Arc Thruster for nanosatellites, developed

at Kyushu Institute of Technology, Laboratory of Spacecraft Environment Interaction Engineering (LaSEINE). Thruster was developed for student satellite project Horyu-IV, as a functional mission demonstration and with improved characteristics can be used as an effective deorbit system for CubeSats. Vacuum Ar Thruster has a head mass of 6 gramm and together with electric circuit total weight is 35 gramm plus additional DCDC converter. This mass characteristic in comparison with competitors has a huge advantage. Operation voltage 300V-800V converted from 5V of DCDC convertor, specific impulse 1300 sec, thrust 4.8 nN and efficiency 2.5%. Discharge occurred in LEO plasma condition without any igniter, that avoid uses of high voltage on-board and increase satellite safety.

1.2.1. Vacuum arc.

The terminology of a vacuum arc is used to describe a current-driven arc discharge that exists between anode and cathode electrodes within a vacuum condition. Vacuum arcs on the cathode material characterized by the electron emission and plasma production [5]. On the cathode surface form small arc spots and they produce plasma emission. These spots are microscopic and they are formed in the area of highly concentrated electric field ($\sim 10^9$ V/m). This high power density can support a sufficient heat, vaporization and cathode material ejection during a very short time like 10-100 ns, when the cathode material could transform from the solid phase into the plasma. Emitted material collides with the electron cloud and forms highly ionized plasma. Plasma generation process on the cathode surface includes some simple area dominated by ionization, diffusion and emission. Ions ejected to the plasma from the cathode surface are expand outward with ions that going back to the cathode and by the bombardment heat of a cathode surface until the vacuum arc will destabilized and initiate a new arc spot in the new close place. Cathode's arcs were found to be the most common arc mode of choice in literature for operating vacuum arc thrusters.

Finally, the electron emission and plasma density would be decreased to some level where the discharge could be stopped. Due to decreasing in electric field and

conductivity of the cathode, the voltage between the cathode and anode electrodes increases. If the discharge is stopped but the plasma condition near the cathode area in combination with increased voltage is enough for ionization, cathode propellant emits electrons from the area that is more suitable for that, such as microprotrusion. This suitable location of microprotrusions could be heated by the ion bombardment energy together with heating of electrons by the Joule heat. Increasing temperature gives a escape situation when additional electrons emit and increase ionization, that provide additional ion bombardment, temperature increasing and electron emission. The thermal runaway near the microprotrusion in a very short period of nanoseconds will destroy it and a new cathode spot will be formed in this phase [6].

1.2.2. Cathode material and geometry.

Due to the high density and good electrical and thermal conductivities, metals are well suited as a propellant for vacuum arc thruster with additional high melting and boiling points. Therefore, for some previous research were used metallic elements as a propellant (Aluminum, Molybdenum, Titanium, Tungsten etc.).

Each material has own and exclusive combination of electrical and thermal properties, that change depending on the state of the cathode surface, presence of microparticles and pollution with vacuum arc [Polk et. Al. 2008]. So, it is possible that some cathode materials (clear metals or some compounds or metalized plastic) has not been tested yet and can show some better operation compare to current results.

Thrust can be reduced by the impossibility of acceleration of the cathode material to high, as ions, velocities. It is depend to the cathode material properties, such as thermal conductivity and low melting that provide greater erosion. This problem could be solved by decreasing discharge pulse period to ~ 10 usec.

Regarding to the previous works (e.g. Kandah and Meunier) and some industrial tests, some materials based on carbon or graphite are a good propellant for vacuum arc thrusters. Carbon for example has high temperature resistance and

it sublimates rather than melting and its resistance decreases with temperature increasing. Compared to the carbon metallic counterparts, they can show some better erosion rate results and high ion. This work will describe a test for some different propellants, including carbon based one.

The most common used cathode electrode geometry is a rod shape. This provides simple illustration and cathode manufacturing process. Experimental measurements by Miernik & Walkowicz (2000) also showed that the profile of the cathode surface can have a significant effect on the spatial distribution of emitted macro particles from the vacuum arc [7]. For our test was used cathode with rod geometry and was not included some comparison results for cathodes with different geometries.

1.3. Development effective satellite deorbit system based on Vacuum Arc Thruster.

Because of the large number of satellites in orbits, there is a question of how much space debris can be accepted (Figure 6) [8].

For today, more than 20,000 objects are traced and saved to the catalogue and around 66% of this debris concentrated on the LEO orbit. To keep spacecrafts on the orbit, use few “universal orbits” such as sun-synchronous orbit, polar orbit. Sun-synchronous orbit keeps a constant angle between the orbital plane and the Sun. Polar orbit crosses the Earth polar regions. Debris population on the LEO orbit is much higher and frequent approaches up to 15 times per day can occur between objects.

Collision between space debris can occur any time and from any direction due to the Earth’s gravitational field changing and disruption. The Kessler syndrome in this case can apply to the LEO orbits, and collision can be on the speed up to twice to the orbital speed- 16 km/s, or, as it happened in 2009, on a speed 11.7 km/s was head-on collision, when particles can cross other orbits and create a cascade effect. The LEO orbit could be impossible for operation in reason of some large enough collision, like between space station and some satellite for

example [9].

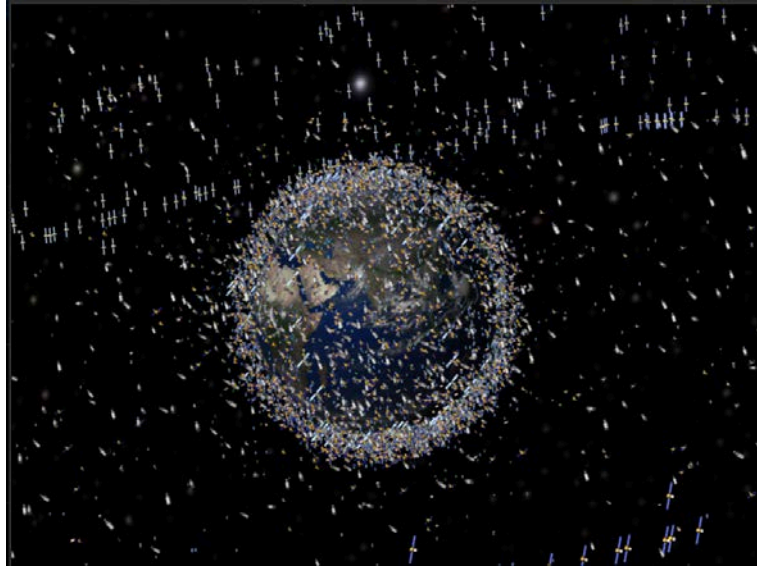


Figure 6. Model of space debris around the Earth.

At 400 km (250 mi) and below where the air drag helps clear zones of fragments mostly are manned missions. In 90th, one of the factors that reduced debris density was increasing drag on the critical altitudes due to space weather and the atmospheric expansion. Also was decreased number of launches compare to 70th and 80th when was done most of the launches by USSR.

Total number of debris in LEO according to size is: 0.1-1 cm are 20 million objects, 1-10 cm are 400,000 objects and > 10 cm are 15,000 objects. Operational payloads number that orbiting around the Earth are less than 10%. Other objects are non-operational payloads (26 %), rocket bodies (18 %), mission related objects (10 %), fragments (40 %) [10].

Purposed solution for debris removal is: solar sail, electrodynamic tether, drag augmentation, electric propulsion etc.

As example M. Keidar purposed to provide CubeSat deorbiting by arcing discharges on the solar cells surface and use a satellite structure as a propellant. In this case the satellite substrate material could be used as the anode in such kind of “vacuum arc thruster” and silicon material of solar cells as a cathode. It means that satellite panel will have two arcing places- vacuum arcs- that occurred on the

boundary between satellite substrates- anodes and solar cell silicon material- cathode. These discharges should occur in pairs to escape a rotation moment (Figure 7). To control pairs discharges is very difficult in case of passive ignition in LEO plasma condition, so accuracy of this method for now is low.

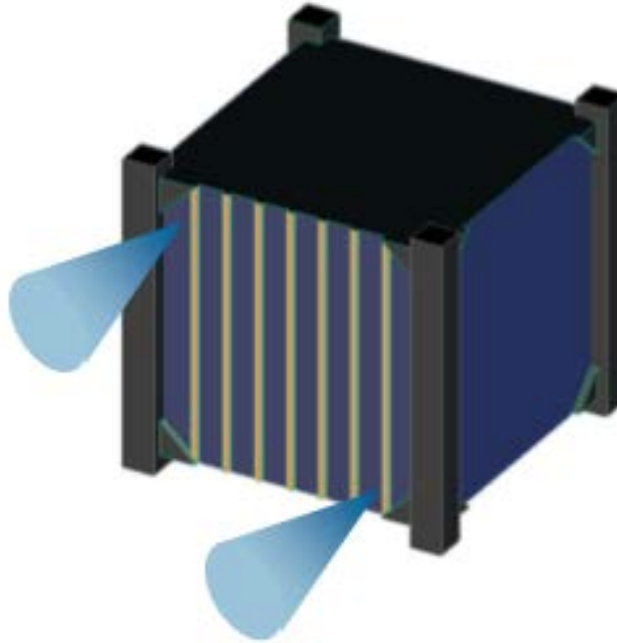


Figure 7. Concept for self-consuming satellite (solar cells are used as the cathode in a vacuum arc propulsion system).

This work will describe CubeSat deorbit system based on Vacuum Arc Thruster (VAT) [11,12] as a propulsion system.

The requirements for the satellite with deorbit system on-board:

- picosat 10cm x 10cm x 10cm;
- mass below 1 kg;
- power consumption below 1 W.

Deorbit system requirements:

- Power consumption less than 1 W;
- Small size;
- Small weight;
- Simple design;

- Deorbit time less than 25 years;
- Deorbit from the 800 km altitude to the 400 km.

The main idea is an installation to the satellite ram side a vacuum arc thruster that will produce a thrust, opposite direction to the movement of the satellite. VAT with passive ignition required a specific plasma concentration to heat the propellant and emit electrons from the cathode. This work confirms a possibility of the discharge in space plasma by the thruster testing in the same artificial vacuum condition provided by electron cyclotron plasma source (ECR) and present deorbit results for CubeSat with some prediction about the improvement of this data.

1.4. Novelty.

The novelty of this work is a Vacuum Arc Thruster that doesn't use any igniter to provide a discharge on the working surface. System, that does not use igniter is more safe to the satellite because does not use high voltage to support ignition. Discharge is occurred by passive ignition, in LEO plasma with some required number of ions ($\sim 10^{12} \text{ m}^{-3}$), that heat the propellant- CFRP-plastic, that already has a positive charge, and it is provide electron emission, electric field concentration between insulator and anode becomes stronger, and the electrons accelerate furthermore. Sufficiently accelerated electrons collide with the ambient molecules and ionize them. Finally, the cathode and anode will be electrically connected, and vacuum arc discharge occurs.

Propellant/cathode electrode such as Carbon Fiber Reinforced Plastic can expand thruster lifetime, because of insulator coating on the main propellant/cathode surface to provide a positive charge and electron emission. Such kind of insulators have their own lifetime, that minimize total thruster lifetime.

One more additional part of this work and some kind of novelty is a development the deorbit system for nanosatellites based on Vacuum Arc Thruster. The purpose is to provide CubeSats deorbiting from the LEO orbit in time less than

25 years (ISO 24113). The deorbit system presented as a one thruster- VAT, on-board 1U CubeSat, with mass- 35 gramm and applied voltage at 800 V through DCDC converter. Presented modeling and results for altitude 800km with deorbiting by VAT to 400 km (continue by the atmospheric drag).

1.5. Objectives.

This work aims to study and develop an electric propulsion thruster for potential use on board a conceptual nanosatellite (1 kg, 10 cm cubic) within an average power limit of 1 W to perform satellite deorbit mission from LEO altitudes (800 km to 400 km in time less than 25 years). A vacuum arc thruster, powered by a capacitive discharge power circuit, was designed, built and tested at the Laboratory of Spacecraft environment and interaction engineering in Kyushu Institute of Technology. Model of the vacuum arc thruster was developed to predict and characterise thruster behaviour and performance. Thrust measurements were performed. Presented results for efficiency improving by attaching permanent magnet to the thruster. Was presented results for efficiency improvement by using a new thruster propellant, manufactured in the laboratory and based on the Carbon Fiber Reinforced Plastic (CFRP). It is the intention of this work to develop a theory of vacuum arc thruster performance and aspects of vacuum arc thruster design.

There are many features of vacuum arc thruster design and operation that need to be studied and expanded upon. This study will investigate the following areas with the over- all goal of improving the performance of vacuum arc thrusters:

1. Development of Vacuum Arc Thruster;
2. Development deorbit system for nanosatellites based on Vacuum Arc Thruster.

2. Experimental apparatus and test setup.

This chapter provides descriptions of the development and performance of test facilities, thruster diagnostic tools and equipment used in this work. Section provides some background on the tool, its function, design specifications and an assessment of its performance and ability to accomplish this work's study objectives. Major test equipment included the Impulse bit measurement system, Quadrupole mass spectrometer (QMS), ECR plasma source, and erosion rate was measured by weight machine.

All experimental testing was performed at the Laboratory of Spacecraft Environment Interaction Engineering (LaSEINE) in Kyushu Institute of Technology, Japan.

2.1. LEO chamber.

Experimentation with LEO plasma simulation was performed in a stainless steel ring vacuum chamber with internal dimensions 1000 mm diameter \times 1200 mm length (Figure 8). This chamber includes a rotary pump, two turbo pumps and also ECR plasma source (Figure 9). Highest vacuum level that could be performed by this pumps is $1 \cdot 10^{-4}$ Pa, and ECR source produce a plasma with next parameters: density $1 \cdot 10^{12} \text{ m}^{-3}$ and electron temperature around 1 eV. Vacuum level was measured by two pressure reading sources: low-vacuum Edwards PK-10 Pirani gauge (atm– 10^{-2} mbar abs.) and a high-vacuum Leybold-Heraeus PM41 Penning Gauge (10^{-2} – 10^{-9} Torr). ECR source use a Xenon gas as a source of plasma.

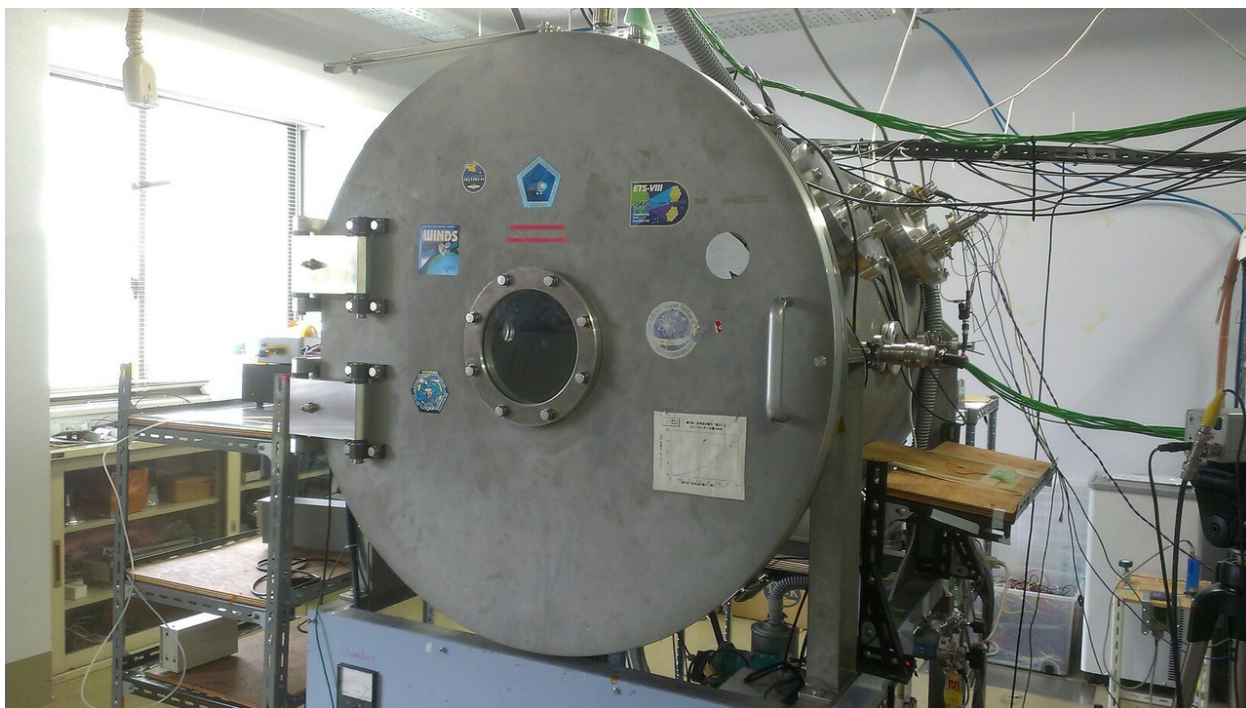


Figure 8. LEO vacuum chamber.

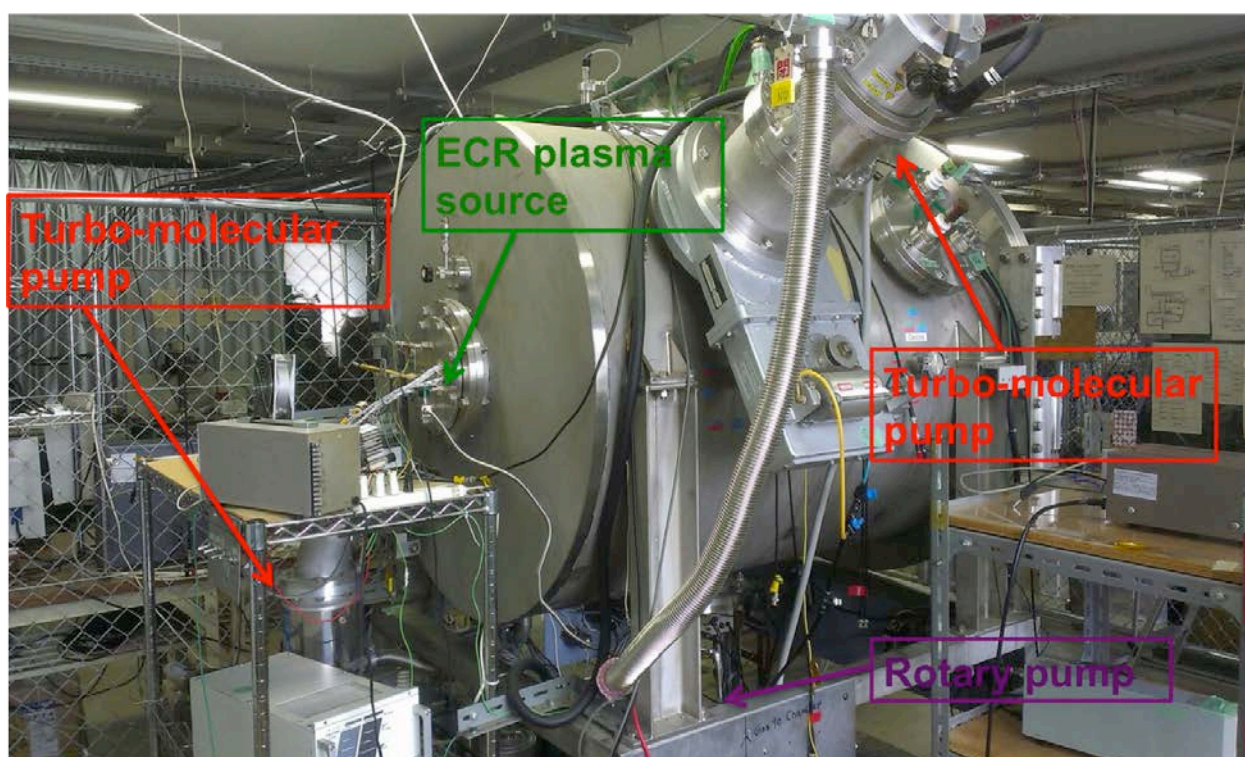


Figure 9. LEO's chamber apparatus.

On the Figure 10 presented a power source for the plasma ignition. Ignited voltage is $\sim 55\text{-}58$ Volts and a current ~ 0.001 A.

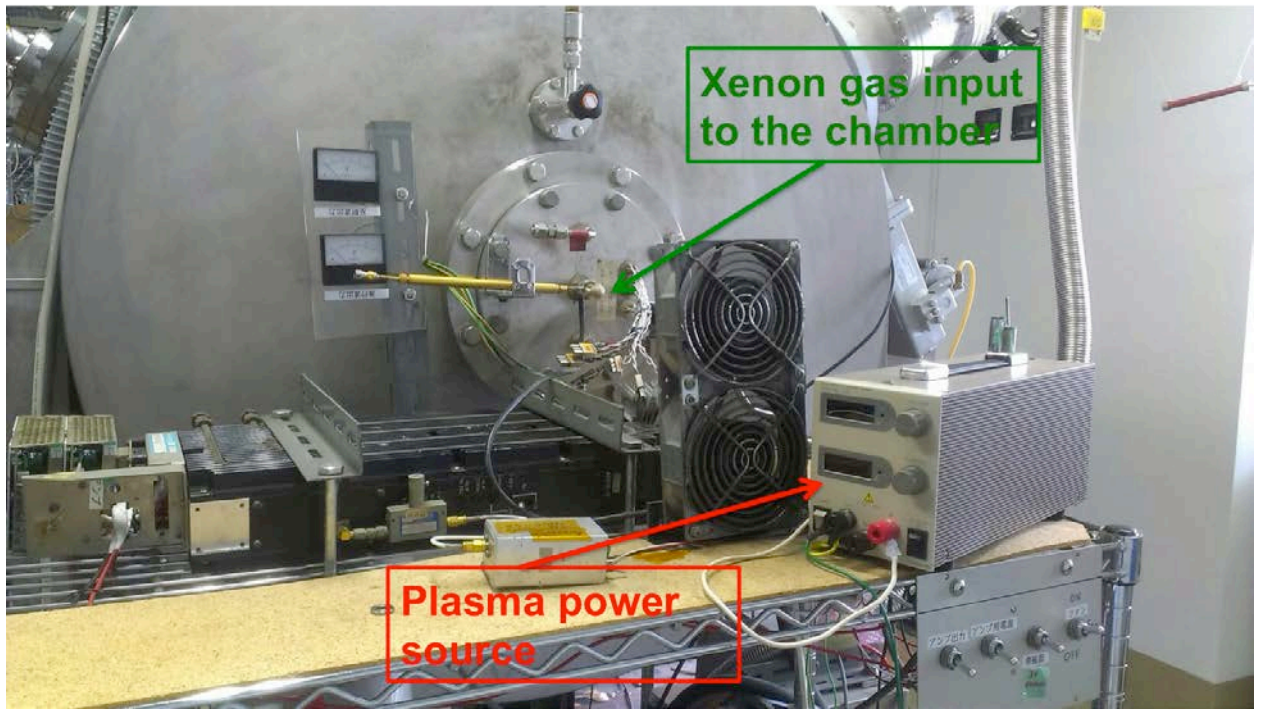


Figure 10. ECR plasma power source.

Inside the LEO chamber is installed a Langmuir probe that can measure electron density, electron temperature and plasma potential that allow the determination of the physical plasma properties. Langmuir probe consist of one or more electrodes, inserting into the plasma with electric potential between that could be constant or varying.

2.2. Quadrupole Mass Spectrometer.

To evaluate the performance of the vacuum arc thruster using a CFRP propellant, the exhaust velocity, v_e , of the metal vapor was measured in the vacuum chamber. The experimental configuration is shown in Figure 10. A Quadrupole Mass Spectrometer (QMS) (Figure 11) was used to detect the metal vapor ejected by CFRP (mass to charge ratio, m/z : 12; with m : mass number, and z : charge amount). QMS (model number: RGA200) made by SRS was used in this experiment. QMS mainly consists of an ionizer, quadrupole rods, a Faraday cup (to detect ion), and a Secondary Electron Multiplier (SEM) [13]. During arcing, CFRP vapor is ionized and flies through the quadrupole rods, which generate an electric field. Ions, except for ones with a specific mass-to-charge ratio of 12, collide with

the quadrupole rods. The ions with a specific mass-to-charge ratio of 12 are detected by the Faraday cup. The output from the Faraday cup is then amplified by the SEM, which measures signal. However, the signal intensity does not relate to the gas mass, and the vertical axis unit therefore uses arbitrary unit (a.u.) to show the relative relationship. In this experiment, the m/z ratio was set to 12 to detect carbon molecules.

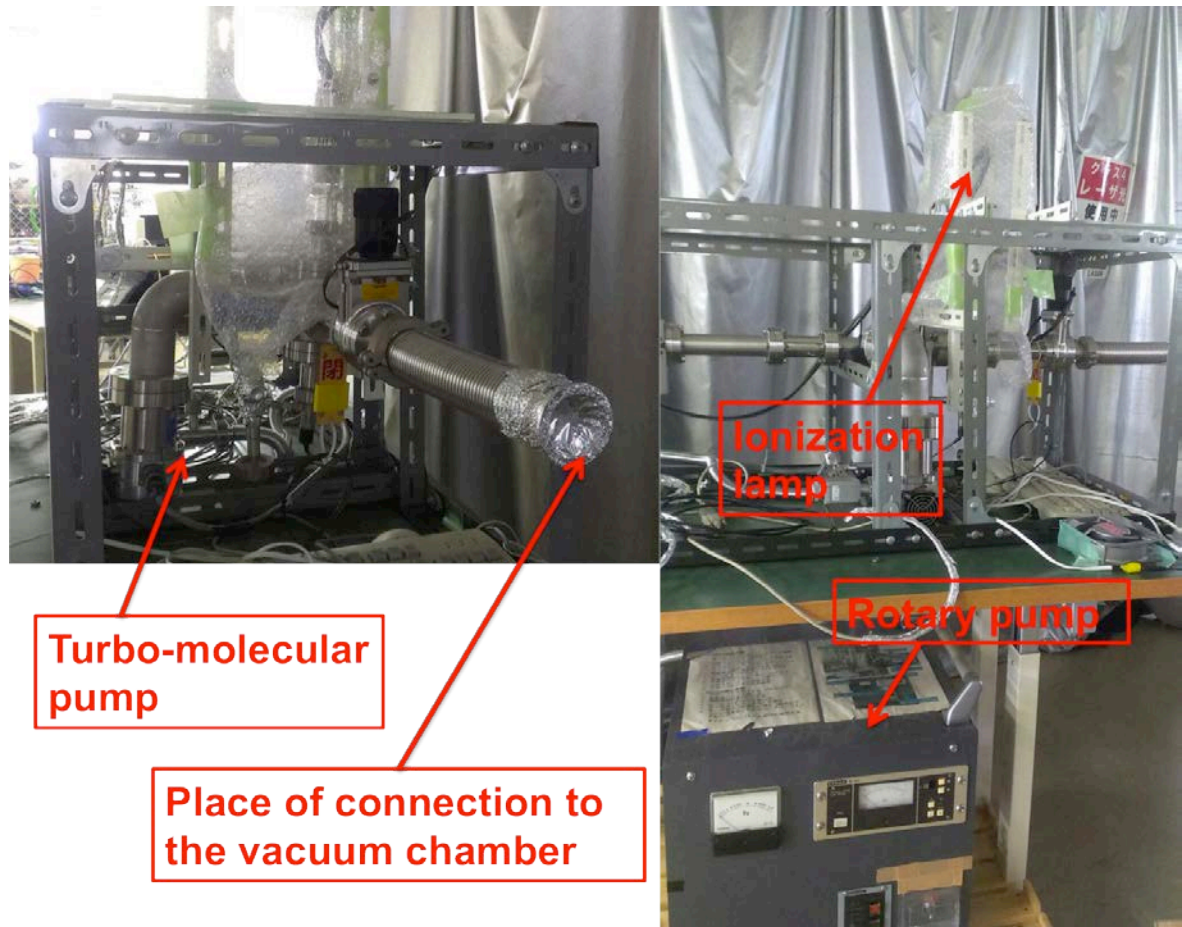


Figure 11. Quadrupole Mass Spectrometer.

2.3. General purpose chamber.

For some experiments, when number of measurements is high, was used a General Purpose Chamber [Figure 12], that doesn't has any plasma simulation sources and discharge on the thruster initiated here by an igniter system. An experimental apparatus consist of vacuum chamber (diameter 450 mm x 500 mm height), rotary pump and diffusion pump. Highest vacuum level that could be

performed by this pumps is $4 \cdot 10^{-4}$ Pa. Vacuum level was measured by two pressure reading sources: low-vacuum Edwards PK-10 Pirani gauge (atm– 10^{-2} mbar abs.) and a high-vacuum Leybold-Heraeus PM41 Penning Gauge (10^{-2} – 10^{-9} Torr).

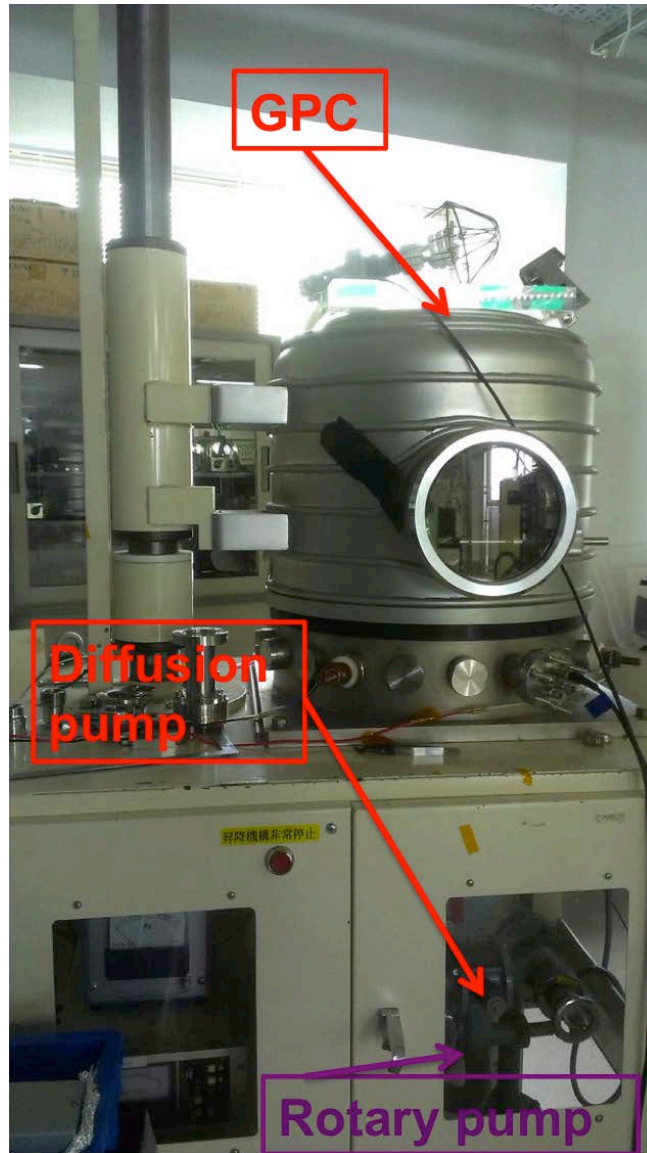


Figure 12. General Purpose Chamber (GPC).

2.3.1. Igniter system.

An igniter was used in order to generate a single discharge on the surface of VAT, when the test was performed without space plasma conditions (in the LEO chamber produced by ECR plasma source). The thruster circuit and igniter circuit were electrically isolated from each other. Therefore the igniter had no influence

on the vacuum arc discharge process. The igniter used was a compact type igniter CKB-108A, with an input voltage of 3.0 VDC, electric current consumption of 100 mA, and output voltage of 15 kV (Figure 13).

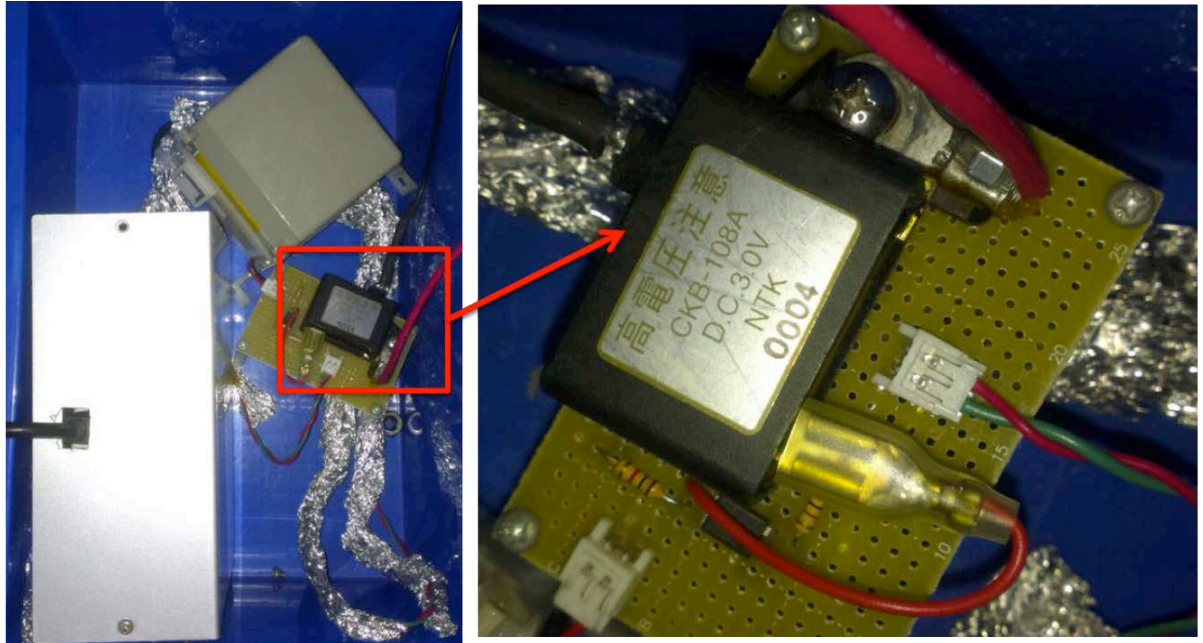


Figure 13. Igniter system.

2.4. Thruster's electric circuit.

Difference between tests setup in the LEO chamber and GPC chamber is only use an igniter in the GPC chamber, because of high number of measurements that was done in this tests and if we will perform it in the LEO chamber with simulated plasma condition, and passive ignition, we have to wait for the each discharge and total test time will be huge. In LEO chamber was measures arc rate/frequency data for VAT with different configurations and different propellants, average velocity for the carbon molecules as a main component for the VAT propellant CFRP and was performed ed-to-end satellite test in collaboration with High Voltage Sollar Array as a main direct drive power source for the thruster. General purpose chamber was used for impulse bit measurements with different thruster configurations (propellants, magnetic system, nozzle), long life test experiment

(10,000 discharges). This implies a large number of measurements therefore was used an igniter system.

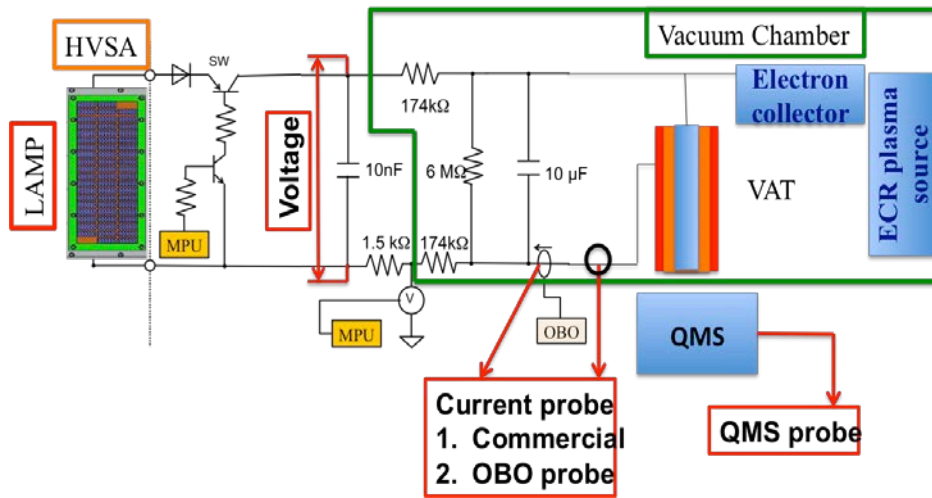


Figure 14. Electric circuit for the test performed in the LEO chamber.

On the Figure 14, we can see two different current probes on the thruster cathode line. One of them was commercial and a second one- hand-made current probe developed for the Horyu-4 satellite and using on-board for the VAT's discharge current measurements (Figure 15). Commercial current probe was used for measurements correlation and checking. QMS spectrometer was installed in the opposite to the thruster surface direction, in one of the chamber window, in such a way that the cathode molecule (Carbon) during the discharge flew straight into the barrel of the QMS spectrometer. As a power source for the thruster was used a HVSA or a commercial power source (Figure 16). Points for voltage measurements was mentioned only for the confirmation of the power supply level from HVSA as a power source.

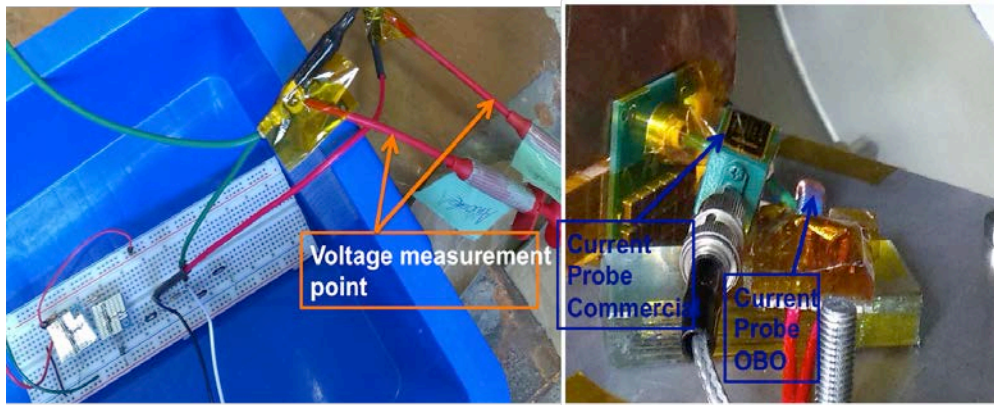


Figure 15. Current and voltage probe connections.



Figure 16. Power source.

For arc rate measurements was used a quick lock camera system that includes a personal computer that receive a signal from the oscilloscope (Figure 17), across from the Delay pulse generator (DPG) (Figure 18), and send a signal to the camera (Figure 19) to detect a moment of discharge, make a photo and count numbers.

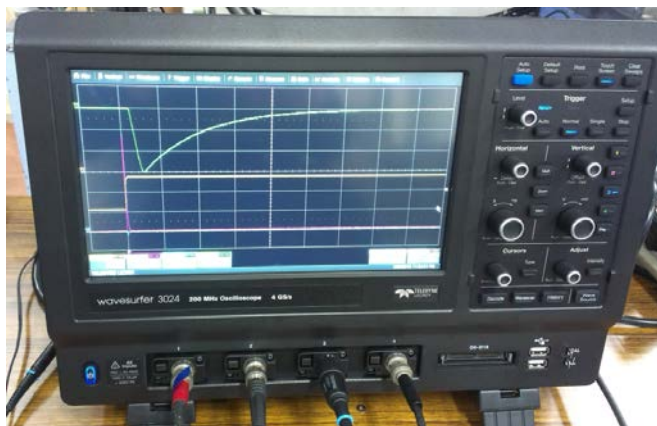


Figure 17. Oscilloscope "Wavesurfer 3024".



Figure 18. Delay pulse generator



Figure 19. Quick look camera.

For the test in a General-purpose chamber was used an electrical circuit presented on the Figure 20.

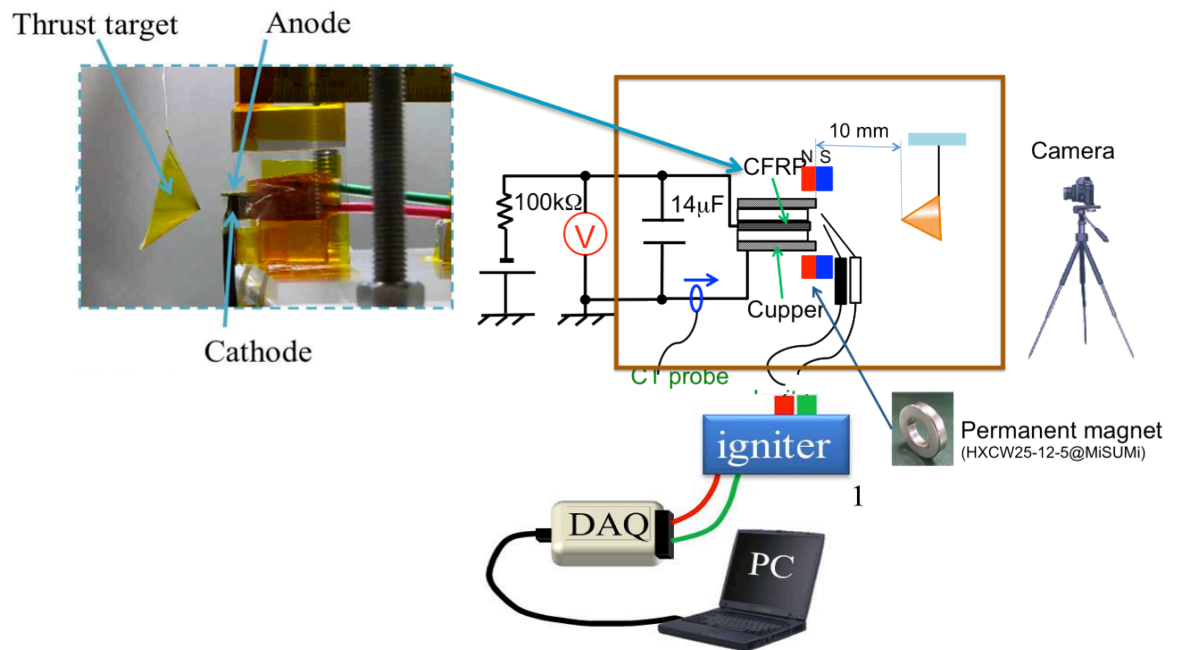


Figure 20. Electric circuit for the test performed in the GPC.

For the long life test was used a quick look system to count number of discharges on the VAT and 8-channel oscilloscope, that could save data faster than “Wavesurfer 3024”.

3. Vacuum Arc Thruster.

This chapter provides a brief outline of Vacuum Arc Thruster (VAT): the design, the work mechanism, general performance. It describes the basic principle of selection of the working body or thruster cathode. These characteristics will be presented: impulse bit, discharge current, average velocities, arc rate. Long-life test results are also included. The thrust measurements were done in the nano-Newton range.

3.1. An Introduction to Vacuum Arc Thruster.

The idea of using electric power to accelerate the working material in rocket engines was made by K. E. Tsiolkovsky in 1911. Mr. Oberg has shown that despite the low values of thrust, we obtain in the electro devices through long duration of their work, the spacecraft can be accelerated up to a significant speed. The world's first plasma rocket engine (developed by academician V. P. Glushko) was designed as a camera with a nozzle, in which the working substance is heated to a high temperature and accelerated pulse discharge capacitor bank with energy 3200 J.

Practical work on electro-motors started in 1970. The Vacuum Arc Thruster was studied from the 1960's, but VAT methods received significant attention after the publication of works by the Alameda Applied Science Corporation, California, during the 1990's. And VAT was patented by Schein in 2004, as a source device using a low mass, compact energy storage circuit, with electrodes acting as the propellant themselves. Vacuum Arc Thruster is the closest competitor to the Pulsed Plasma Thruster (PPT) in terms of electric propulsion [14, 15].

3.2. VAT theory and Performance.

The propulsion system for nano-satellites must be simple because the satellite does not have enough space to mount complex equipment. Vacuum arc thrusters

can be made simple and lightweight. As a propellant, vacuum arc thrusters use a solid metal rod that does not require additional equipment, such as piping, valve and fuel tank, as does a liquid or gas type propellant. A vacuum arc thruster's electrodes act as the propellant themselves, and the number of parts required for propulsion is therefore greatly reduced.

Upon thrust of the vacuum arc, metal vapor and plasma are ejected. When a vacuum arc is generated between the electrodes, vapor is exhausted from the cathode. Therefore, the performance of the vacuum arc thruster depends on the exhaust velocity, which results from the power input, cathode erosion (cathode material) that extends the operational lifetime, and others [16,17,18].

The novelty of this research is using Carbon Fiber Reinforced Plastic (CFRP) as propellant material. CFRP is a material often used as the back face material of a solar paddle. Past studies show that CFRP generates discharge easily and the discharge threshold voltage is less than 100 V in plasma inverted gradient. The vacuum arc thruster of this research uses this discharge for ignition of the vacuum arc.

Moreover the vacuum arc thruster presented in this paper proposes to use solar cells as the direct drive, so that the booster circuit is not necessary in this system configuration. The direct drive is carried out by high voltage solar array (HVSA) that can generate a voltage beyond the threshold voltage [19]. The high voltage solar array can supply stable 350 V and was demonstrated in orbit by a micro-satellite "HORYU-II" developed at Kyushu Institute of Technology (Kyutech) in 2012 [20]. This paper also describes the performance measurement results of the vacuum arc thruster using CFRP propellant.

Figure 21 shows the vacuum arc thruster developed by Kyutech. The main components for this vacuum arc thruster are: electron supply source (electron collector), capacitor, voltage source and protective resistor. The voltage source must supply a voltage higher than the electric discharge threshold value. Therefore, in this research the voltages used were from 300V up to 800V. The protective

resistor value must be larger than the plasma resistance, therefore a 100 k Ω protective resistor was used.

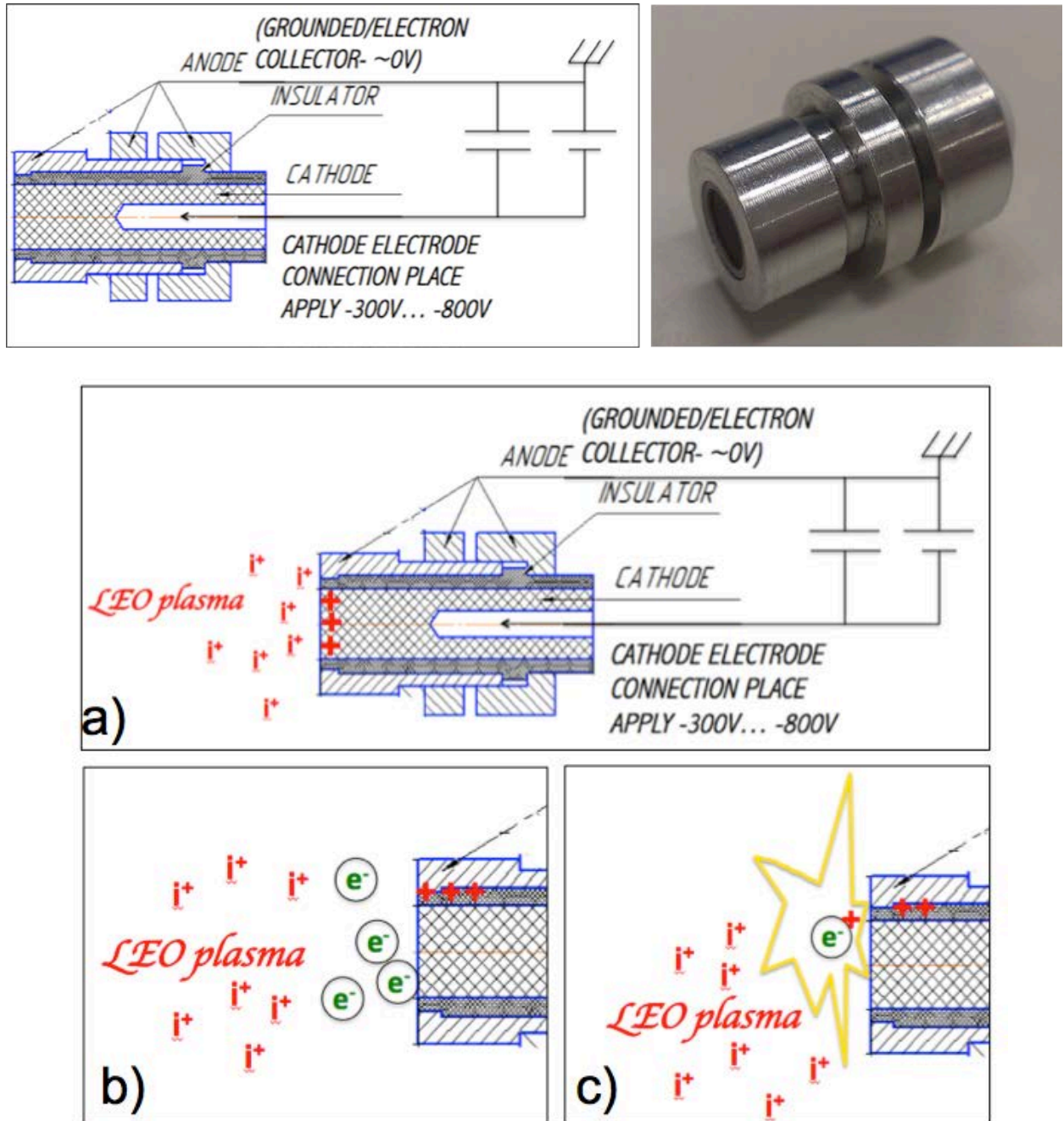


Figure 21. Kyutech's Vacuum Arc Thruster

Following the description of this thruster operation, the ion plasma environment, based on the Xe gas, (with a high density plasma, 10^{12}m^{-3}) (LEO conditions), charges an insulator and/or dielectric (Figure 21 a.). Electric field concentration is generated at the boundary of the cathode and insulator (HVSA supply -350 V to the cathode) and from the cathode accelerated electrons are emitted (Figure 21 b.).

These move to the insulator to neutralize the potential difference. Charging of insulator becomes larger because of the collisions between accelerated electrons and as a result emitting secondary electrons. Electric field concentration becomes stronger, and the electrons accelerate furthermore. Sufficiently accelerated electrons collide with the ambient molecules and ionize the molecules. Finally, the cathode and anode will be electrically connected, and vacuum arc discharge occurs (Figure 21 c.). The vacuum arc between the anode and cathode is formed by the charges stored in the capacitor ($10\mu\text{F}$), and upon vacuum arc generation, metal vapor is ejected from the cathode's discharging point. The reaction of this ejected metal vapor results in the generation of thrust that propels the satellite to move [21].

3.3. Design of Vacuum Arc Thruster.

On the Figure 22 and Figure 23 are shown a prototype design of the Vacuum Arc Thruster. Here, thruster head mounted to the electric circuit (main discharge capacitor, that storage energy for the discharge). The outer case is cylindrical and made from aluminum (Al 7075). The cathode electrode works as a thruster propellant and made from the Carbon Fiber Reinforced Plastic (CFRP). It has the form of a cylinder. To ensure isolation between the propellant (CFRP, cathode) and the aluminum case (Anode), boron nitride was used.

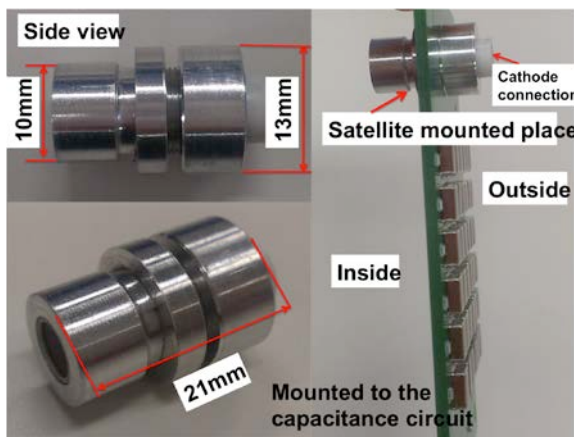


Figure 22. Vacuum arc thruster head head

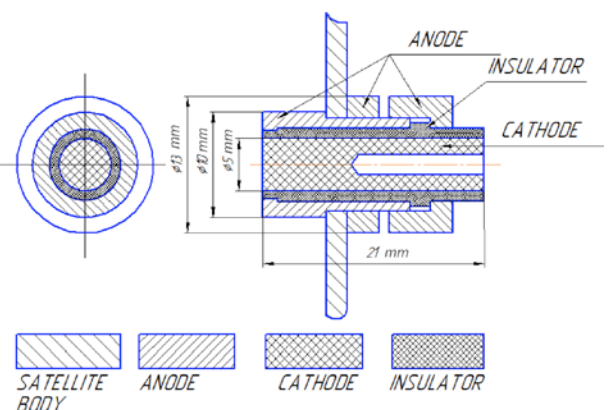


Figure 23. Schematic of thruster

Anode, Figure 24, consists of 3 parts. Between two of them fixing electric circuit with conductive layer inside, to connect anode electrode to the electron collector. The cathode connection is made by using AWG22 cable and conductive glue “Araldite”. The position of connection shown on the Figure 22 (a hole with 10 mm depth). Cathode-cable connection place isolated by RTV glue (Figure 25).

Total weight of the thruster body is 6 grams, including cathode or propellant with weight – 1.8 gram and side $\phi 5$ mm x 19 mm (length). VAT head together with electric circuit have a weight of 35 grams. The thruster head size is 13 mm x 21 mm and circuit size is 40 mm x 85 mm. The circuit includes the main discharge capacitor that has 10 μ F capacity and additional resistors in total 6.3 M Ω .

The cathode electrode connects to the power source (with DC/DC converter or direct drive from High Voltage Sollar Array (HVSA)~ 330 V). The anode connects to the electrone collectore or ground (ground test). For DCDC was used 5AV800 convertor from 5 V input and 800 V output and maximum aoutput power- 1.25 W [22].



Figure 24. VAT's assembling

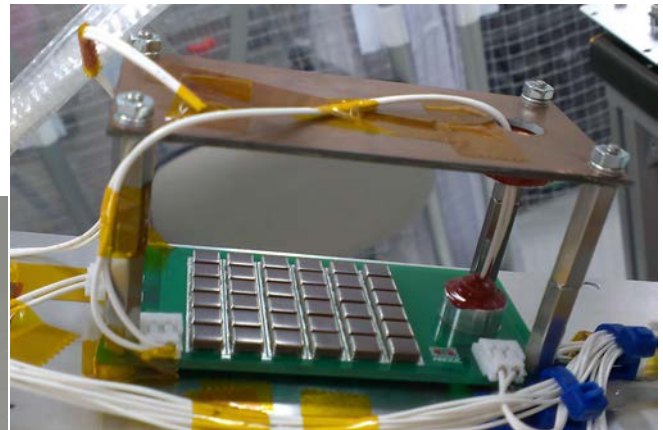


Figure 25. VAT mounting to the satellite wall.

The original circuit design is shown in Figure 26, where is a green line-charging line, a red line-discharge line. On the figure, the abbreviation GND- is an

electron collector with the potential of plasma, in space condition, and ground- 0V, on the ground test. Power source applied voltage up to 800V.

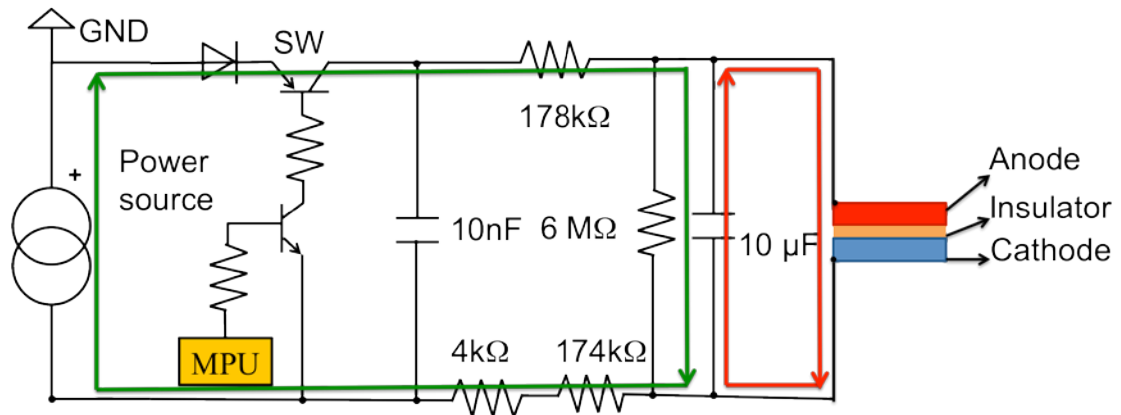


Figure 26. VAT's electric circuit (green-charging line, red- discharge line).

3.4. Vacuum Arc Thruster's propellants.

Vacuum Arc Thruster, regarding to his theory, does not have an igniter, and the ignition process is possible, only in plasma condition similar to LEO plasma, where the concentration of ions is enough to heat the propellant and initiate electron emission from the surface. The effectiveness of thruster usually shows thrust parameters. Required measurement of the two parameters that define thrust, namely, the propellant mass flow rate and propellant velocity or average velocity of particles, emitted and accelerated from the propellant surface.

Important part of the VAT research is the cathode erosion rate that can decrease thruster lifetime. Methods of measuring the cathode erosion rate include the weight loss method and measuring changes in cathode geometry. In addition, gross melting propellants make the thruster inefficient, since less mass is being ionized to produce useful thrust.

Were tested some materials for the Vacuum Arc Thruster propellant. For each propellant material were compared vapor velocity results. Tested materials were aluminum, tungsten, and Carbon Fiber Reinforced Plastic (CFRP) (Figure 27, 28, 29).



A Quadrupole Mass Spectrometer (QMS) was used to detect the metal vapor ejected by CFRP (Carbon Fiber Reinforced Plastic), Tungsten, and Aluminum. A QMS (model number: RGA200) made by SRS was used in this experiment [23].

QMS mainly consists of an ionizer, quadrupole rods, a faraday cup (to detect ion), and a Secondary Electron Multiplier (SEM). During arcing, propellant vapor is ionized and flies through the quadrupole rods, which generates an electric field. Every ion, except for the ones with a specific mass-to-charge ratio (for CFRP it is 12), collides with the quadrupole rods. The ions are detected by the Faraday cup. The output from the Faraday cup is then amplified by the SEM, which signal is measured. However, the signal intensity does not relate to the gas mass, and the vertical axis unit therefore uses arbitrary units (a.u.) to show the relative relationship.

The time-of-flight between the thruster and the QMS was measured. The exhaust velocity V_e was calculated using Eq. (1).

$$V_e = \frac{d}{t} \quad \text{Eq. 1}$$

Where, d [m] is the distance between the thruster and the QMS, and t [s] is the time-of-flight.

In this experiment, the m/z ratio was set to 12 to detect carbon. The QMS pressure was 10^{-4} Pa. The chamber pressure was 10^{-3} Pa. The capacitance was 10 μF to change the arc discharge scale, and the supply voltage was 300V.

Measurements were carried out in a general vacuum chamber with vacuum in 10^{-3} Pa. Tube of QMS which has an aluminum plate with a hole in a one side was

connected to the chamber (Figure 30). Accelerated Carbon molecules from the VAT cathode came to the hole in the Aluminum plate and were registered by QMS.

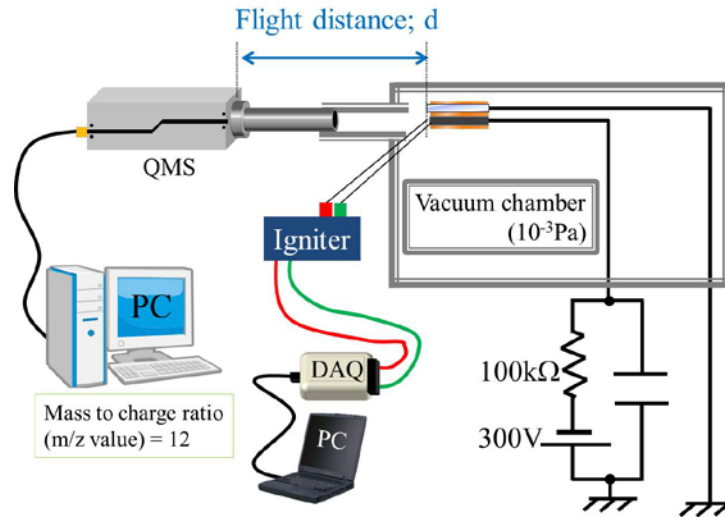


Figure 30. Scheme of experiments to measure average velocity

In this experiment, an igniter was used in order to generate a single discharge. The thruster circuit and igniter circuit were electrically isolated from each other. Therefore the igniter had no influence on the vacuum arc discharge process. The igniter used was a compact type igniter CKB-108A, with an input voltage of 3.0 VDC, electric current consumption of 100 mA, and output voltage of 15 kV.

Figure 31 shows the QMS output signal. The vertical axis shows the detected amount of carbon by QMS in the arbitrary unit (a.u.). This figure shows the carbon distribution corresponding to the time at which the discharge occurs. The measurement was made at the moment the oscilloscope detects discharge current maximum according to the trigger level. This means that at this same moment the average velocity of carbon is also at maximum.

The exhaust velocity distribution calculated Eq. 1 is shown in Figure 32, where, $P(v)$ represents the velocity distribution function. Weighted velocity distribution was calculated using Eq. 2 in order to calculate an average exhaust velocity. $Q(v)$ represents the weighted velocity distribution function, Figure 33. The average exhaust velocity was calculated using Eq. 3, and the specific impulse

was calculated using Eq. 4. However, it should be noted that the average velocity represents the average of the velocity distribution of the injected carbon atoms for one shot.

In this experiment, data of each capacitance value were acquired and the average velocity was calculated. Figure 34 shows the experimental results. The vertical axis is the average exhaust velocity and the horizontal axis is the energy of the vacuum arc discharge. Results present for three propellants.

$$Q(v) = v_e \times P(v) \quad \text{Eq. 2}$$

$$\bar{v}_e = \frac{\int Q(v) dv}{\int P(v) dv} = \frac{\int v_e \times P(v) dv}{\int P(v) dv} \quad \text{Eq. 3}$$

$$I_{SP} = \frac{\bar{v}_e}{g} \quad \text{Eq. 4}$$

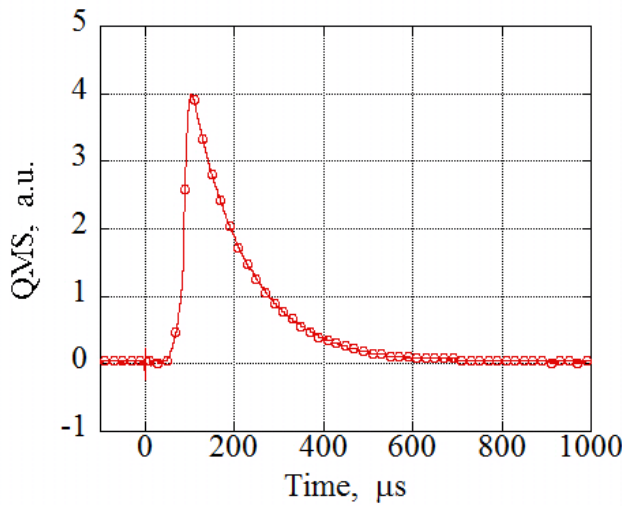


Figure 31. QMS output signal

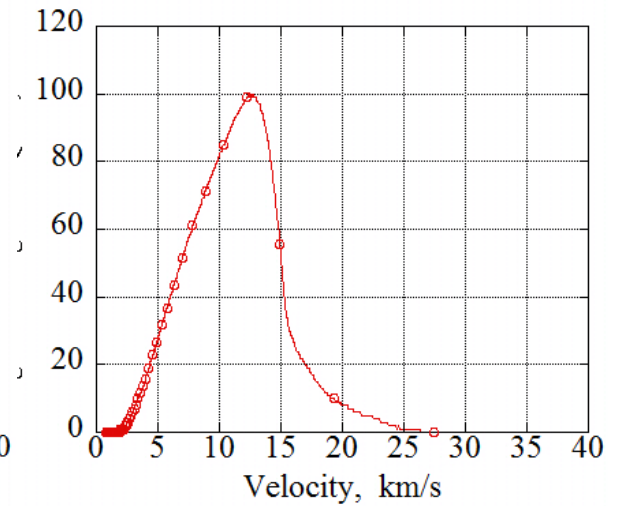


Figure 32. Velocity distribution

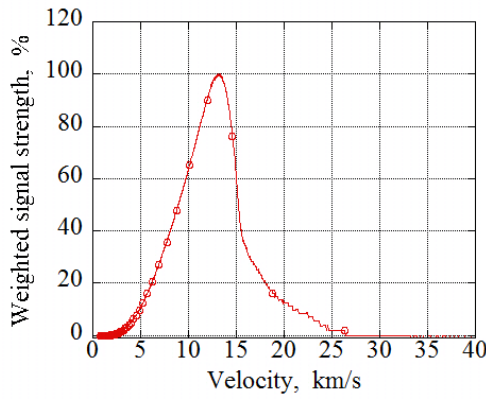


Figure 33. Weighted velocity distribution

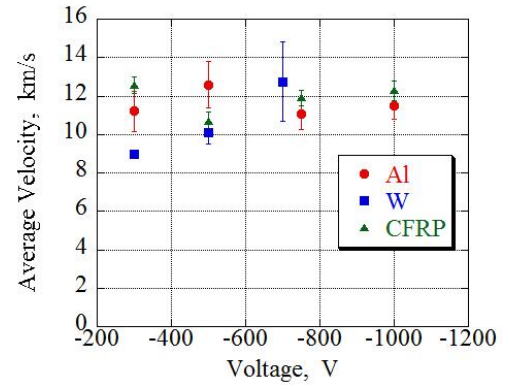


Figure 34. Average velocity vs. vacuum arc energy

On the cross section of CFRP material was identified many triple junction points on the boundary of conductor and insulator. Small discharges that occur between them (conductor (negative charge) and insulator (positive charge)) because of the potential difference works like an igniter. Therefore the system mainly does not need the electrical igniter. We think that CFRP is useful as a material of the propellant [23]

3.5. Vacuum Arc Thruster's work parameters.

Vacuum arc thruster was tested in the laboratory to verify possibility of passive ignition. We cannot control the frequency of VAT discharges with passive ignition because an igniter system for thruster ignition is not used, and have to wait for discharges. Test setup and conditions are shown in Figure 35.

In this experiment, the plasma environment was simulated using ECR mechanism. The background pressure was 10^{-3} Pa and the electron density was 10^{12} m^{-3} with a temperature of 2 eV. A capacitor of $10 \mu\text{F}$ was used, the electrone collector was made from Copper, and a high voltage solar array was used to generate 300 V.

The entire propulsion system (including the thruster head, capacitor, electron collector, and protective resistance) was placed in a vacuum chamber with no

connection to external units to check whether the prototype could operate without an igniter (passive ignition in LEO plasma).

For discharge parameters measurement was used two current probes: commercial current probe and hand-made current probe (used on-board microsatellite Horyu-IV), voltage probe (measured the level of the applied voltage from the HVSA). HVSA and a sun simulator (a lamp) was installed outside the vacuum chamber.

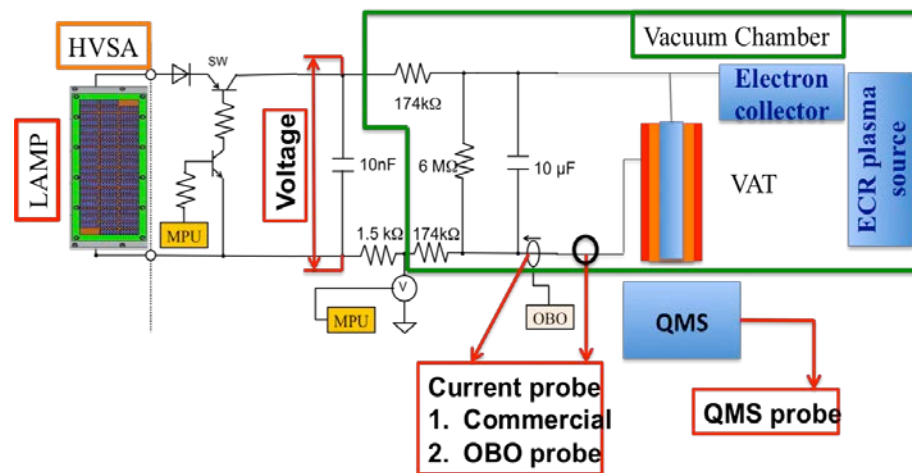


Figure 35. VAT setup condition.

The discharge current waveform is presented on the Figure 36. It was detected that each discharge has a length of $\sim 5 \mu\text{s}$. Maximum arc current is $\sim 650\text{--}700 \text{ A}$ (with a direct drive power source- HVSA, $\sim 300\text{--}330 \text{ V}$). In $5 \mu\text{s}$ we have a main capacitor discharging and the next charging until the new VAT's discharge will occur. More emission sites accommodate higher current levels. These emission sites are initiated at locations where there are local microprojection or dielectric inclusions, which cause local enhancement of the applied electric field. The ion bombardment and Joule heating keep the temperatures required for cathode material vaporization and electron emitting. If we loss a cathode material, it is cause cathode's material craters, and because of this the power deposition decrease, by ion bombardment and ion heating [24]. It affects the frequency of

discharges. The frequency was measured in LEO chamber, with a plasma source for passive ignition.

Testing to measure VAT discharge frequency was done in about 30 min. In that period an arc vision camera installed outside of the vacuum chamber detected 65 discharges. Each arc discharge detected triggered the camera, which made photos of discharges and counted them. Arc rate data is presented in Figure 37 together with the discharge, photographed by the camera from outside the chamber.

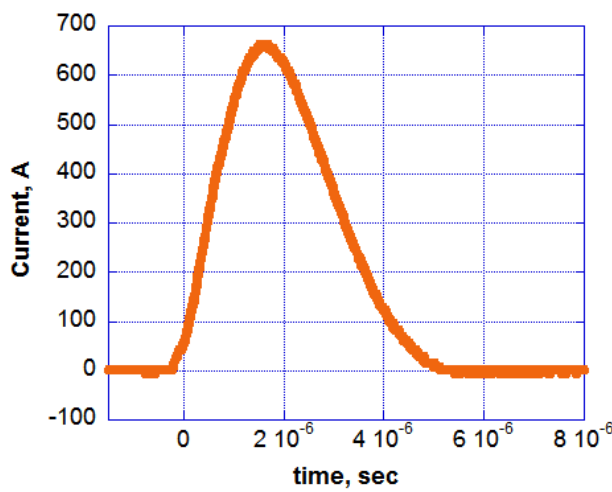


Figure 36. Discharge parameters for VAT with CFRP

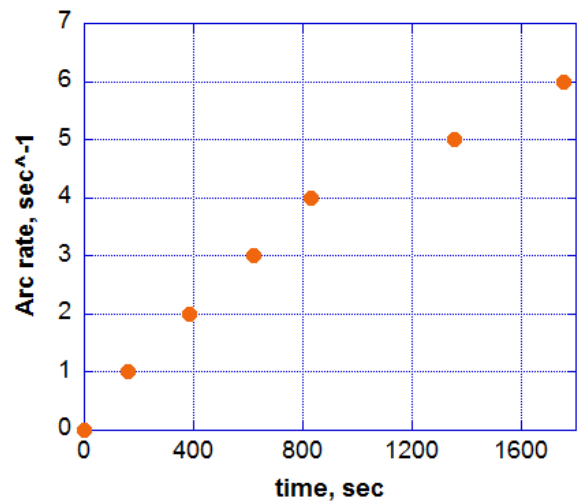


Figure 37. Arc rate data of VAT

The arc rate of VAT, from Figure 37, is 0.0031 sec^{-1} , for the thruster configuration with a commercial CFRP cathode (propellant), Aluminum anode, capacitor $10 \mu\text{F}$ and applied voltage of 327 V from the HVSA (direct drive power source).

To measure discharge frequency or arc rate was done the test in the same plasma condition but with different level of the applied voltage. The HVSA was replaced by power source and was applied voltage from 300 V up to 800 V. Was measured current waveforms and arc rate (discharge frequency). Results are presented on the Figure 38, for the discharge current and Table 2 shows arc rate of VAT depends to the voltage.

For CFRP material as for the main propellant, originally was ordered two different configurations. First is – CFRP with zero degree carbon fiber direction and second one is- CFRP with 45 degree carbon fiber direction.

For both of them was done a discharge test. And if for the CFRP with zero degree carbon fiber direction we got past data, or CFRP with 45 degree, passive discharge was not occurred. Plasma condition, electric circuit configuration and test parameters were absolutely same. We describe it by the higher impedance for this material. Some small discharges was occurred very close to the propellant working surface, but was not detected by the camera or by the oscilloscope with the trigger level in 5 A. On the Figure 39, we can see a CFRP propellant with 45 degree carbon fiber direction, thruster configuration, scheme of the experiment and schema of discharges on the propellant working surface.

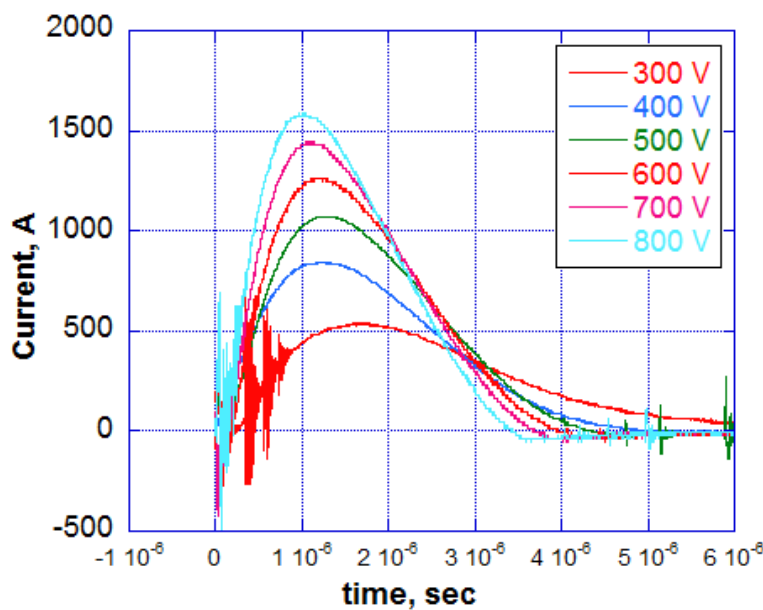


Figure 38. Discharge current waveforms for 300V-800V voltage level.

Table 2. VAT's arc rate

Voltage, V	Arc rate, sec ⁻¹
300	0.0032
400	0.0036
500	0.017
600	0.038
700	0.04
800	0.031

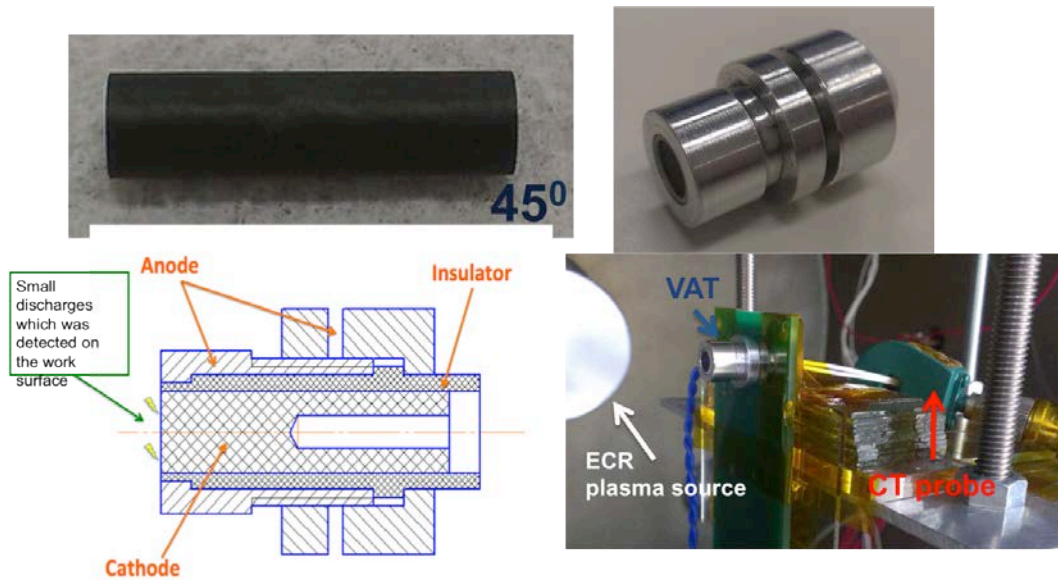


Figure 39. CFRP with 45 degree carbon fiber direction and test configuration

3.6. Impulse bit measurement.

To count VAT's thrust, we have to know not only the arc rate, we need impulse bit data. This parameter depends to the average velocity of the cathode material particles, and amount of charge in the capacitor. In case of the space condition, when we have passive ignition and uncontrolled discharges, discharge could occurred even if capacitor was not full charged. In this case, we can talk about some average thrust parameters. To see an impulse bit, and a thrust for one single and a full discharge, means when discharge occurs use full energy stored in the capacitor, we used a vacuum chamber that does not have the plasma simulator equipment, but we can connect an igniter and control a discharge by the computer from outside.

A special polyimide target provided experiments for impulse bit measurements. The target was located on the distance of 10 mm to the surface of the propellant and at the moment of discharge we could see target inclination (displacement).

The experiment setup is presented on the Figure 40. The applied voltage varied from 300 to 800 V. The back pressure during the test was 10^{-3} Pa. An igniter was used to control the number of vacuum arc occurrences (active ignition, without ECR plasma source).

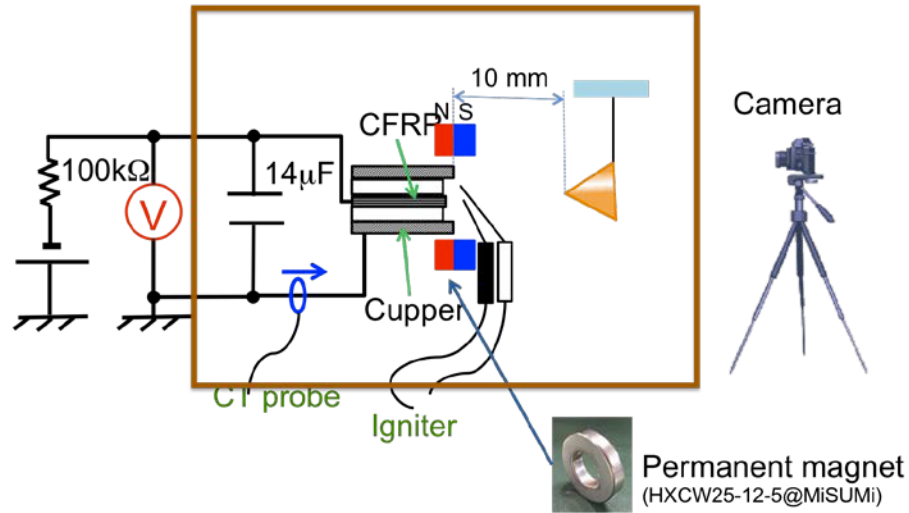


Figure 40. Experiment setup for impulse bit measurement.

The impulse bit was calculated using Eq. 5 in which the displacement x was measured from the thrust target displacement upon metal vapor ejection. The thrust target was injected with metal vapor that was emitted by one vacuum arc, and the displacement of the thrust target was recorded by a digital camera (CASIO EX-F1). The thrust target mass is 20 g and a plate target was used, but reflected ions increase the momentum twice and impulse bit data was two times larger. The cone structure of the target reflects ions and gives zero momentum [25]. The thread was made from nylon and length was 140 mm in triangle. The mass of the thrust head was measured together with thread. Nylon thread thickness is about 1 mm, small to add some reaction.

$$I_{bit} = M \sqrt{2g(L - \sqrt{L^2 - x^2})} \quad \text{Eq. 5}$$

Where, M is the weight of thrust target, g is the gravitational acceleration (taken as 9.8 m/s²), L is the thread length, and x is the displacement of the thrust target.

A photograph at the moment of arc discharge is shown in Figure 41. Figure 42 shows the target displacement.



Figure 41. VAT's discharge.

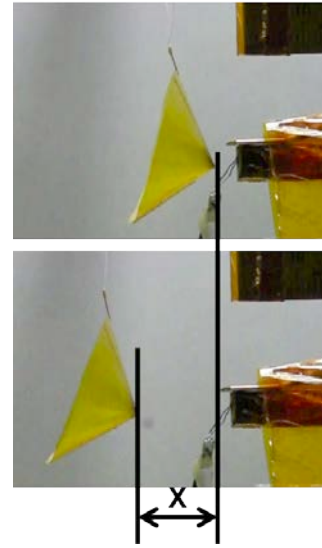


Figure 42. Target displacement after the discharge.

Results are presented on the Figure 43, depends to the level of applied voltage (300 V-800 V). For each point the test was done three times.

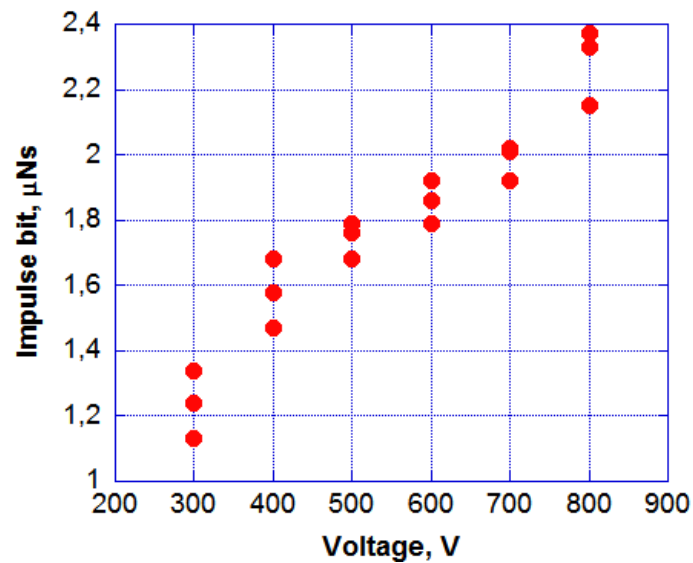


Figure 43. Impulse bit data for VAT with CFRP

The thrust for discharge period and impulse bit which were known were calculated for VAT in Eq. 6, which will operate on-board Horyu-4 with 300 V direct drive from the HVSA and CFRP propellant (commercial) with an arc rate of 0.0032 sec^{-1} :

$$F = I_{\text{bit}} \cdot f = 1.5 \cdot 10^{-6} \text{Ns} \cdot 0.0032 = 4.8 \text{ [nN]} \quad \text{Eq. 6}$$

and an efficiency of this thruster (Eq. 7):

$$\delta = \frac{I_{\text{bit}} \cdot V_e}{2 \cdot W} \cdot 100\% = \frac{1.5 \cdot 10^{-6} \text{Ns} \cdot V_e}{C \cdot U^2} \cdot 100\% = 2.5 \% \quad \text{Eq. 7}$$

where C- is the discharge capacitance in main electric circuit, 10 μF , U-apply voltage, 300 V, V_e - average velocity, 12 km/sec.

3.7. Methods of efficiency improving.

As the main parameter for efficiency – thrust, was purposed to develop the new water adopt CFRP propellant. So, to the CFRP sheet was added the water, as an absorber for water was used silica powder, and a glue, to connect everything together (glue was "Araldite" type). Water molecules can accelerate a discharge, and increase frequency [26].

For the new VAT's propellant model was cut a line of a CFRP sheet with a size of 10 mm x 13 mm. Silica powder was mixed with water and glue (Araldite). This mixture was applied to apart of the CFRP sheet and was twisted into the shape of a cylinder around the copper rod through which electricity is fed to the cathode. As the anode, an aluminum plate and insulator- polyimide was used (Figure 44, 45).



Figure 44. The Mechanism of water adopt CFRP propellant development.



Figure 45. Water adopt CFRP propellant, silica powder and “Araldite” glue.

If we assume that such a working body can improve the cathode working characteristics, was purposed to manufacture water adopt CFRP in three configurations, different in composition. Material #1 consists of: CFRP, silica powder, water and glue. Material #2 consists of: CFRP, Silica powder, glue. Material #3 consists of: CFRP, water, glue. Manufactured materials are presented on the Figure 46.



Figure 46. Water adopt CFRP configurations.

3.7.1. Water adopt propellant testing.

For Vacuum arc thruster with the configuration includes a water adopt CFRP was confirmed passive ignition. Test setup and conditions are same as in chapter 3.5. The plasma environment was simulated using ECR mechanism. The background pressure was 10^{-3} Pa and the electron density was 10^{12} m^{-3} with a

temperature of 2 eV. A capacitor of $14\ \mu\text{F}$ was used, the electron collector was made from Copper, and a power source was used to generate 300 V.

The outstanding camera that gets a trigger signal from the oscilloscope detected the moment of the discharge. Test was done for three propellant (Material #1, Material #2, Material #3). Figure 47 shows discharges for the each water adopt propellant.

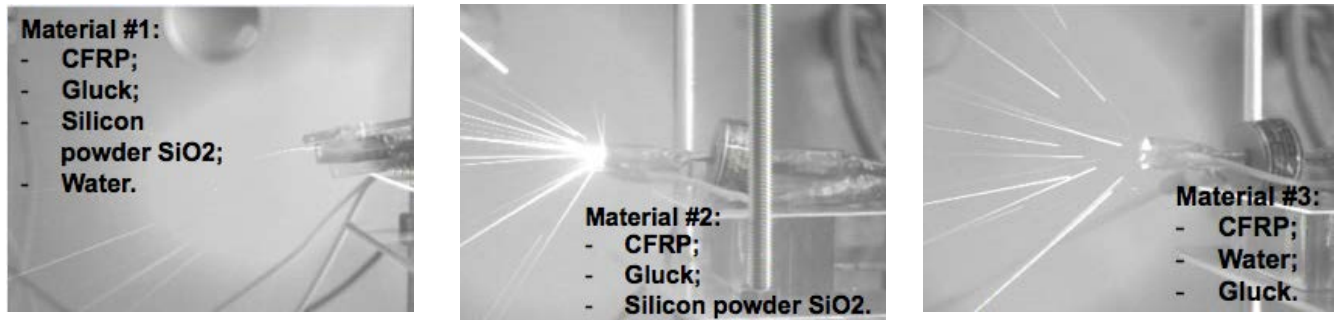


Figure 47. Water adopt propellant's discharges

Each propellant has a different material composition. Water adopt CFRP was twisted into the shape of a cylinder around the copper rod through which electricity is fed to the cathode, and from the Figure 47 we can see, that for Material #2 and #3, the plasma plume probably consist from the discharges of the Copper rod. For Material #1, plasma plume looks more “clear”. Depends to the speed of the electron emission from the propellant, the discharge will occurred in passive emission process. Because of this was measured arc rate, to know possibility of discharges in time and discharge current waveforms (Figure 48, 49).

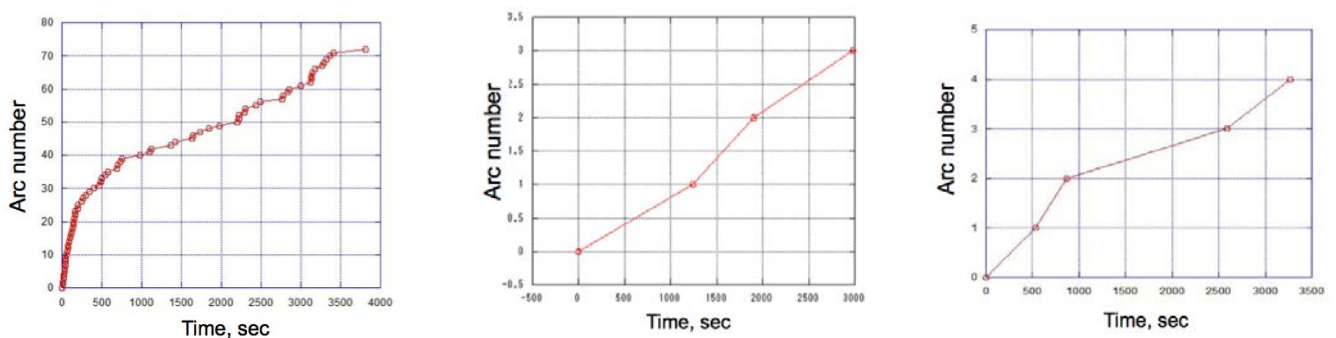


Figure 48. Arc rate data for each water adopt propellant (#1, #2, #3)

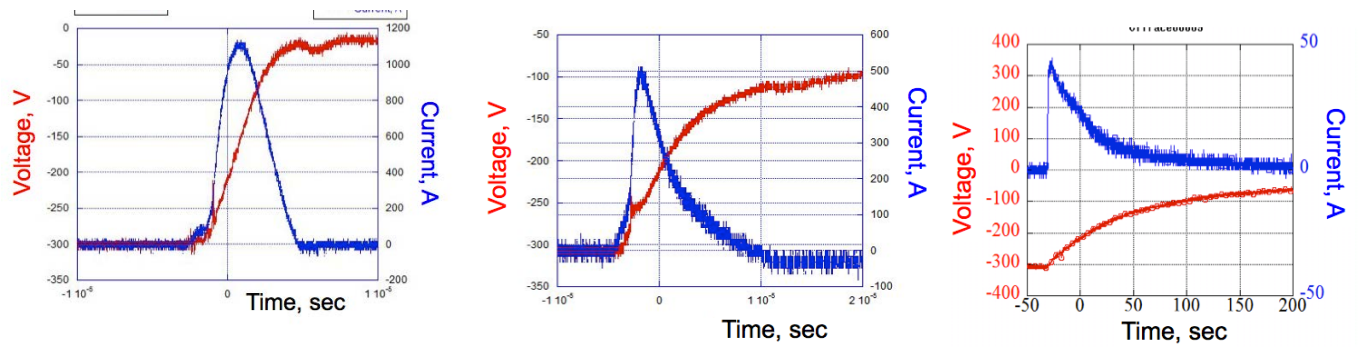


Figure 49. Discharge current of VAT with water adopt CFRP (#1, #2, #3)

We already have data for the commercial CFRP propellant, and now compare discharge test results with water adopt CFRP (Figure 50) we decided to use for next testing propellant “water adopt CFRP #1” and commercial CFRP.

For water adopt propellant, to decide the configuration of anode was done an impulse bit measurement test with two different anodes, made from the Aluminum and made from the Copper materials (Copper has a better electrical conductivity than aluminum). Impulse bit measurement test was done in the General purpose chamber, was used igniter to initiate discharge and measurement provided by the polyimide target as described in the chapter 2.6. Results are presented on the Figure 51. Was used water adopt CFRP (with water, silica powder, and glue) and aluminum anode (plate) or cylindrical copper anode.

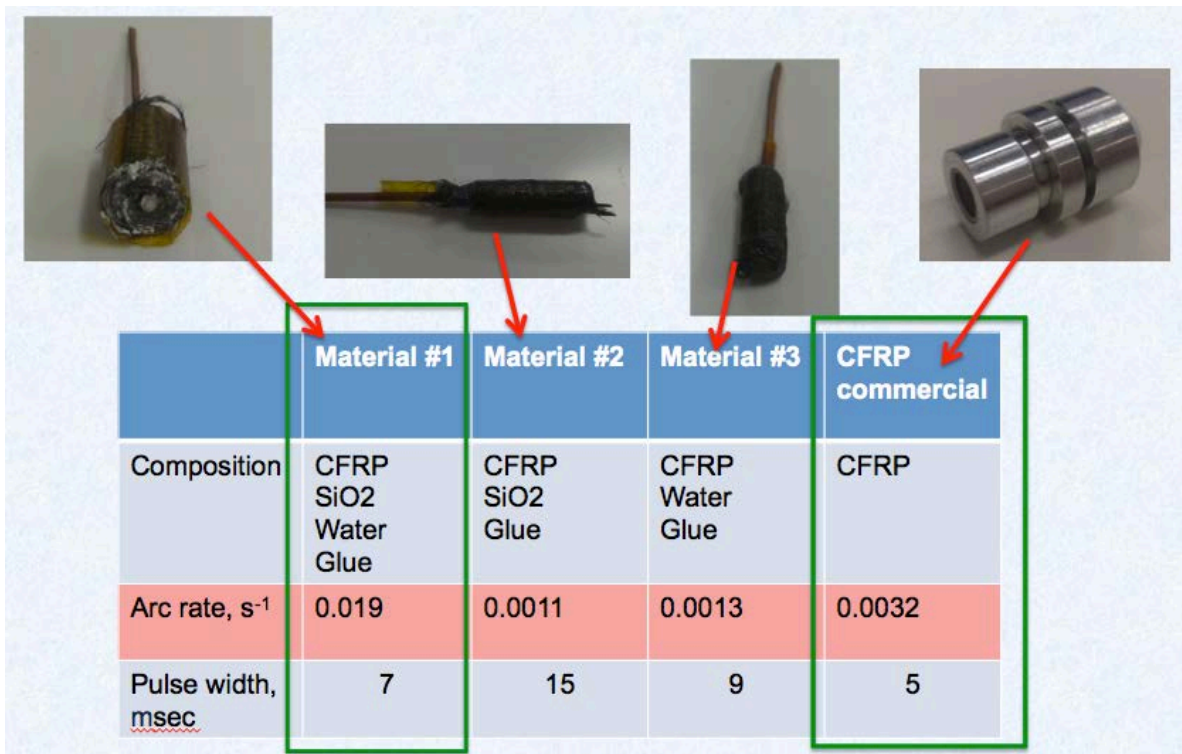


Figure 50. Comparison of VAT's propellant material.

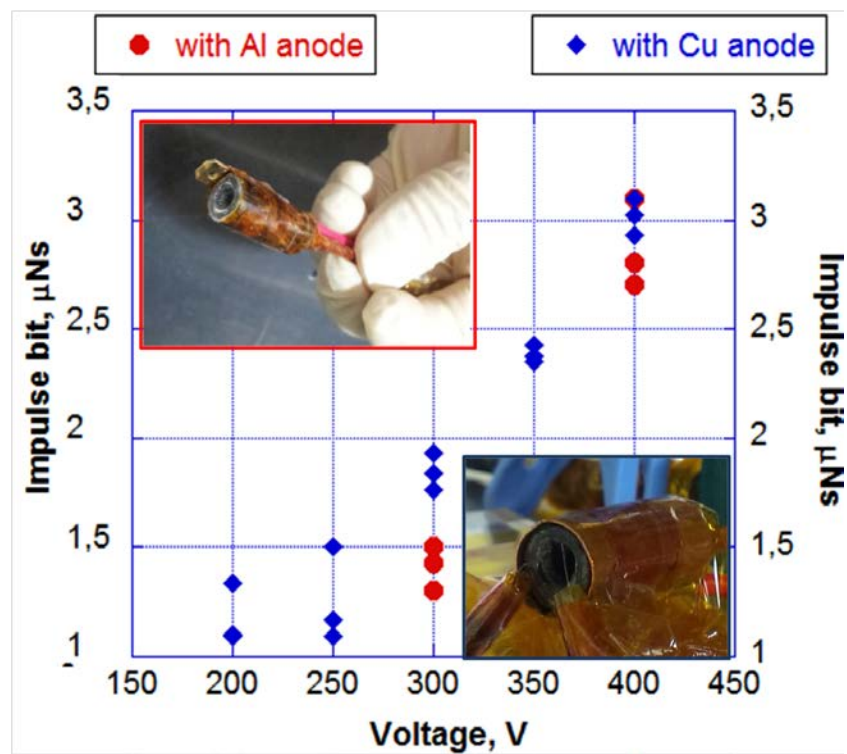


Figure 51. Impulse bit measurement for water adopt CFRP with Al and Cu anode.

As we can see, results are almost the same within the error. For the next test decided to use cylindrical copper anode, because this configuration (cylindrical) is more similar with the original VAT configuration, which was designed in the parallel for the satellite project Horyu-IV.

3.8. Magnet system.

Reducing contamination and increasing thrust could be possible by confining the expanding plasma with the magnetic field produced by the permanent magnet. For example, M. Keidar (2005) developed a magnetically enhanced vacuum arc thruster to restrict plasma, but was used the inductive driver [17]. So, for our test was decided apply to the system a permanent magnet with a magnetic field of 0.3 T (Figure 52, Table 3).



Figure 52. Permanent magnet

Table 3. Permanent magnet parameters

Material	Neodymium
Adsorption force, kgf	73.8
Surface Magnetic Flux Density, mT	330
SMFD at center, mT	120
Size, mm	25 x 12 x 5

Magnet system was located in the two different positions to the thruster (thruster on the middle of permanent magnet, thruster on the cross section of magnet) (Figure 53). This configuration was purposed to identify in which position of magnetic field lines, the plasma could be confine more effective. Data was compared with VAT configuration without permanent magnet.

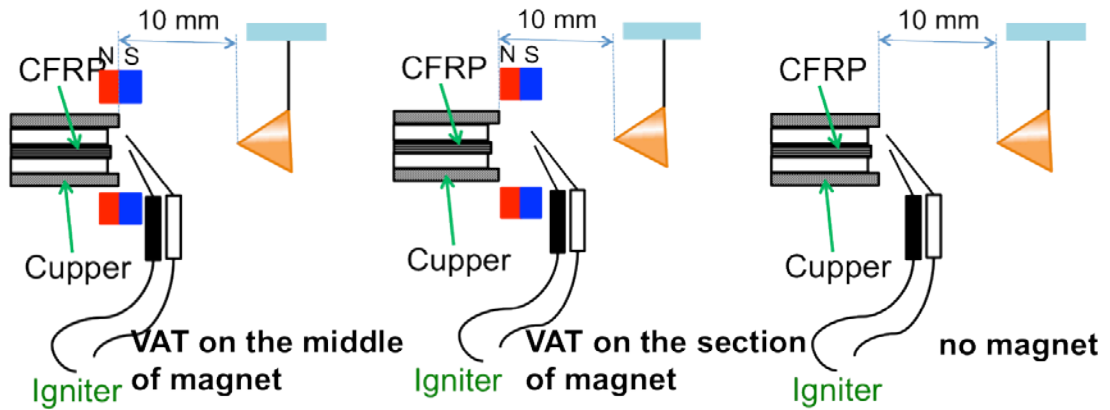
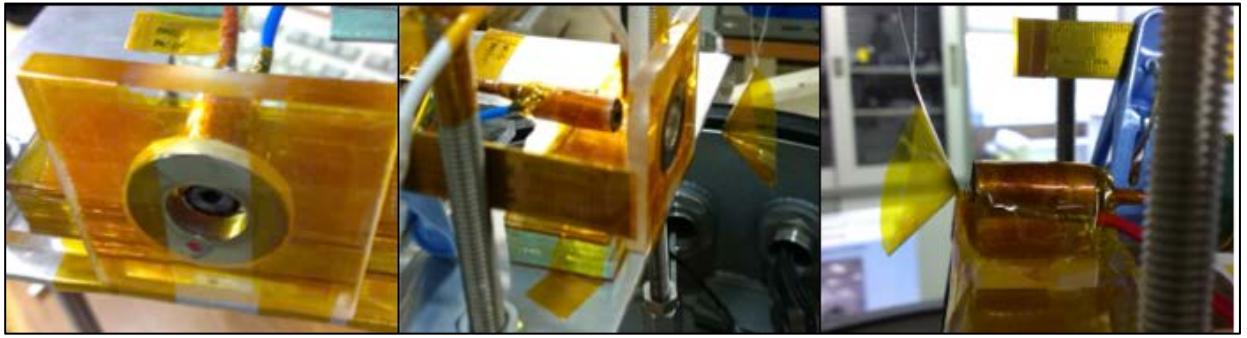


Figure 53. VAT's configuration with permanent magnet

Impulse bit was measured. At first, presenting results for the water adopt CFRP and copper anode with polyimide insulator. Presented results compared to the thruster without permanent magnet in the assembly with the Copper anode. Too, were changed poles of the permanent magnet that added two more configurations. So, magnet was installed at the section of the VAT and VAT was in the middle of the magnet, when poles were faced to the VAT by "N" pole (as on the Figure 53) and by "S" pole. Results presented on the Figure 54.

Results for the system with magnets in the cross section of the thruster and when thruster locates in the middle of magnet are the same within the error. However, in the system without magnets, we can see an improvement of ~30%.

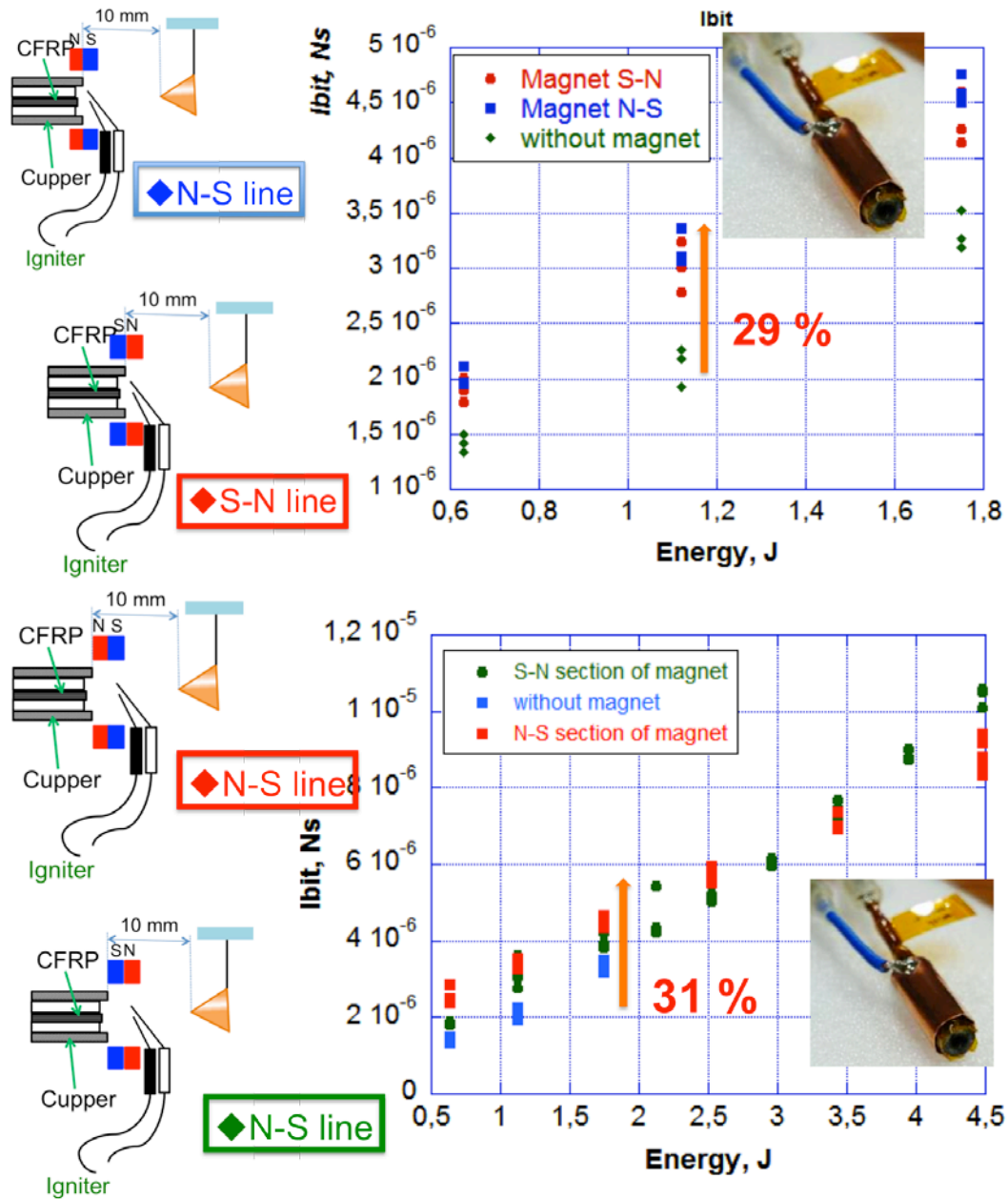


Figure 54. Impulse bit for VAT with water adopt CFRP and permanent magnet of the different configuration.

For the commercial CFRP with 0 degree carbon fiber direction was done the same test. Configuration with permanent magnet, plasma condition was same and was used a general purpose chamber with the ignition system.

As we can see from the Figure 55, impulse bit increases if the level of applied voltage increases. It was confirmed that permanent magnet can improve the characteristics of Ibit in about 30 % in level of applied voltage of 800 V. It is can be attributed by the results of Joule heating and cathode material evaporation in this process.

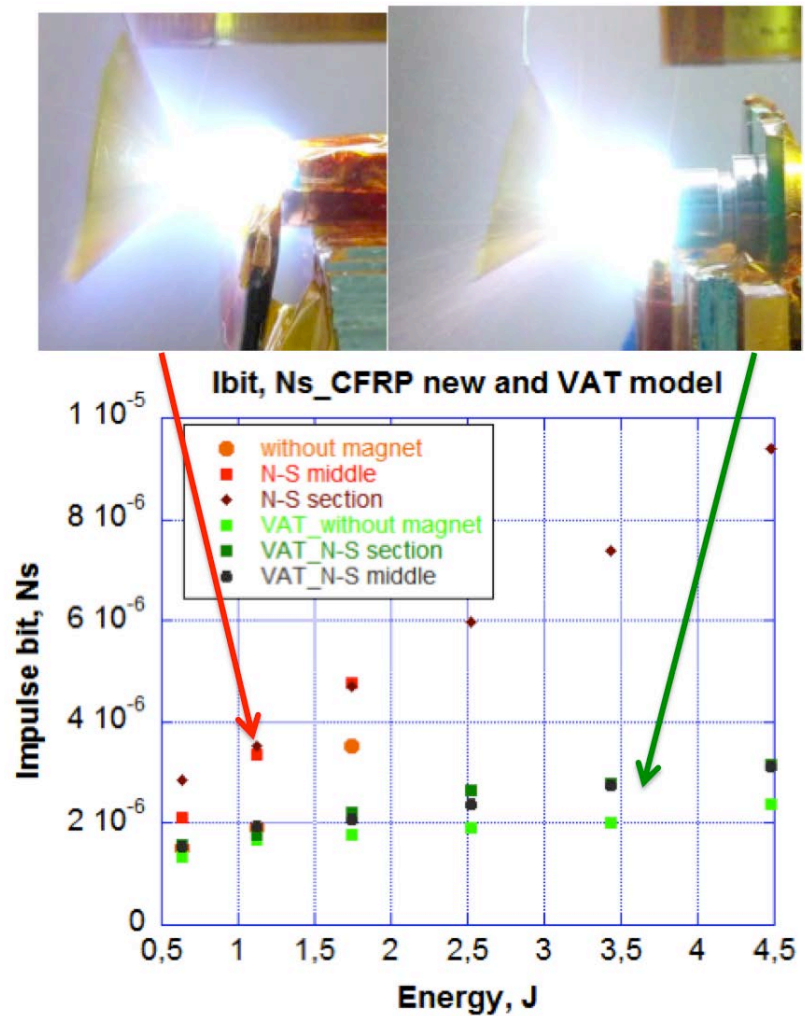


Figure 55. Impulse bit for VAT with the CFRP commercial with 0 degree and water adopt CFRP in different configuration with permanent magnet.

3.9. Applied nozzle to the VAT head

Magnetic field can improve thruster performance and the same we know that nozzle can improve a thrust by increasing pressure in the thruster channel. Test was done for the thruster configuration with commercial CFRP propellant, with Aluminum anode and a nozzle with length in 5 mm (Figure 56). The nozzle length was decided the same as a diameter of cathode electrode (propellant).

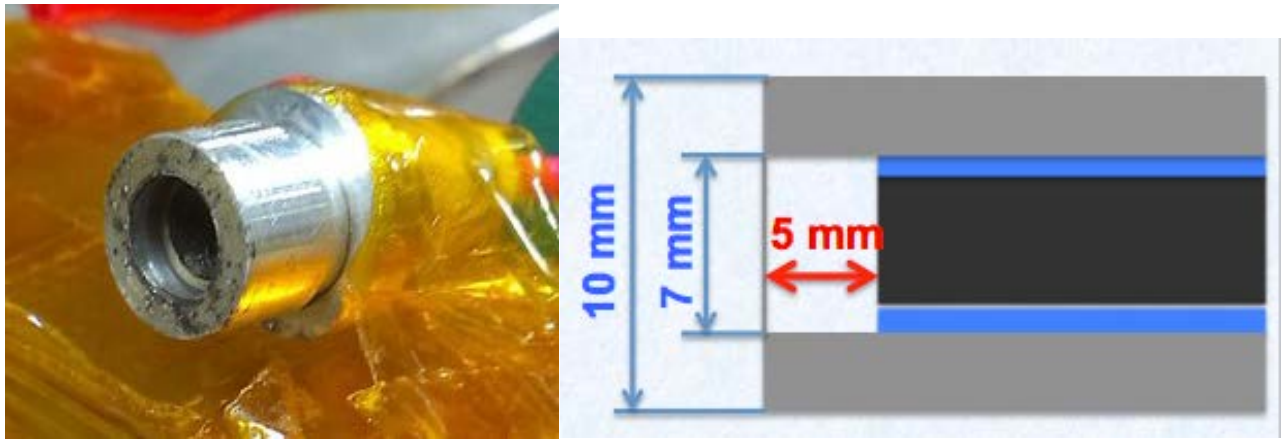


Figure 56. VAT configuration with nozzle.

Capacitance in the circuit was 10 μF . Test was done in the General purpose chamber with igniter system. Applied voltage from 300 V to 800 V. To compare the results with VAT's configuration without nozzle was measured impulse bit data for thruster configuration with nozzle. On the Figure 57 are presented a photos of discharges for the VAT configuration with 5 mm nozzle, depends to the applied level of voltage.

Impulse bit was measured as described before. Was used polyimide target with mass 0.2 gr and located in a distance 10 mm from the thruster head. In moment of discharge target was inclined and by this inclination Impulse bit was measured (Figure 58).



Figure. 57. VAT's discharges for configuration with nozzle.

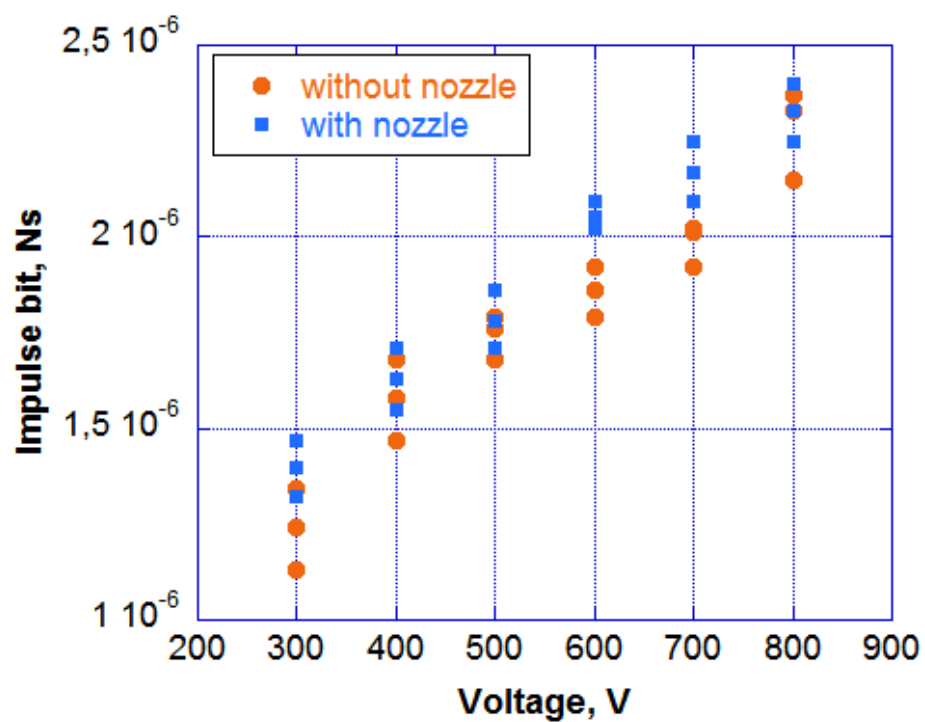


Figure 58. Impulse bit for VAT configuration with 5 mm nozzle and without nozzle.

From these results we can see that they are almost the same within the error. The thruster configuration with different length of nozzle was not tested, but could show better results and if together with nozzle will be attached a magnetic field too.

3.10. Long life test for VAT

As important design factors that regard initiation reliability are a reliable feed mechanism and minimal satellite contamination from exhausted propellant or-cathode erosion, by Polk et al. (2001).

In addition, gross melting makes the thruster inefficient, since less mass is being ionized to produce useful thrust. Methods of measuring the cathode erosion rate include the weight loss method, measuring changes in cathode geometry and measuring crater volumes (Boxman et al. 1995). The weight loss method appears to be the most common of all methods due to it is relative simplicity and fundamental accuracy over other methods, since it measures the erosion rate of the entire cathode structure (Shalev et al. 1985, Polk et al. 2001). Boxman et al.

For Vacuum arc thruster was done the long life test, included 10,000 controlled discharges by the igniter system. Was measured a mass before and after the test by weight loss method and was detected cathode (propellant) changes in process. This test was done in the general purpose chamber, with vacuum 10^{-3} Pa, igniter system, power source (applied voltage was 800 V), 10 uF capacitor was installed inside the vacuum chamber. Current probe on the cathode line inside the chamber detected the discharge current and trigger signal send the command to detect a discharge. That give us a confirmation, that each discharge was occurred, and discharge signal that was detected is not from the igniter system. By the number of discharge images we calculated number of occurred discharges. On the Figure 59, photos of VAT with commercial CFRP and zero degree carbon fiber direction after some number of discharges.

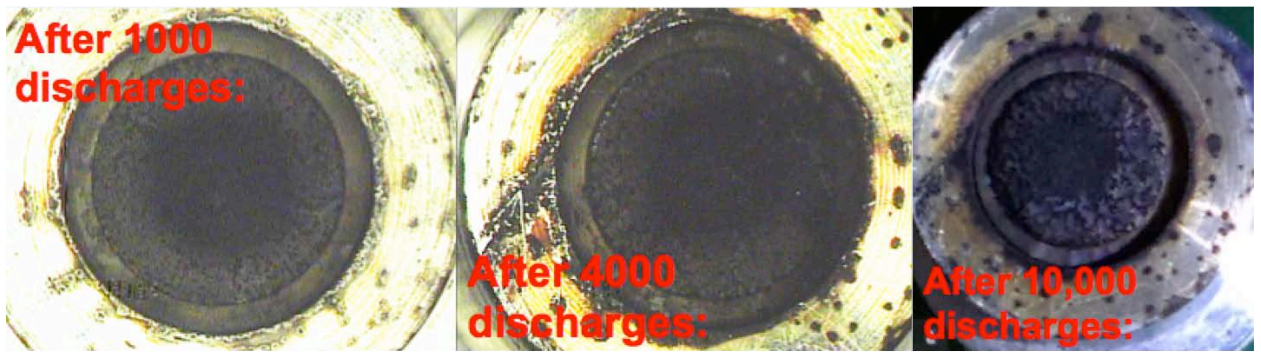



Figure 59. Cathode profile in term of long life test

Before the test was started, propellant mass was 1.8 gr. After 10,000 discharges mass was measured again and calculated mass rate – $3.7 \cdot 10^{-10}$ kg/discharge.

3.10.1. Arc rate after long life test.

After the long life test in 10,000 discharges was measured arc rate in LEO chamber with ECR plasma source (vacuum was $7 \cdot 10^{-3}$, plasma density $n = 2.2 \cdot 10^{11} \text{ m}^{-3}$) for the same thruster configuration (capacitance 10 uF, commercial CFRP with 0deg carbon fiber direction in the propellant and with Aluminum anode). Results are presented in the Table 4 with comparison for arc rate measured before long life test.

Table 4. Arc rate data for VAT before and after the long life test.

Discharge	Voltage V	Arcs	Arc rate after long life test, sec^{-1}	Arc rate before long life test, sec^{-1}
	300	5	0.00139	0.0032

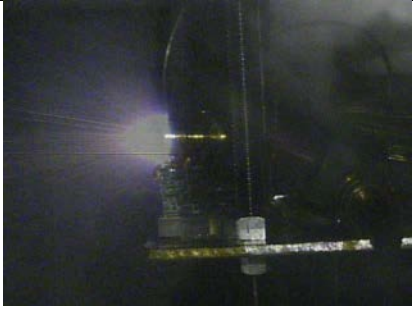
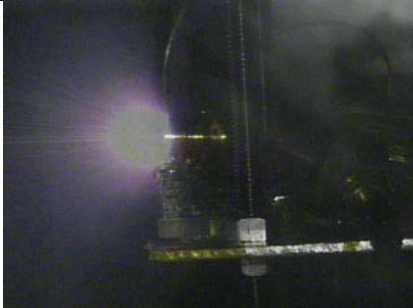
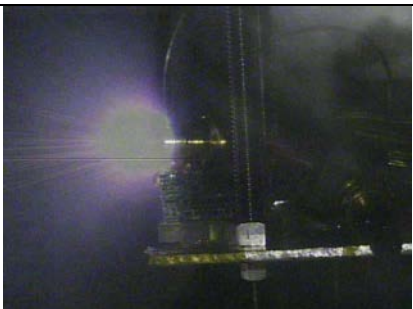

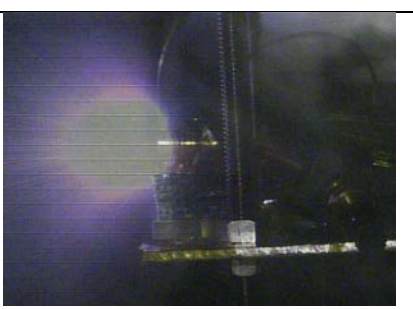
	400	3	0.00083	0.0036
	500	6	0.0017	0.017
	600	5	0.00139	0.038
	700	6	0.0017	0.04
	800	6	0.0017	0.031

Table 4 (continue). Arc rate data for VAT before and after the long life test.

3.11. VAT testing with different capacitors.

Parameters of the discharge are depending to the exhaust velocity of emitted particles. Emission process will be different if the level of the apply voltage changes or the main energy storage source- capacitor, will have a different amount of charge- capacitance [27]. This chapter describes the difference in impulse bit measurement, depends to level of applied voltage and for 2 different capacitors - 10 uF and 14 uF.

For this test, for the correlation was choose commercial CFRP propellant with zero degree carbon fiber direction with cylindrical Aluminum anode (data presented for this configuration is before and after the long life test), water adopt CFRP with Copper anode, commercial CFRP with 45 degree carbon fiber direction and with cylindrical Aluminum anode, but for the last configuration, in the propellant was made a hole with diameter 2 mm and insert inside a Copper electrode. Copper electrode was installed on the depth at 4 mm inside (same as water adopt propellant and Copper rode inside it).

Test was made in the general purpose chamber with igniter system. Vacuum level was $2 \cdot 10^{-3}$ Pa, applied voltage 300 V-800 V from the power source. For measurement was used the described system with polyimide target and outstand high resolution camera. For the 10 uF capacitor and four configuration of the thruster, impulse bit results are presented on the Figure 60.

For 14 uF capacitor case, test results are presented on the Figure 61. Here, for the configuration with commercial CFRP 45 degree, was changed Copper electrode position. From the 4 mm depth, it was moved to “+” axis, and the electrode was on the same section as propellant- cathode. It is decreased propellant impedance and increase a discharge current. Results presented in comparison to water adopt CFRP and commercial CFRP with zero degree of carbon fiber direction.

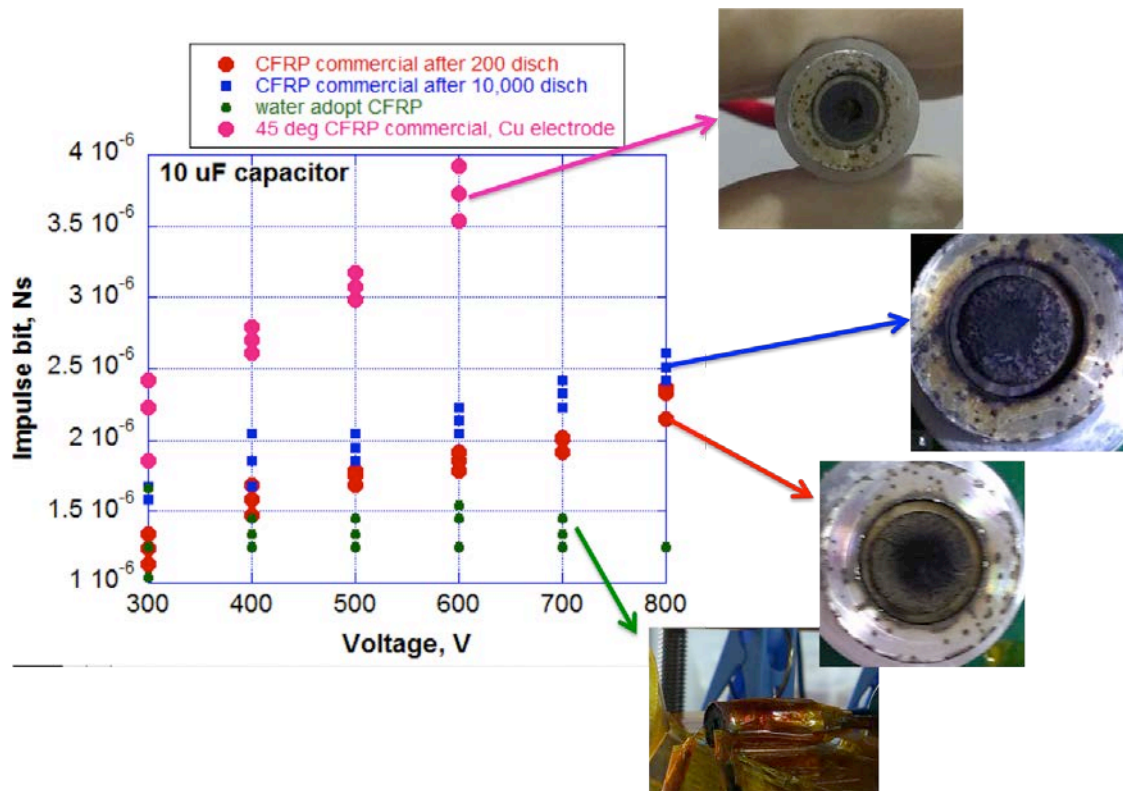


Figure 60. 10 uF capacitor impulse bit test.

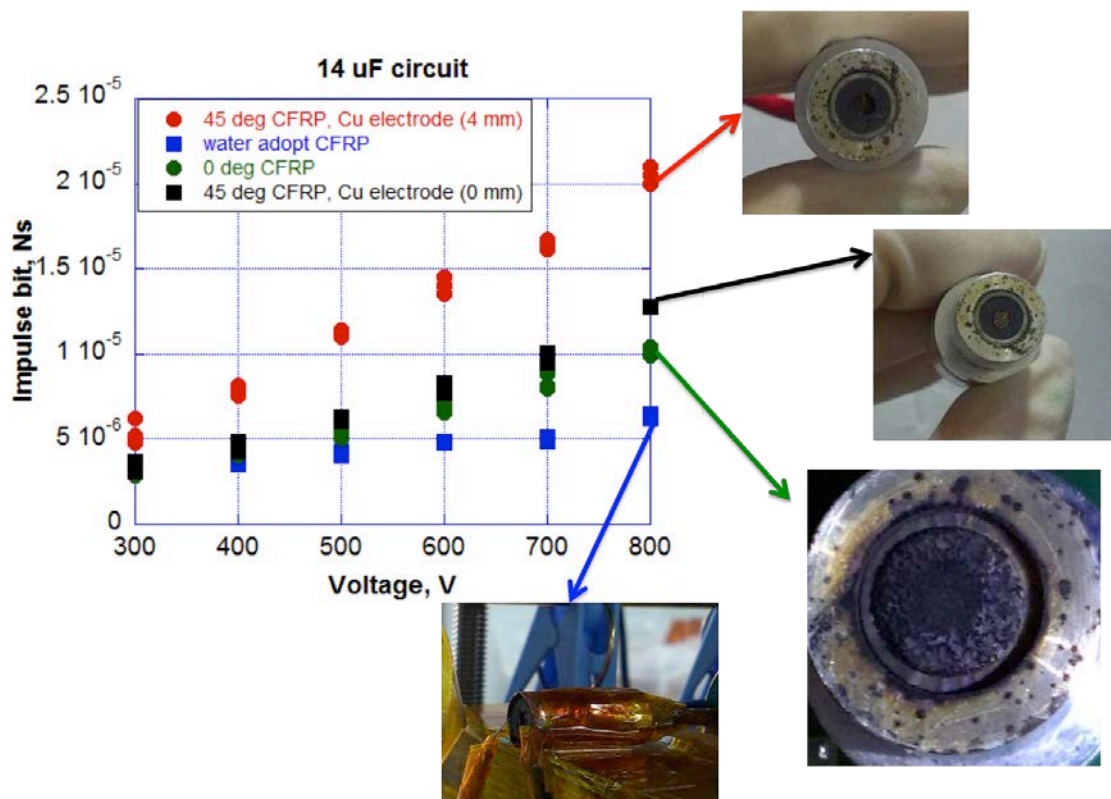


Figure 61. 14 uF capacitor impulse bit test.

Discharge current waveforms are presented on the Figure 62.

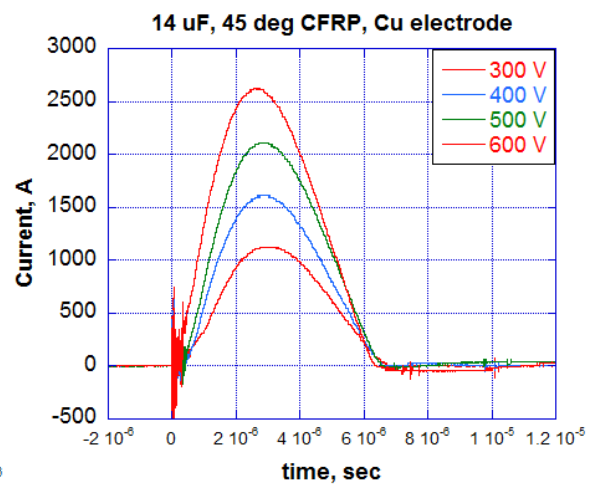
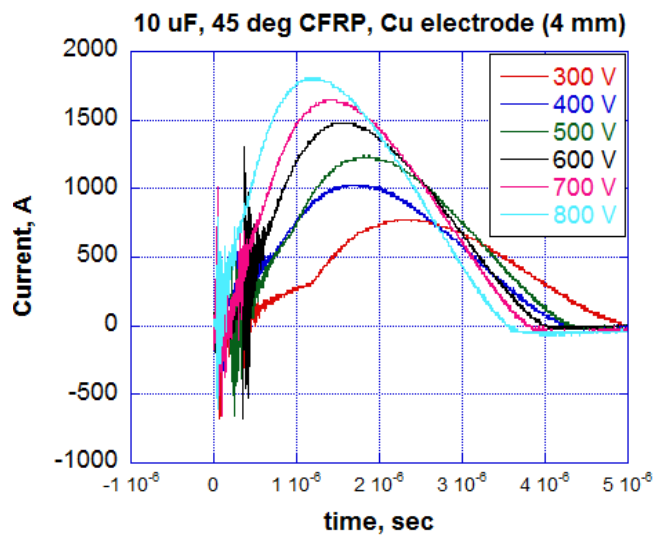
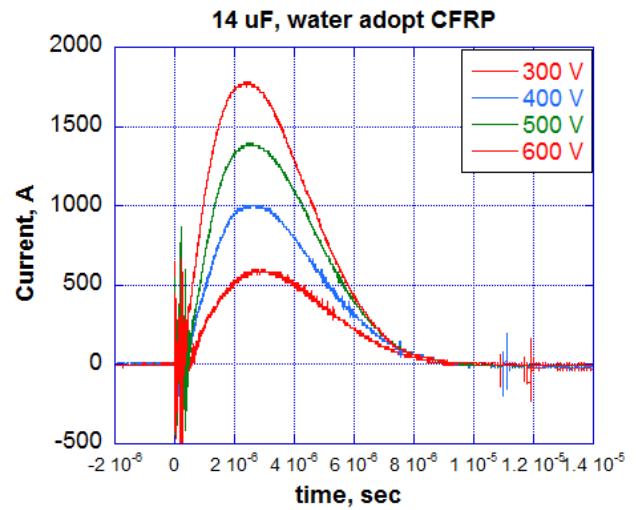
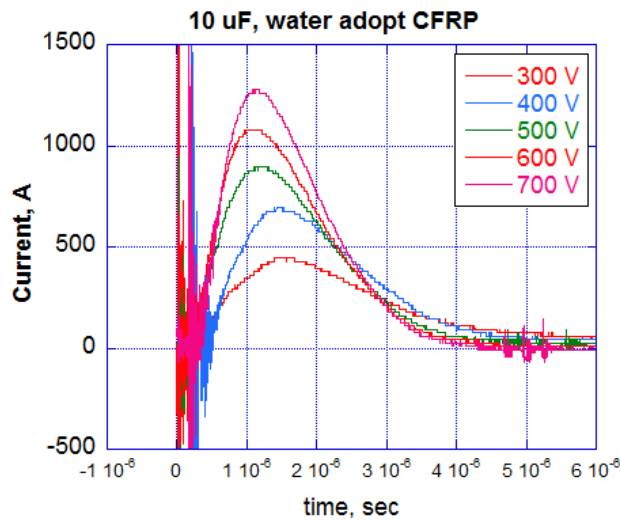
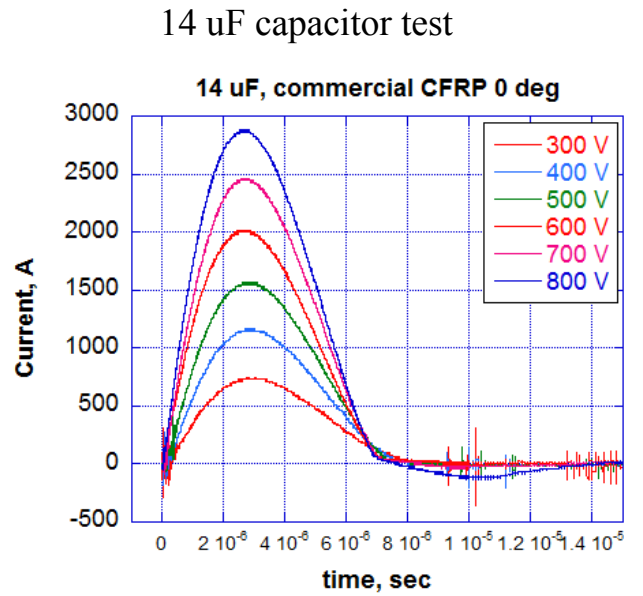
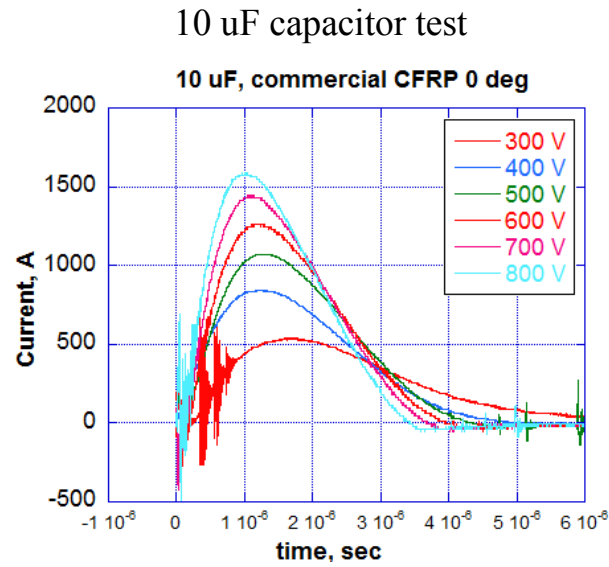


Figure 62. Discharge current waveforms for test with 10 uF and 14 uF capacitors with four VAT's configurations.

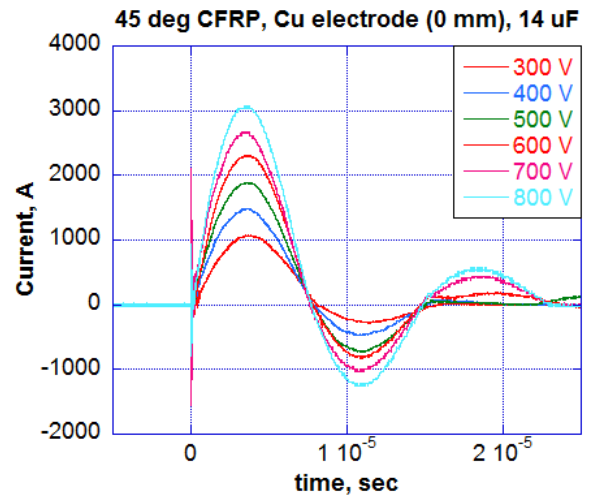


Figure 62 (continue). Discharge current waveforms for test with 10 uF and 14 uF capacitors with four VAT's configurations.

Highest impulse bit results showed a VAT with commercial CFRP and Copper electrode inside, with depth 4 mm compare to 0 mm. Was decided to measure impulse bit for the same thruster configuration but with depth in 8 mm. On the Figure 63 presented results for VAT configuration with copper electrode on three positions- 0 mm, 4 mm, 8 mm and current waveforms for VAT with 8 mm depth of electrode inside the cathode.

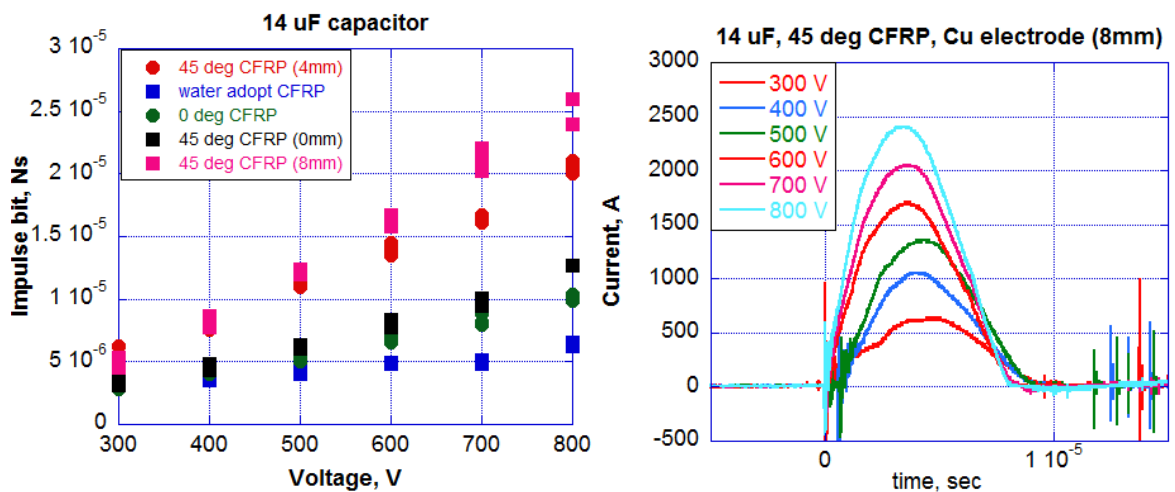


Figure 63. Impulse bit for VAT with commercial CFRP (8 mm) and current waveforms.

From the results on the Figure 63 we can see impulse bit results improved with increasing an electrode depth. It could be described by the low impedance and some kind of nozzle inside the propellant. To confirm results need to measure arc rate for different electrode depth in cathode.

The less discharge current we got with configuration of VAT included 10 uF capacitor and commercial CFRP with zero degree of carbon fiber and for VAT included 14 uF capacitor and a water adopt CFRP.

For these two thrusters was done the arc rate test in LEO plasma condition. Was used LEO chamber, ECR plasma source (the background pressure was 10^{-3} Pa and the electron density was 10^{12} m^{-3} with a temperature of 2 eV), passive ignition, power source and applied voltage was 300 V-800 V, current probe for triggering and image capturing.

For arc rate test and water adopt propellant with cylindrical Copper anode was used 14 uF capacitor, test was done in 3816 second and was detected 72 discharges. For commercial CFRP with zero degree carbon fiber and cylindrical Aluminum anode test was for 1727 sec and was detected 65 discharges. Was applied 300 V in both cases. Results are presented on the Figure 64.

In the Table 5 are presented arc rate data for both VAT's configurations for different applied voltage level (from 300 V up to 800 V). As we can see, arc rate increases if voltage increases.

Table 5. Arc rate depends to the voltage

Voltage, V	Arc rate, sec⁻¹ (water adopt CFRP)	Arc rate, sec⁻¹ (commercial CFRP)
300	0.019	0.0032
400	0.029	0.0036
500	0.038	0.017
600	0.0542	0.038
700	0.1614	0.04
800	0.1899	0.031

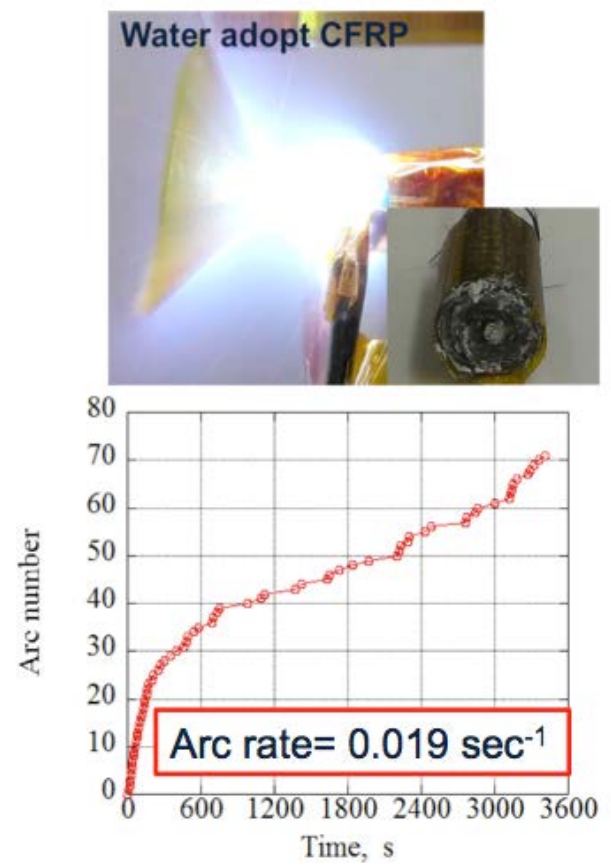
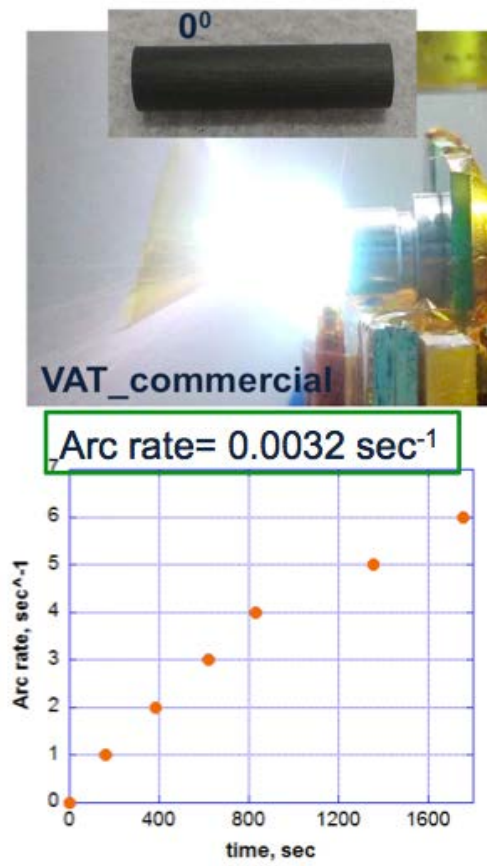


Figure 64. Arc rate test for commercial CFRP and water adopt CFRP.

4. Satellite deorbit system based on the Vacuum Arc Thruster

This chapter describes the possibility of development of an effective deorbit system for CubeSat based on Vacuum Arc Thruster. Results are presented for altitudes from 800 km to 400 km by the VAT and from 400 km to 200 km by the atmospheric drag. Results are presented for the circuit with DCDC converter that increase voltage from 5 V to 800 V, and has power consumption of 1 W.

4.1. Requirements for the satellite deorbit system.

For the all space history, fulfilled spacecrafts was not deorbited or send to the burial orbits, they was just keep in space orbits that increase debris population together with a total debris mass, which is about 2 million kg. The uncontrolled space debris population increasing has to be avoided to maintain the life for spacecrafts in future. Engineers and space users need to take care and keep acceptable level, especially on the LEO orbit, where numbers of debris are highest.

Some studies and publications confirm collision probability increasing for the spacecraft and debris objects [28, 29]. If no measures are taken, number of debris will increase in around 5% per year. Even very small particles that have a speed around 10 km/sec can destroy operational satellite [30].

To reduce debris population presented two ways: debris removal and avoidance of debris. The most effective method to avoid the problem with debris population is active debris removal or satellite deorbit after the end of their mission.

All space debris classified by size and place of life (orbit). Debris, as a source of rocket bodies, engines, asteroids, satellite after the end-of-life, operational payloads, mission related objects depends to the object size and space location is presented in the Figure 65.

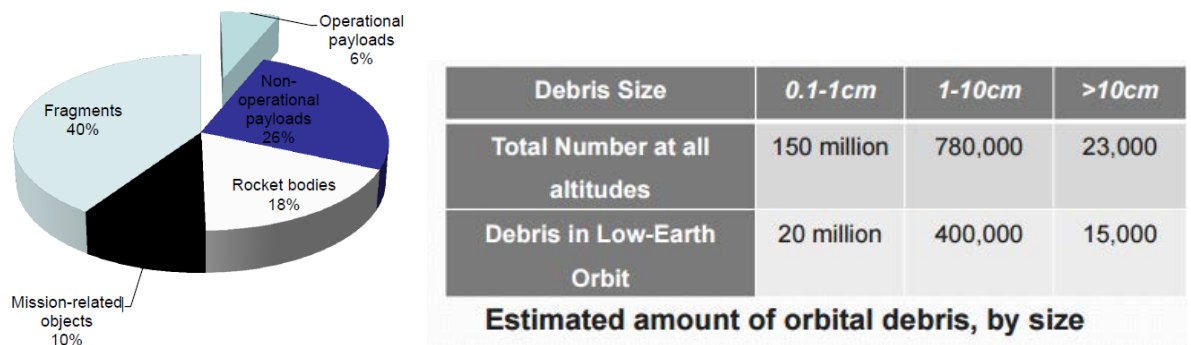


Figure 65. Space debris classification. Classification by size in all altitudes and in the LEO orbit.

If target on the microsatellite CubeSat class with size >10 cm, on the Figure 66, described effective number of objects depends to the year. Presented number of collisions for cataloged, non-cataloged and total object for LEO, MEO and GEO orbits [31].

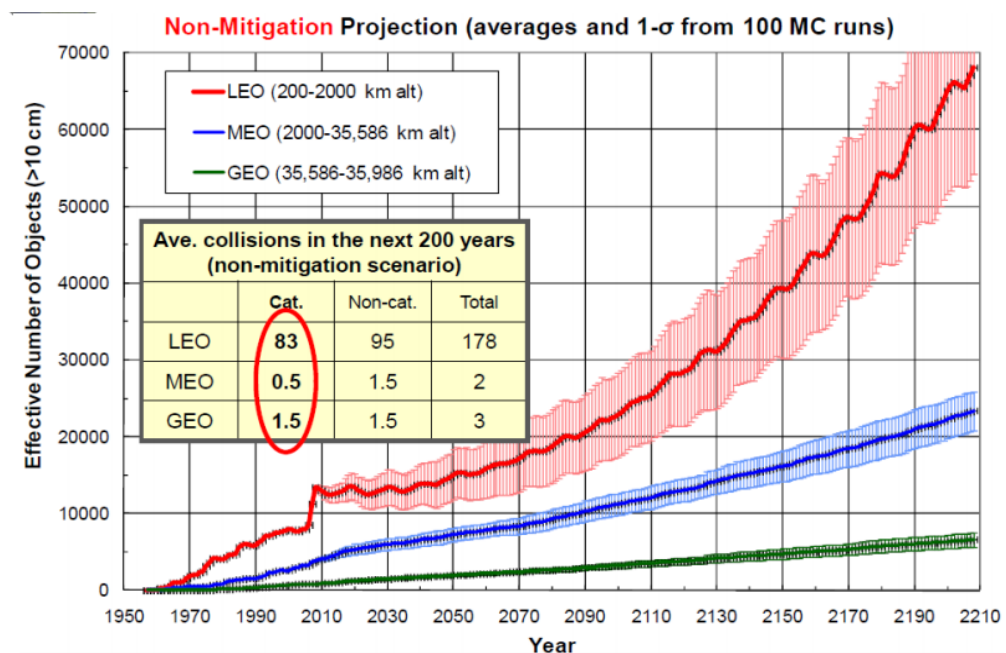


Figure 66. Effective object numbers on the orbits (collision results for the cataloged and non-cataloged objects with size >10 cm)

Satellite deorbit time from the LEO orbit, should be in less than 25 years by the ISO 24113, at 2011. The 25-year limit is derived from IADC guidelines as a result of studies on the forecast of evolution of the population of space systems and

debris in LEO. It is a compromise between the limitation in the debris environment increasing over the next 100 years and programs and projects cost for implementing measures to limit the presence on orbit after end of mission.

There are few solutions for debris removal, such as solar sail, electodynamic tethers, drag augmentation and one of the effective deorbiting method is propulsion-related methods for LEO spacecraft.

For one unit CubeSat, with size 10 cm x 10 cm x 10 cm, weight around 1 kg and power consumption at 1 W, deorbit system requirements are these:

- Power consumption less than 1 W;
- Small size;
- Small weight;
- Simple design;
- Deorbit time less than 25 years.

The purpose is- Deorbit system for microsatellite based on Vacuum Arc Thruster.

VAT, it is a thruster with a passive ignition in LEO condition. Ion plasma conditions, with a high density plasma (LEO conditions), charges an insulator and/or dielectric. Electric field concentration is generated at the boundary of the cathode and insulator and from the cathode accelerated electrons are emitted. These move to the insulator to neutralize the potential difference. Charging of insulator becomes larger because of the collisions between accelerated electrons and as a result emitting secondary electrons. Electric field concentration becomes stronger, and the electrons accelerate furthermore. Sufficiently accelerated electrons collide with the ambient molecules and ionize the molecules. Finally, the cathode and anode will be electrically connected, and vacuum arc discharge occurs. So, discharge could occur in specific plasma condition. If specify satellite as a one unite CubeSat with one thruster system on-board, installed on the ram side of the satellite, we should confirm possibility of VAT ignition in space, on the LEO orbit (Figure 67).

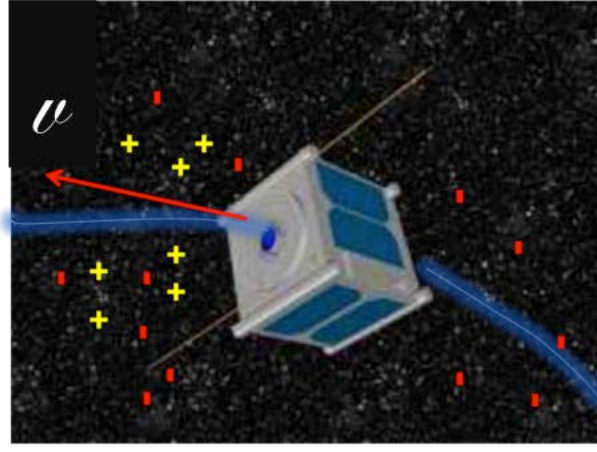


Figure 67. VAT position on the RAM side.

The parameters for mean maximum plasma densities from IRI for the LEO orbit is temperature $T=2,327$ K and oxygen ion density $n_{O^+}=1.3 \cdot 10^{11} \text{ m}^{-3}$ [32], was used to calculate the ion concentration on the ram and wake side for 800 km altitude.

RAM side compression region would be ion concentration- n_0+n_r , behind the satellite body- n .

$$v_{th} = \sqrt{\frac{2 \cdot k \cdot T}{m_p}} = \sqrt{\frac{2 \cdot 1.38 \cdot 10^{-23} \cdot 2327}{2.6 \cdot 10^{-26}}} = 1572 \text{ km/sec} \quad \text{Eq. 8}$$

where is $k=1.38 \cdot 10^{-23}$ (J/K) Boltzmann constant, $m_p=2.6 \cdot 10^{-26}$ (kg) mass of oxygen molecule.

$$n_{O^+} = 1.3 \cdot 10^{11} (\text{m}^{-3})$$

$$n_0 + n_r = n_0 \cdot \left(1 + \frac{V_0}{v_{th}}\right) = 1.3 \cdot 10^{11} \cdot \left(1 + \frac{7800}{1572}\right) = 7.75 \cdot 10^{11} (\text{m}^{-3}) \quad \text{Eq. 9}$$

As we can see from the Eq. 9, the ion concentration is the same (within the error), that was used for the VAT testing in the ground tests with LEO condition. It can confirm possibility of discharges in the LEO altitude for the Vacuum Arc Thruster, and it is effective source for the satellite deorbit purpose.

4.2. Satellite deorbit time realized by Vacuum Arc Thruster.

The modeling and calculation for the deorbit by vacuum arc thruster was done for altitudes 800 km to 400 km. Satellite mass from 1 kg, or one Unit of CubeSat to 4 kg, four unit CubeSat. Deorbit time by VAT was calculated by Eq. 10.

$$T_{deorbit} = \frac{N_p}{f(\text{frequency})} \quad \text{Eq. 10}$$

where N_p - required number of discharges (thruster's pulses) for CubeSat deorbiting from 800 km to 400 km, f - arc rate, sec^{-1} .

Equation of energy Eq. 11:

$$\frac{mv_1^2}{2} - G \frac{Mm}{R+h} = \frac{mv_2^2}{2} - G \frac{Mm}{R+H} \quad \text{Eq. 11}$$

where m -satellite mass, 1...4 kg, v_1 - satellite orbit velocity before the maneuver made by VAT, km/sec, v_2 - satellite orbit velocity after the maneuver (after a discharge occurred), km/sec, h =800 km, altitude of start the maneuver, H =400 km, final deorbit altitude, $M=6 \cdot 10^{24}$ (kg), mass of the Earth, $R=6.37 \cdot 10^6$ (m), Earth radius, $G=6.67 \cdot 10^{-11}$ (J/K), gravitational constant.

Satellite orbit velocity (Eq. 12):

$$v_1 = \sqrt{G \frac{M}{R+h}} \quad \text{Eq. 12}$$

and an equation of momentum (Eq. 13):

$$mv_1 - mv_2 = I_{bit} \quad \text{Eq. 13}$$

can give a satellite velocity after a thruster's discharge occurred (after maneuver) (Eq.14):

$$v_2 = v_1 - \frac{I_{bit} \cdot N_p}{m} \quad \text{Eq. 14}$$

Eq. 12 and Eq. 14 we use in Eq. 11 and found a relationship between a number of pulses N_p and a thruster impulse bit parameter I_{bit} , that depends on the altitude, and velocity changes before and after satellite maneuvers created by VAT (Eq. 15):

$$N_p = \frac{m}{I_{bit}} \left[\sqrt{G \frac{M}{R+h}} - \sqrt{2 \cdot G \frac{M}{R+h} - G \frac{M}{R+H}} \right] \quad \text{Eq. 15}$$

Impulse bit data we got from the experiments for different thruster configurations. Data was analyzed by software “Curve Expert” and describe results as a function, that depends to the applied voltage level (Figure 68).

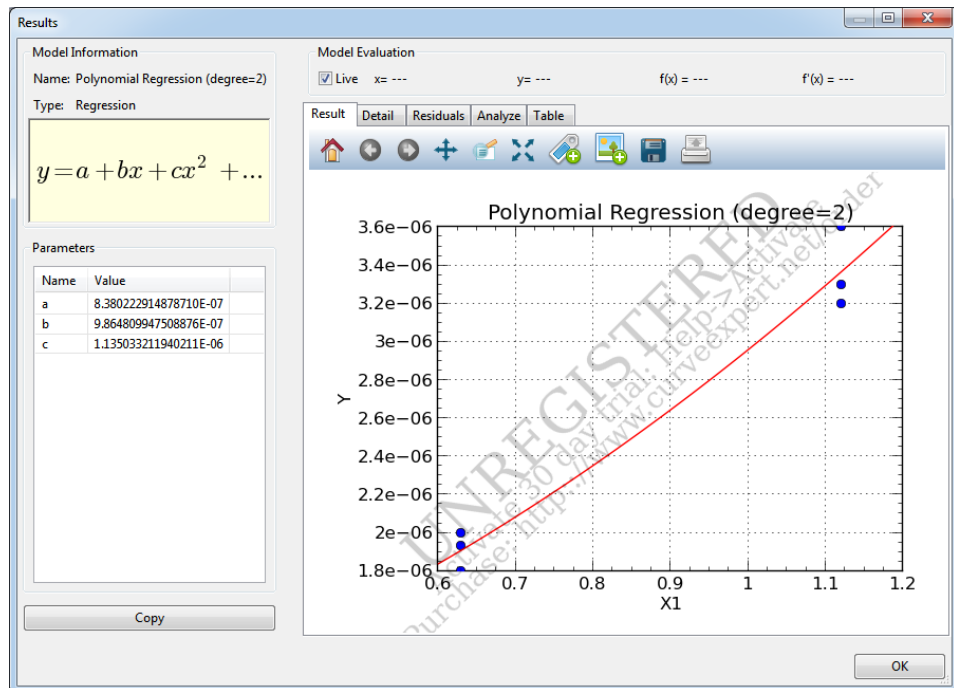


Figure 68. Impulse bit data equation predicted by “Curve Expert”.

Impulse bit equation from the software (Eq. 16):

$$I_{bit} = 8.38 \cdot 10^{-7} + 9.87 \cdot 10^{-7} \cdot U + 1.135 \cdot 10^{-6} \cdot U^2 \quad \text{Eq. 16}$$

And final results for the number of pulses (Eq. 17):

$$N_p = \frac{m}{8.38 \cdot 10^{-7} + 9.87 \cdot 10^{-7} \cdot U + 1.135 \cdot 10^{-6} \cdot U^2} \left[\sqrt{G \frac{M}{R+h}} - \sqrt{2 \cdot G \frac{M}{R+h} - G \frac{M}{R+H}} \right] \quad \text{Eq. 17}$$

Results in Figure 68 and Eq. 16, 17 are presented as an example for one of the many tests for the water adopt CFRP propellant included CFRP, silica powder, water and glue “Araldite”. Was used thruster configuration with an Aluminum anode.

By the described principle, for the next VAT’s impulse bit measurement tests with water adopt CFRP and commercial CFRP, it was found impulse bit equations for commercial CFRP propellant and for the water adopt CFRP with configuration with permanent magnet and without (Eq. 18-Eq.23).

Water adopt CFRP propellant, no permanent magnet:

$$I_{bit} = -1.5 \cdot 10^{-6} + 1 \cdot 10^{-8} \cdot U + 1.04 \cdot 10^{-4} \cdot U^2 \quad \text{Eq. 18}$$

Water adopt CFRP propellant, N-S middle of the permanent magnet:

$$I_{bit} = 1.54 \cdot 10^{-9} + 2.9 \cdot 10^{-9} \cdot U + 1.265 \cdot 10^{-11} \cdot U^2 \quad \text{Eq. 19}$$

Water adopt CFRP propellant, N-S section of the permanent magnet:

$$I_{bit} = 1.75 \cdot 10^{-7} + 5.3 \cdot 10^{-9} \cdot U + 6.76 \cdot 10^{-12} \cdot U^2 \quad \text{Eq. 20}$$

Commercial CFRP propellant, no permanent magnet:

$$I_{bit} = -1.78 \cdot 10^{-8} + 6.54 \cdot 10^{-9} \cdot U - 8.8 \cdot 10^{-12} \cdot U^2 + 5.2 \cdot 10^{-15} \cdot U^3$$

Eq. 21

Commercial CFRP propellant, N-S middle of the permanent magnet:

$$I_{bit} = 1 \cdot 10^{-8} + 7.72 \cdot 10^{-9} \cdot U - 1.04 \cdot 10^{-11} \cdot U^2 + 7.12 \cdot 10^{-15} \cdot U^3$$

Eq. 22



Commercial CFRP propellant, N-S section of the permanent magnet:

$$I_{bit} = 1 \cdot 10^{-9} + 5.2 \cdot 10^{-9} \cdot U - 1.52 \cdot 10^{-12} \cdot U^2$$

Eq. 23

For both propellants (commercial CFRP and water adopt CFRP) was measured arc rate- frequency of discharges (Table 6).

Table 6. Arc rate dates for the commercial CFRP and for the water adopt CFRP.

 VAT with commercial CFRP 10 uF capacitor		Water adopt CFRP 14 uF capacitor 	
Voltage, V	Arc rate, s ⁻¹	Voltage, V	Arc rate, s ⁻¹
300	0.0032	300	0.019
400	0.0036	400	0.029
500	0.017	500	0.038
600	0.038	600	0.0542
700	0.04	700	0.1614
800	0.031	800	0.1899

By the equations of impulse bit and Eq. 17, we got number of pulses (Table 7, 8), needed for the satellite deorbit. We divided these results by arc rate data, and calculate deorbit time for one unit of CubeSat from altitude 800 km to 400 km. Results are presented for different thruster configurations (cathode electrode-propellant) (Figure 69).

Table 7. Number of pulses needed for 1U CubeSat deorbit (VAT configuration with commercial CFRP).

Voltage	without magnet	NS middle	NS section
300	1.73E+08	1.41E+08	1.57E+08
400	1.47E+08	1.18E+08	1.22E+08
500	1.31E+08	1.04E+08	1.01E+08
600	1.20E+08	9.18E+07	8.69E+07
700	1.10E+08	8.10E+07	7.72E+07
800	<u>9.96E+07</u>	<u>7.04E+07</u>	<u>7.01E+07</u>

Table 8. Number of pulses needed for 1U CubeSat deorbit (VAT configuration with water adopt CFRP).

Voltage	without magnet	NS middle	NS section
300	1.63E+08	1.11E+08	9.42E+07
400	9.97E+07	7.02E+07	6.62E+07
500	6.74E+07	4.85E+07	4.95E+07
600	4.86E+07	3.55E+07	3.86E+07
700	3.67E+07	2.72E+07	3.11E+07
800	<u>2.87E+07</u>	<u>2.15E+07</u>	<u>2.56E+07</u>

As we can see from the Figure 69, deorbit time decrease with applied voltage level. The propellant heating can describe it and it can improve a process of electrons emission. Figure results more detailed presented on the Table 9.

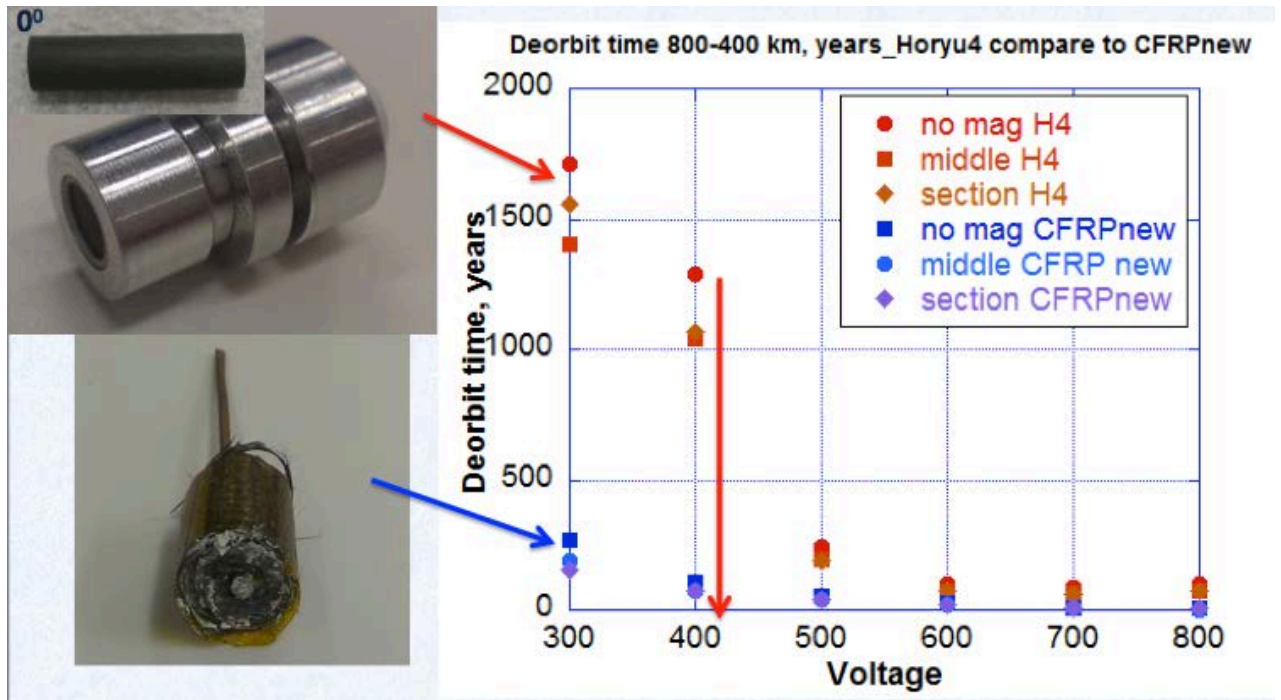
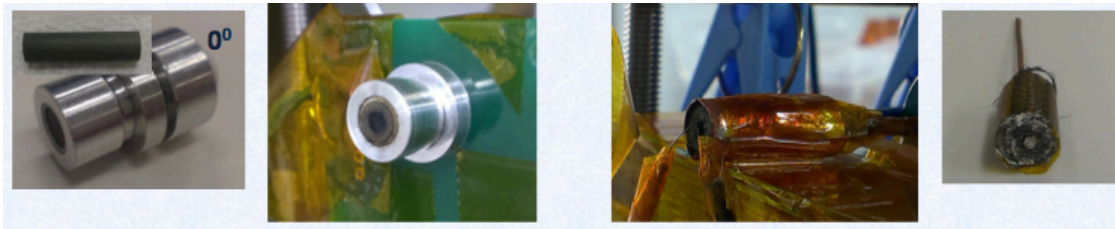


Figure 69. CubeSat deorbit time, realized by VAT.

Results that are presented on the Table 9 were calculated for commercial CFRP with Aluminum anode and 10 uF capacitor, and for the configuration with water adopt CFRP, Aluminum anode and 14 uF capacitor circuit. For the water adopt propellant and 800 V apply level, we have a deorbit time in around 4.8 years, for the configuration of thruster without permanent magnet. And the most optimistic result is for the same configuration but with permanent magnet, when VAT is installed on the middle of this magnet- 3.6 years. This result is much less than 25 years for the deorbiting from the LEO orbit- 25 years.

Calculation was done for the deorbit from 800 km altitude to the 400 km altitude. From the 400 km to 200 km altitude deorbiting will be done by atmospheric drag. From the on-line software [33] it will take 685.8 days or around 1.9 year for one unit of CubeSat. So, total deorbiting time is 5.5 years from altitude 800 km to 200 km by VAT with water adopt propellant, and capacitor in 14 uF.

Table 9. Deorbit time for CubeSat for the commercial CFRP and for the water adopt CFRP.



deorbit time, years	without magnet	NS middle	NS section
300	1710	1400	1560
400	1290	1040	1070
500	245	193	188
600	100	76.6	72.5
700	87.2	64.2	61.2
800	102	72	71.7

deorbit time, years	without magnet	NS middle	NS section
300	271	186	157
400	109	76.7	72.4
500	56.2	40.4	41.3
600	28.1	20.8	22.6
700	7.21	5.34	6.1
800	4.79	3.58	4.27

This high number of pulses of course will make propellant erosion, and propellant material weight should be enough to provide deorbiting and continue mission. As was described before, mass loss is $7.2 \cdot 10^{-10}$ gr/dischage. On the Table 10 are presented a propellant consumption data for more electrically loaded situation- 800 V applied voltage. Data shows total mass loss after the end of mission for the deorbiting from 800 km to 400 km for VAT with commercial CFRP and water adopt CFRP with or without permanent magnet.

Table 10. Propellant consumption.

VAT configuration with commercial CFRP propellant			
	Without magnet	NS middle	NS section
800 V applied	36.9 gramm	26 gramm	25.9 gram
VAT configuration with water adopt CFRP propellant			
	Without magnet	NS middle	NS section
800 V applied	10.6 gramm	7.96 gramm	9.47 gramm

Total cathode electrode weight is 1.8 gramm and with mass loss as on the Table 10, this propellant weight is not enough to continue deorbit mission. One more perspective thruster configuration is VAT with 45 degree CFRP propellant that has a hall in 1.5 mm diameter and inside installed Cupper electrode. Depth of electrode position inside CFRP is 8 mm. Exactly this configuration shows the highest impulse bit characteristics. For this thruster configuration was calculated number of pulses needed for the deorbit and deorbit time (Table 11).

Table 11. Deorbit results for VAT with Cu electrode (8 mm depth).

Voltage, V	Number of pulses	Deorbit time, years
300	1.98E+07	33.1
400	1.29E+07	14.1
500	9.11E+06	7.6
600	6.81E+06	3.98
700	5.29E+06	1.04
800	4.24E+06	0.707

This thruster has one disadvantage - a great erosion in the channel where was installed Cu electrode. To check it need to provide a long life test. From the calculation, mass shot is $3.7 \cdot 10^{-10}$ kg/discharge, for most loaded situation- 800 V, for $4.24 \cdot 10^6$ number of pulses (needed for satellite deorbit from 800 km to 400 km) we will have 1.57 gramm of mass loss for the full mission. With total propellant mass 1.8 gr, propellant consumption for the presented thruster configuration is not enough, but not so critical as for the VAT with 10 uF capacitor and commercial CFRP with zero degree carbon fiber direction (Table 10). To solve this problem, cathode electrode/propellant diameter could be increased to survive with presented propellant consumption.

4.2.1. VAT testing with DCDC converter.

The highest results for the deorbiting were got at 800 V voltage level. This amount of energy can heat the propellant and initiate the emission of electrons

quicker, that at 300 V for example. To get 800 V on-board microsatellite was purposed to use DCDC converter series AV/SMV- 5AV800, that convert from 5 V of input voltage to 800 V output. Power consumption is ~ 1 W [34] (Figure 70). Test was done for the thruster configuration with commercial CFRP and Aluminum anode.

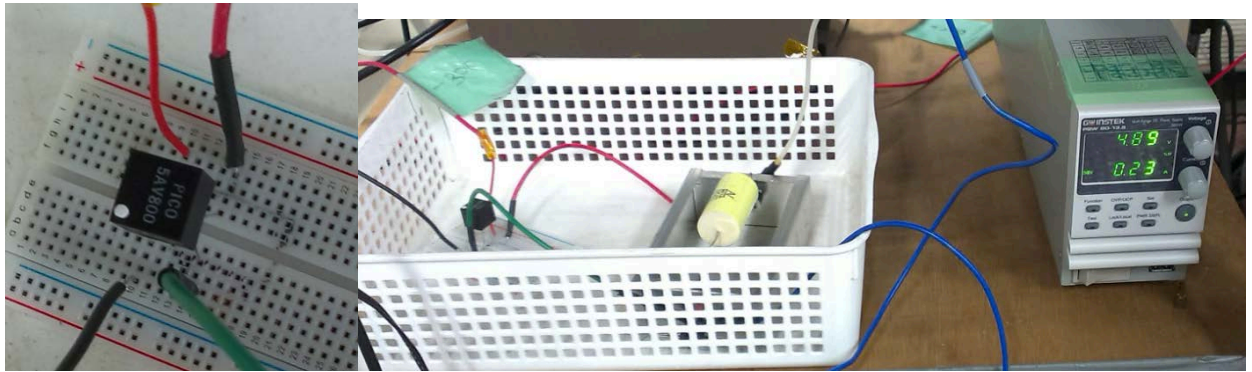


Figure 70. DCDC converter configuration.

Arc rate was measured (Figure 71) and the deorbit time for one unit CubeSat from 800 km altitude to 400 km altitude was calculated.

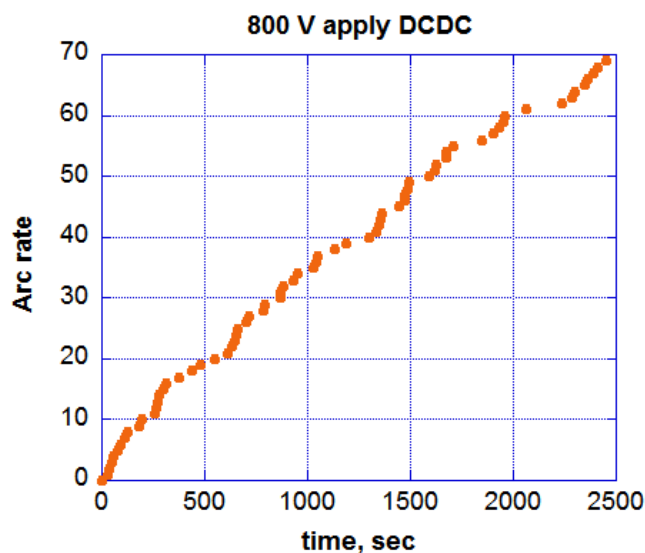


Figure 71. VAT's arc rate with DCDC.

Comparison results for the deorbit time if we apply 800 V to the cathode-propellant are presented on the Figure 72 (configuration with and without DCDC converter).

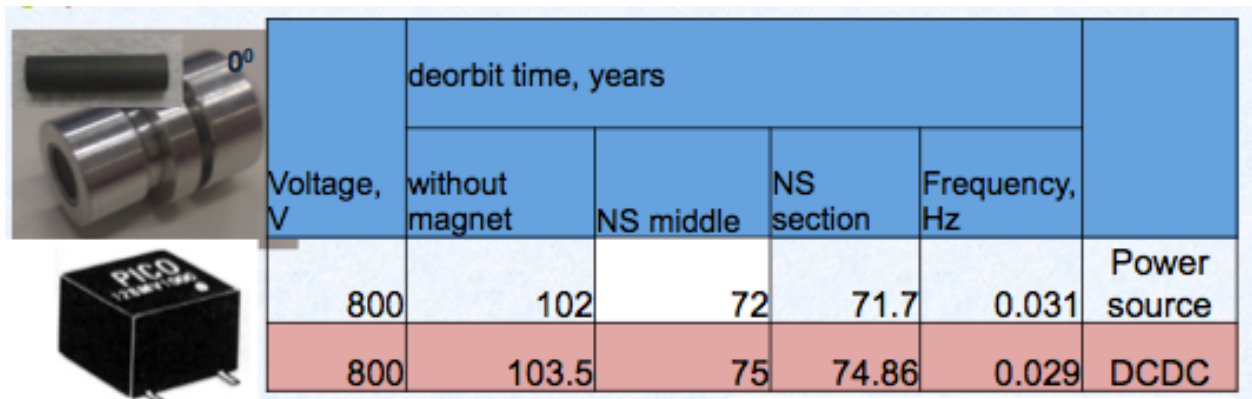


Figure 72. Deorbit time for thruster's circuit configuration without and with DCDC.

As we can see from the last figure, results of the deorbit time are almost same within the error. That confirms a possibility of use for this circuit as original on-board CubeSat thruster configuration, if we have to apply 800 V to get highest results of arc rate and confirm shorter deorbit time.

For the VAT configuration that was used for deorbit calculation (VAT with commercial CFRP and in the circuit with 10 uF capacitor and VAT with water adopt CFRP and 14 uF capacitor) on the Figure 73 and Figure 74 are presented efficiency results and impulse bit results depends to the power consumption.

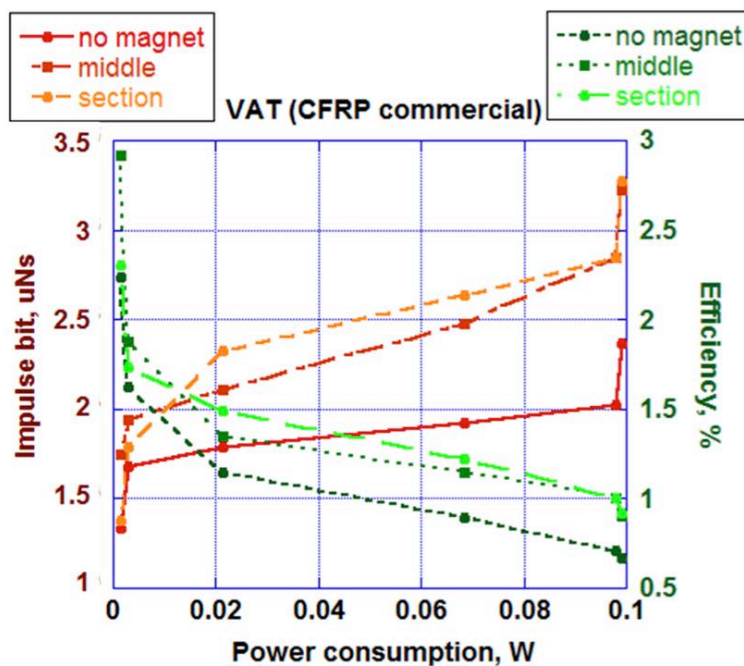


Figure 73. VAT efficiency in configuration with commercial CFRP propellant.

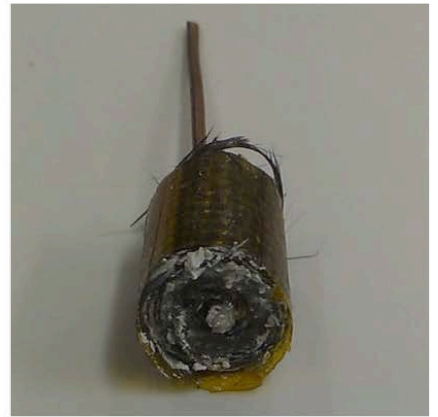
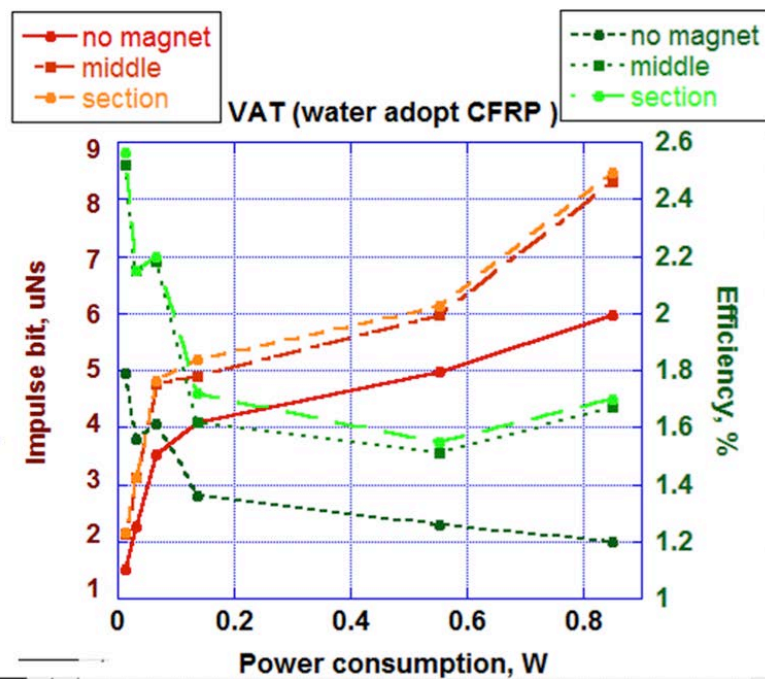


Figure 74. VAT efficiency in configuration with water adopt CFRP propellant.

For both cases, power consumption is less than 1 W, as was required for the deorbit system for CubeSat.

5. Vacuum Arc Thruster on-board satellite Horyu-4

This chapter describe the configuration of the Horyu-IV satellite. Presented main missions, and a configuration of Vacuum Arc Thruster with results for end-to-end test with other satellite sub-systems.

5.1. Horyu-4 satellite project.

Microsatellite Horyu-IV (Figure 75) was designed at the Kyushu Institute of Technology and was launched in February 2016 by H2A rocket. Forty-three students have taken part in the project including international students from 16 countries. The name of this satellite is Arc Event Generator and Investigation Satellite (AEGIS), Horyu-IV. HORYU-IV is a cubic-shaped nano-satellite with dimensions of 490 mm \times 490 mm \times 495 mm, including antennas and mirror holder, with an approximate mass of 10 kg. The size of the satellite main external structure is 331 mm \times 285 mm \times 331 mm, without antennas and mirror holder. The planned orbit altitude is 575 km with an inclination of 31 deg. The main mission is to conduct discharge experiments on-board. The secondary mission is to test high voltage solar arrays that will produce 350 V, degradation by discharge and Langmuir probe. Extra missions: Vacuum Arc Thruster (VAT), Electron Emitting Film, Camera, Singer others [35, 36].

Satellite development took nearly three years. And 47 members from 18 countries took part in this project.

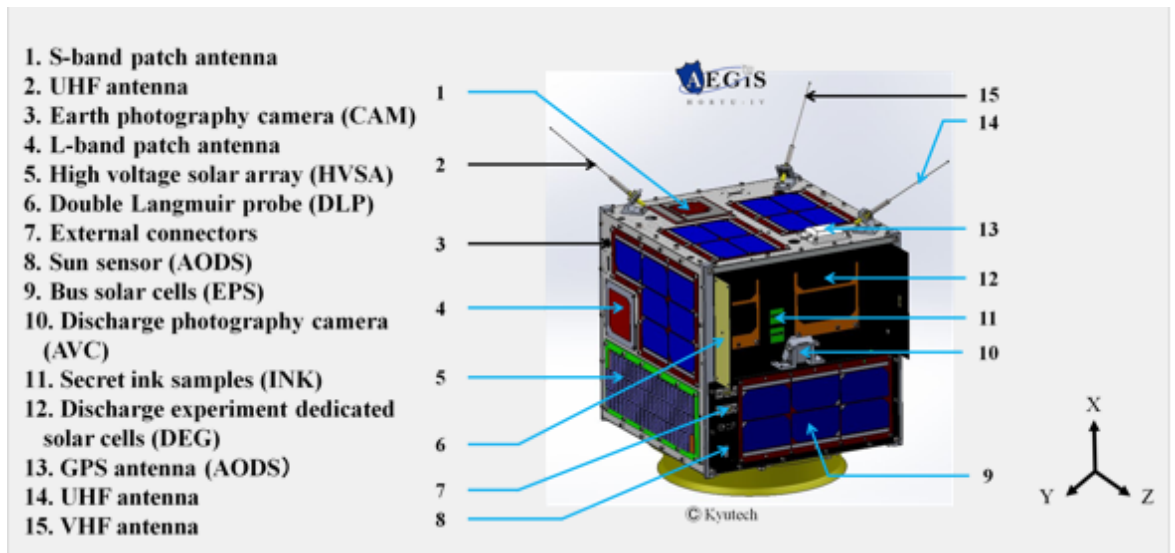
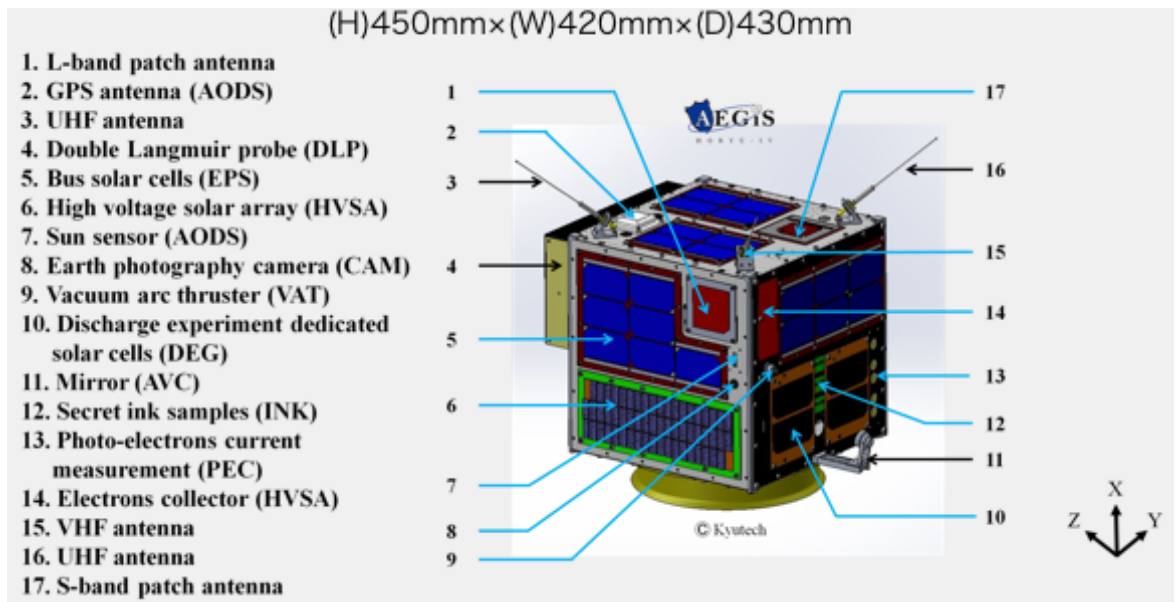


Figure 75. Horyu-IV satellite and sub-system description.

5.2. Vacuum Arc Thruster sub-system.

Main mission of Vacuum Arc Thruster is on-orbit demonstration of a trigger-less discharges on VAT, which circuit is directly connected to the high voltage solar array (HVSA).

The VAT electronics is located on an electronic board called the Big Apple board as shown on the Figure 76. This board also has 3 other missions: double langmuire probe (DLP), photo-electrons current measurement mission (PEC), electron-emitting film (ELF)/surface charging monitor (SCM) mission. These four missions share a microcontroller that controls the operations, how power is

distributed, and how data are saved. The Big Apple microcontroller receives command from the on-board computer (OBC) to carry out any of the four missions and also to downlink mission data. The power supplied from the electric power system (EPS) to this board is a 5V.

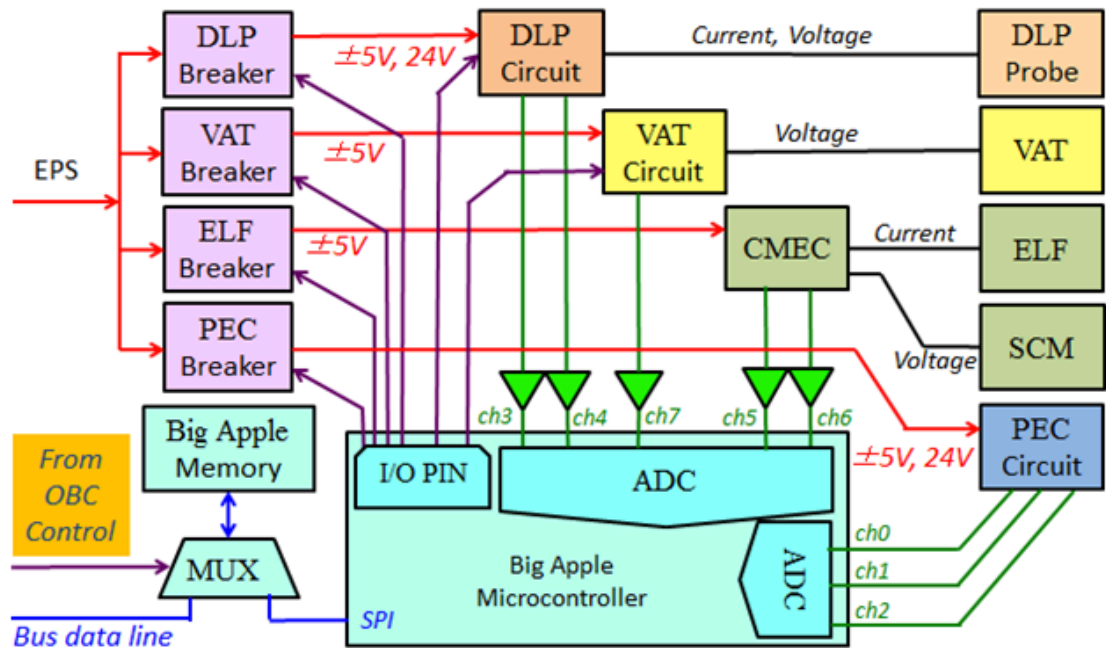


Figure 76. Big Apple mission board.

Vacuum Arc Thruster locates on the “-Z” panel, and power directly supplied from High voltage solar array (HVSA) system. VAT is installed to his own electric circuit with 10 uF capacitor and total resistor value 6.35 M Ω . Main circuit has a conductive layer inside to which thruster’s anode connected by screwing using threads (Figure 77).

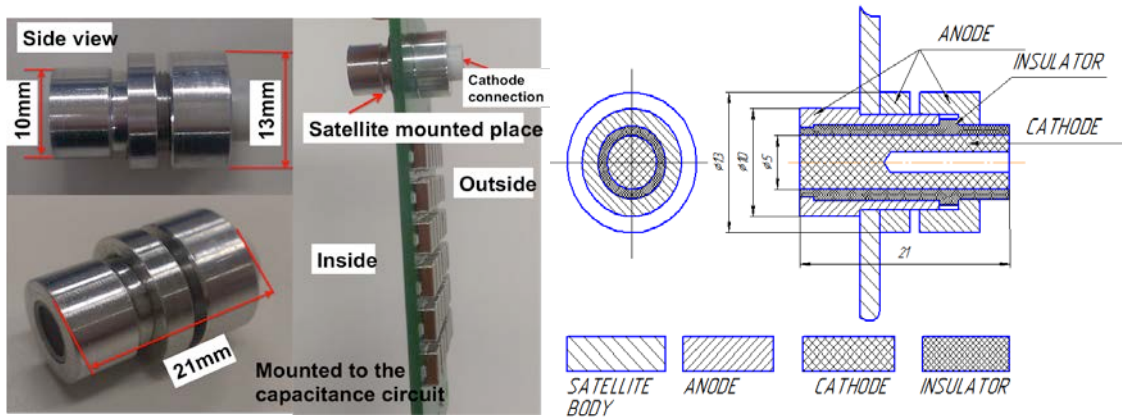


Figure 77. VAT mounting to the capacitor circuit.

VAT circuit (same as on the Figure 26, Chapter 2) was mounted to the satellite wall by four screws and washers that installed between the satellite wall and circuit. In parallel to the VAT's circuit installed a board with current probe, that measure discharge current by on-board oscilloscope (OBO) and a trigger system send a signal to the arc-vision camera (AVC) to detect a moment of discharge. AVC installed on the “-Z” panel. Satellite’s “-Z” panel showed on the Figure 78 with a VAT head and a circuit.

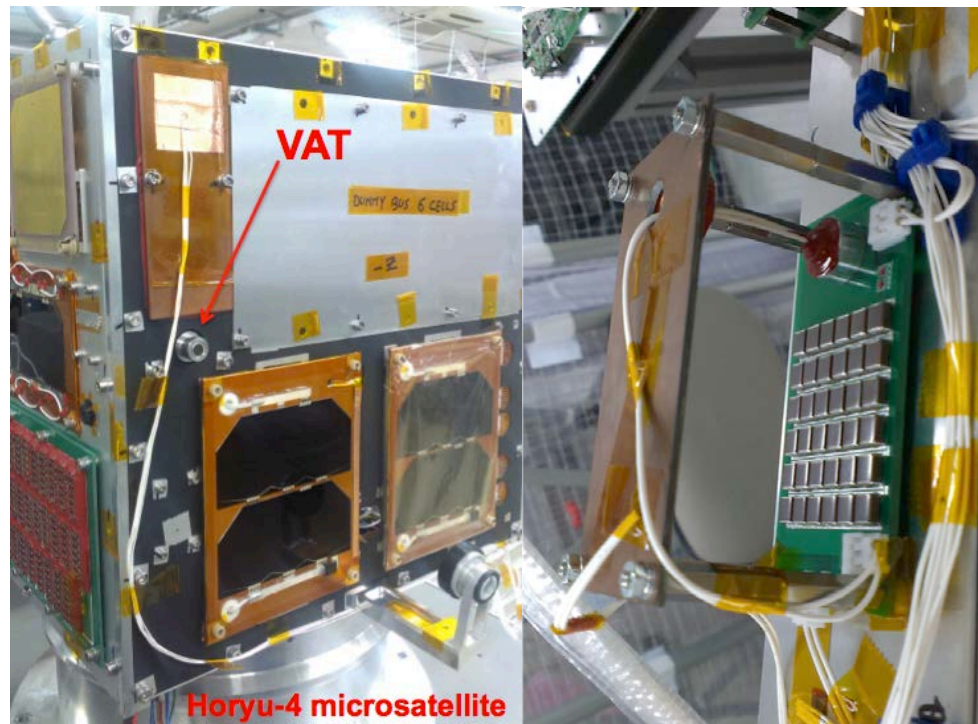


Figure 78. VAT position on-board satellite Horyu-IV.

The end-to-end test was done together with on-board oscilloscope (OBO) and high voltage solar array (HVSA applied ~ 330 V). In parallel, to check the possibility of measurements for Horyu-4 OBO, was used commercial oscilloscope. After the discharge occurred, satellite's on-board current probe measured a discharge current and sent a signal to the OBO trigger system. After that, AVC takes a photo of discharge. The second commercial current probe measured the same discharge current by the commercial oscilloscope, to compare the results. The discharge current detected by the on-board current probe, and by the commercial current probe are presented on the Figure 79.

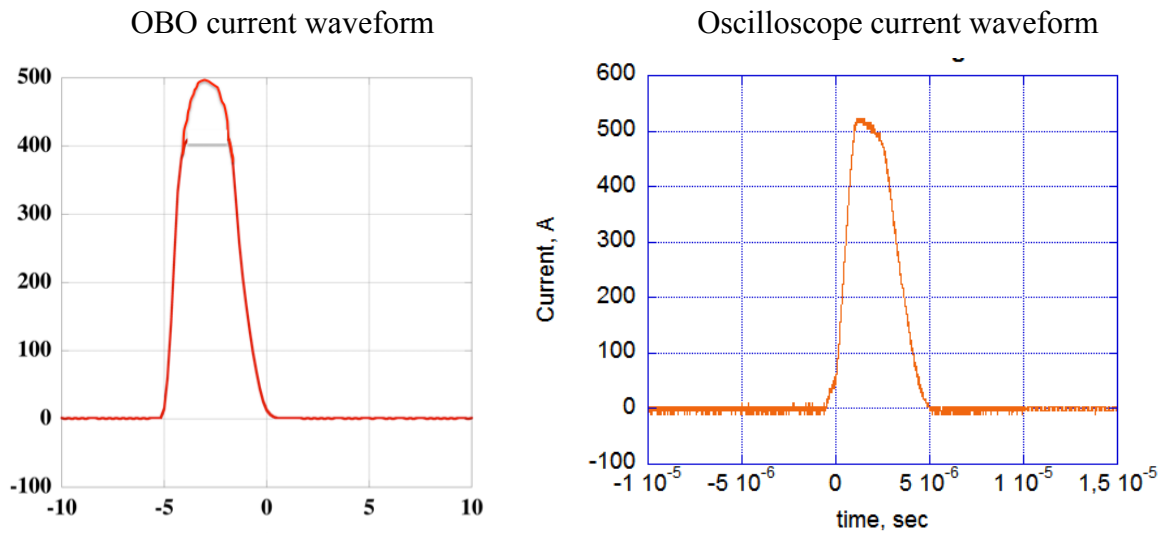


Figure 79. OBO current waveform and commercial oscilloscope current waveform.

From the Figure 79 we can see that discharge current measured by the OBO probe and by the commercial probe, within the error is same. Maximum discharge current is around 500 V and discharge period is ~ 5 usec.



Figure 80. VAT' discharge detected by AVC (end-to-end test).

In this end-to-end test was done 15 discharges (0.028 sec^{-1}). After each discharge, a memory of both oscilloscopes saves a dates of the current. By the number of this waveforms saved to the memory, we get arc rate. By trigger from commercial oscilloscope was detected in the test 15. Because of data saving speed, not all current waveforms was saved to the internal USB flesh card, was saved just 7 curves.

By OBO_Horyu4 system was detected the same number of discharges- 15, and was saved all data to the OBO memory. OBO can detect number of discharges by numbers of saved data. Photo of the discharge detected by the AVC camera after the trigger signal from OBO is presented on the Figure 80.

6. Conclusions

For expanding the satellite agility, capability, life-time (period) of the satellite mission needed micro-thrusters. The most safe and attractive solution can show Vacuum Arc Thruster as it was showed in this work. For now, VAT didn't been tested enough yet and doesn't has a long flight experience. This work described some VAT's design, operation concept, material properties with cathode electrode material solution and some possibility of efficiency improvement. And confirm the novelty of this work- design Vacuum Arc Thruster with passive ignition (no igniter) and develop nanosatellite deorbit system based on VAT.

To perform work objectives was used a high-vacuum facilities together with some diagnostic equipment and measurement tools that installed in the Laboratory of Spacecraft Environment Interaction Engineering (LaSEINE), Kyushu Institute of Technology, Japan. Was used Quadruple Mass Spectrometer to measure the average velocity of molecules emitted and accelerated from the propellant, Electron Cyclotron plasma source to provide LEO plasma conditions, Impulse bit stand based on the polyimide head, Langmuir probe, High voltage solar array as a power source etc.

The main areas of VAT design and operation were undertaken, namely studying: the effect of operating parameters such as level of applied voltage and his affect to the discharge frequency and impulse bit data; electric circuit parameters, such as changing main discharge capacitor and measuring impulse bit; magnetic field effect for thruster discharge parameters and expanding cathode design knowledge through the use of new or untested materials (such as Carbon based material); study of cathode erosion for VAT with Carbon Fiber Reinforced Plastic (CFRP) material and Vacuum Arc Thruster efficiency improvement; developing deorbit system based on VAT for nanosatellites. An overview of each study and its findings are given below.

Was tested few VAT configurations. At first, was decided to use a Carbon Fiber Reinforced Plastic (CFRP) as a cathode/propellant electrode. To decide which

propellant is better was measured an average velocity of emitted electrons from the electrode for Aluminum, Tungsten and CFRP material. The highest number of triple junction points showed CFRP, Carbon based material.

For original VAT design was decided to use a cylindrical electrode configuration. Was ordered from the manufacturer two CFRP propellants: with zero degree of the carbon fiber direction and with 45 degree of carbon fiber direction. Was measured arc rate for this two electrodes and CFRP with 45 degree of carbon fiber direction was rejected because didn't show any successful results. For the next test was decided to use Aluminum cylindrical anode and cathode made from CFRP with zero degree of the carbon fiber direction with cylindrical configuration, too. For this VAT configuration was done the next tests: arc rate measurement, average velocity data measurement, discharge current and voltage waveforms, impulse bit measurements. The basic founded performance is:

- main applied voltage level is 300 V;
- power source- High Voltage Solar Array (HVSA), or power source;
- discharge current is around 600 A;
- discharge time period is around 5 usec;
- discharge arc rate- 0.0032 sec^{-1} ;
- average velocity- 9.5 km/sec;
- specific impulse is around 1300 sec^{-1} ;
- thrust - 4.8 nN;
- efficiency – 2.5 %.

To improve thruster parameters was developed water adopt CFRP propellant, and arc rate data shows around 0.019 sec^{-1} , compare to the commercial CFRP that shows 0.0032 sec^{-1} . Discharge current data was almost same with commercial propellant test results ~600-670 A.

For commercial propellant was done a long-life test results for 10,000 discharges. Was measured arc rate and impulse bit data before and after this test. If the impulse bit range after the long life test within the error was almost same as before, arc rate or discharge frequency was decreased from 0.0032 sec^{-1} to 0.00139 sec^{-1} for 300 V

range of applied voltage for commercial CFRP propellant with Aluminum anode thruster configuration. For 800 V frequency of discharges was decreased from 0.031 sec^{-1} to 0.0017 sec^{-1} . Therefore, the purpose of a water adopt propellant, presented in this work is actual for extending thruster lifetime and keep same working parameters during all mission. For water adopt CFRP propellant/cathode arc rate results before the long-life test was 0.019 sec^{-1} (300 V operational voltage) and 0.1899 sec^{-1} (800 V operational voltage). Need to continue a long life test to compare results.

For VAT configurations with Aluminum anode and commercial CFRP or water adopt CFRP was applied a permanent magnet. Thruster's impulse bit data was improved for $\sim 29\text{-}31\%$. Was applied a nozzle with same geometrical characteristics as a diameter of propellant plus insulator- 5 mm. The data with or without nozzle is same within the error.

Was tested VAT in collaboration with two different main capacitor circuits (10 μF and 14 μF). Results showed that VAT impulse bit increases if capacitance in circuit increases too. Together with that, water adopt CFRP with both capacitances (10 μF and 14 μF) showed smaller discharge current than commercial CFRP in the same circuit with high applied voltage (600 V -800 V).

The practical purpose of this thruster is- microsatellite effective deorbit system. As requirements was decided to build a thruster with a simple design, absence of valves, within the 1 W power consumption to deorbit 1 kg CubeSat from 800 km altitude to 400 km altitude in time less than 25 years. From the results was confirmed that VAT with commercial CFRP propellant and 10 μF capacitor in the circuit can provide a 1U CubeSat deorbit in ~ 102 years. For VAT with water adopt CFRP and 14 μF capacitor this time is much less, 4.79 years. Presented results for 800 V applied to the cathode.

For VAT configuration with Copper electrode inside the propellant on the depth of 8 mm, was calculated deorbit time for 9 months. Calculated erosion showed mass loss ~ 1.57 gramm. With total propellant mass 1.8 gr, propellant consumption for the presented thruster configuration is not enough, but not so critical as for the

VAT with 10 μF capacitor and commercial CFRP with zero degree carbon fiber direction. To solve this problem, cathode electrode/propellant diameter could be increased to survive with presented propellant consumption.

To confirm satellite deorbit time by VAT on-board CubeSat, we purpose to use four thruster on-board. All thrusters are powered from the one circuit. In space condition, discharge on the thruster could occurred only on the ram satellite side, where ion concentration is high. With this configuration no need to worry about satellite orientation or some specific system that will detect the moment when thruster should switch ON. Anytime, on the orbit, when VAT is powered we can get a discharge and provide effective deorbiting.

As a practical use of VAT, was taken part in the student satellite project “HORYU-IV”. Was developed VAT system and installed on-board satellite, launched 17 February, 2016. VAT system works in collaboration with on-board oscilloscope, arc vision camera (to detect a discharge) and High Voltage Solar array as a power source.

For future work, need to finish a discharge test for the water adopt propellant, and measure the arc rate data before and after long life test. Calculate mass shot per discharge for this propellant. Need some circuit improvement work, to determine the dependence of the frequency and completeness of the charge value to the capacitor capacitance. Need to perform VAT test on-board satellite Horyu-IV and confirm possibility of discharges in space condition. Need to specify a possibility of CubeSat effective attitude control, by VAT with highest characteristics.

References

1. <http://www.slideshare.net/mooctu9/rise-of-smallsatellites>
<https://www.google.co.jp/#tbm=isch&q=micro+satellites&imgcr=qx3ahAuEEIzpSM%3A>.
2. Keidar M., Haque S. "Micro-cathode arc-thruster for PhoneSat propulsion", Paper #SSC13-VII-9.
3. http://erps.spacegrant.org/uploads/images/images/iepc_articledownload_1988-2007/2003index/0276-0303iepc-full.pdf
https://www.mpn1.seas.gwu.edu/images/mpn1/publications/conferences/SmallSat-Paper-SSC13-VII-9_FINAL.pdf.
4. stacks.iop.org/PSST/14/661.
5. Anders A. Cathodic Arcs: From Fractal Spots to Energetic Condensation.
6. André Anders , Lawrence Berkeley, "Cathodic Arc Plasma Deposition " National Laboratory, University of California.
7. Jonathan Lun, "Performance improvement of Vacuum Arc Thruster".
8. <http://www.space.bas.bg/sens/Ses2005/SS3.pdf>
9. "What are hypervelocity impacts?" ESA, 19 February 2009.
10. http://www.nasa.gov/multimedia/imagegallery/image_feature_1283.html
11. K. Aheieva, K. Toyoda, M. Cho "Deorbit system based on Vacuum Arc Thruster for microsatellites", IAC 2015.
12. Kazuhiro Toyoda, "Preliminary investigation of space debris removal method using electrostatic force in space plasma".
13. <http://www.thinksrs.com/products/RGA.htm>.
14. K. Aheieva, A. Loyan, V. Gaydukov "Power plant for microsatellite orientation", ISAS 2014, JAXA, Tokyo, Japan.
15. Brown, I. G. (1994), 'Vacuum arc ion sources', *Review of Scientific Instruments* **65(10)**, 3061–3081.
16. James, E. Polk, M. John K. Ziemer. "A Theoretical Analysis of Vacuum Arc Thruster Performance", 27th IEPC, IEPC-01-211.

17. Michael Keidar, "Performance characteristics of Micro-cathode Arc Thruster", Journal of propulsion and power, 2014, Vol. 30.
18. Tony, K. Statom, "Vacuum Arc Nano-Thruster cathode performance for nano-satellite", Air force research laboratory, AIAA 2003-4391.
19. Kazuhiro Toyoda, Hirokazu Masui, Takanobu Muranaka, Mengu Cho, Tomoyuki Urabe, Takeshi Miura, Shirou Kawakita, Yuichiro Gonohe, and Tooru Kikuchi, "ESD Ground Test of Solar Array Coupons for a Greenhouse Gases Observing Satellite in PEO", Plasma Science, IEEE Transactions on (Volume: 36, Issue: 5).
20. Shunsuke, I. Tatsuya, Y. Hirokazu, M. Minoru, I. Kazuhiro, T. and Mengu, C. "On-Orbit Data Analysis of high Voltage Technology Demonstration Satellite HORYU-II", 51st AIAA Aerospace Sciences Meeting, AIAA 2013-0813.
21. K. Aheieva, S. Fuchikami, M. Nakamoto, K. Toyoda, M. Cho "Development of a direct drive Vacuum Arc Thruster passively ignited for Nano-satellite", AIAA, IEEE, January 2016, p. 100.
- Teel, George Lewis. "Development and Characterization of the Heated-Anode Cathode Arc Thruster (HA-CAT).", Proquest, 2014.
22. <http://www.picoelectronics.com/dcdclow/pe65.htm>.
23. K. Aheieva, K. Toyoda, M. Cho "Vacuum Arc Thruster development and testing for micro- and nanosatellites", ISTS/IEPC 2015, Japan, IEPC-2015-425p.
24. Polk, J. E., et al., "A Theoretical Analysis of Vacuum Arc Thruster Performance" - IEPC-01-211.
25. Itsuro Kimura, "New type of target for the measurement of Impulse bit of Pulsed Plasma Thruster", University of Tokyo, AIAA 82-4138.
26. Zhuang, T., Shashurin, A., Brieda, L., and Keidar, M., "Development of Micro-Vacuum Arc Thruster with Extended Lifetime," 31st International Electric Propulsion Conference, Vol. 2009, 2009.
27. Shingo, F. Masayoshi, N. Kazuhiro, T. and Mengu, C. "Development of Vacuum Arc Thruster for Nano-Satellite in Low Earth Orbit Plasma", 29th ISTS.
28. ESA Space debris mitigation handbook, Release 1.0, April 7, 1999.

29. The Orbital Debris Quarterly News- A Decade of Growth, NASA Johnson Space Center, Volume 5, issue 4.
30. D. Rex, P. Eichler: The possible long term overcrowding of LEO and the necessity and effectiveness of debris mitigation measures, Proceedings of the first European Conference on space debris, ESA SD-01, pp 607-615, 1993.
31. R. Janovsky, M. Kassebom, End-of-life de-orbiting strategies for satellites, dglr-2002-028.
32. “Spacecraft environment interaction”, D. Hastings, H. Garret.
33. http://www.lizard-tail.com/isana/lab/orbital_decay/.
34. <http://www.picoelectronics.com/dcdclow/pe65.htm>.
35. K. Aheieva, K. Toyoda, M. Cho “Vacuum Arc Thruster development and testing for micro- and nanosatellites”, ISTS/IEPC 2015, Japan, IEPC-2015-425p.
36. <http://kitsat.ele.kyutech.ac.jp/horyu4WEB/horyu4.html>.